Title
Infrared Spectroscopy of Ionic Clusters

Author
Price, J.M.

Publication Date
1990-11-01

LBL-29920

Lawrence Berkeley Laboratory
UNIVERSITY OF CALIFORNIA

Materials & Chemical Sciences Division

Infrared Spectroscopy of Ionic Clusters

J.M. Price
(Ph.D. Thesis)

November 1990

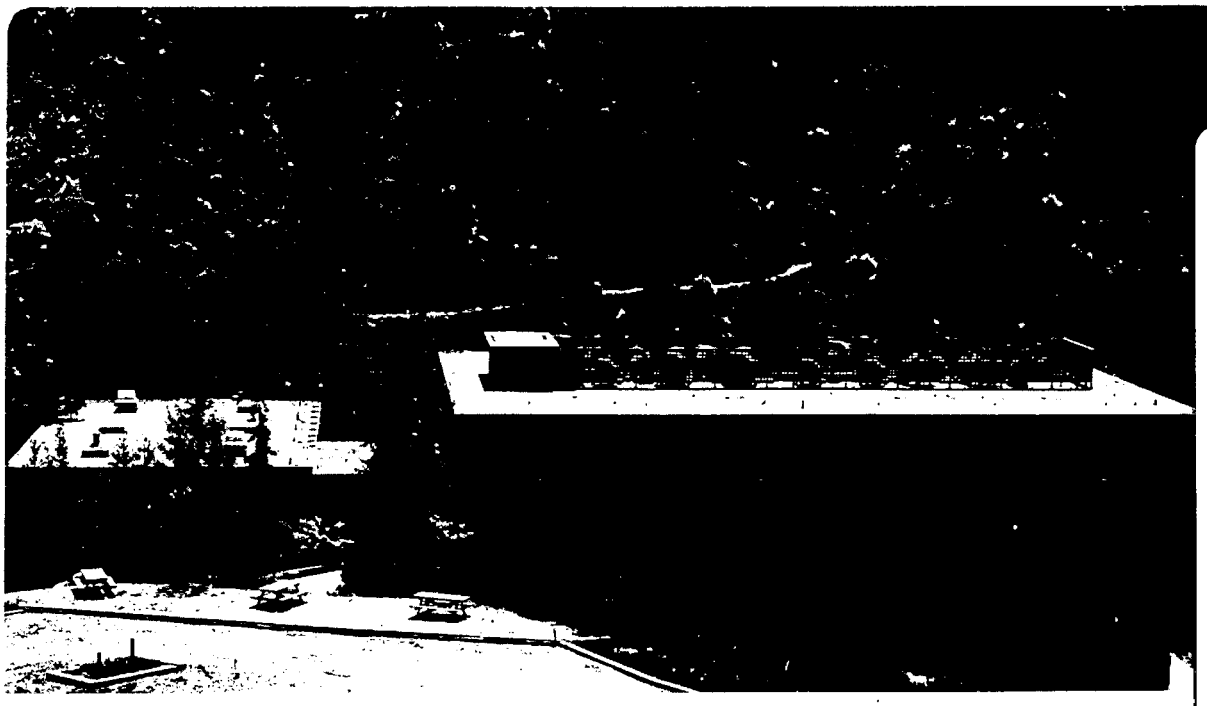

Prepared for the U.S. Department of Energy under Contract Number DE-AC03-76SF00098.

DISCLAIMER

LBL-29920

INFRARED SPECTROSCOPY OF IONIC CLUSTERS

John Michael Price

Department of Chemistry
University of California

and

Chemical Sciences Division
Lawrence Berkeley Laboratory
Berkeley, CA 94720 USA

November 1990

This work was supported by the Director, Office of Energy Research, Office of Basic Energy Sciences, Chemical Sciences Division, of the U.S. Department of Energy under Contract No. DE-AC03-76SF00098.

Infrared Spectroscopy of Ionic Clusters

By

John M. Price

ABSTRACT

This thesis describes new experiments wherein the infrared vibrational predissociation spectra of a number of mass-selected ionic cluster systems have been obtained and analyzed in the 2600 to 4000 cm^{-1} region. The species studied include: the hydrated hydronium ions, $H_3O^+(H_2O)_{3\text{-}10}$, ammoniated ammonium ions, $NH_4^+(NH_3)_{1\text{-}10}$ and cluster ions involving both water and ammonia around an ammonium ion core, (mixed clusters) $NH_4^+(NH_3)_n(H_2O)_m$ (n+m=4). In each case, the spectra reveal well resolved structures that can be assigned to transitions arising from the vibrational motions of both the ion core of the clusters and the surrounding neutral solvent molecules.

For a given ionic cluster, these transitions show systematic frequency shifts with increasing solvation (increasing values of n or m). These shifts and the appearance or disappearance of core vibrational features have been used to determine the number of ligands involved in the first solvation shell about the ions and possibly the number of solvent molecules required for the onset of a liquid-like environment about the core. For the hydrated

hydronium ions described in Chapter II, the first solvation shell fills at m=3. Similarly, for the ammoniated ammonium ions, described in Chapter III, the first shell fills at n=4. For the mixed clusters, described in Chapter IV there is evidence for a number of different structural isomers being present where water ligands preferentially adopt second solvation shell sites before the first shell is filled.

Information has also been gained about solvent-solvent interaction in these systems. For the ionic clusters involving the ammonium ion as the core, structures were observed that can be assigned to transitions arising from the internal rotation of the ligands in the first solvation shell of the cluster about their hydrogen bonds to the ion core. It has been found that this rotation is essentially free, with a very low barrier to the motion (<10 cm^{-1}) for the ammoniated ammonium n=1 cluster. This rotation only occurs when the rotating first shell ligand is not involved in hydrogen bonding with a ligand in the second solvation shell which quenches the free rotation.

ACKNOWLEDGEMENTS:

"I have looked into the face of infinity and laughed..."

-- Jack Burdair Hartung, Jr.
c.a. 1987 A.D.[1]

It was typical in ancient poetry and writings to begin a work with a prayer to the muses; praising them for their powers, and asking them for guidance in the task at hand. The task of the present section is to properly thank those who have helped me during the last four and one half years. The number of people who have aided me, and the strength of the support they have offered makes properly thanking them difficult. -- Perhaps supernatural assistance will be required.

First, I would like to thank Professor Yuan T. Lee for the opportunity to work with him. I have benefitted both from his vast understanding of chemistry, and from his infinite patience. His capacity for hard work and his dedication to science have been a model for me. He told me once that to be a successful scientist you can do one of two things: be very smart, or

work **very** hard. Yuan does both.

Those I have worked with on a day to day basis also deserve recognition. Lisa I-Ching Yeh was the senior student on the project when I arrived at Berkeley. She taught me the mysteries of the experimental apparatus in my first year. Dr. Mark W. Crofton, postdoctoral fellow, gave me many important lessons in spectroscopy and füssball --he is a master of both. I have benefitted from his experimental expertise and his understanding of people. Dr. Gereon Neidner-Schatteburg, a postdoctoral fellow from Göttingen, Germany lent his mastery of computer programming and teutonic attention to detail to the project from which I have learned much. I would also like to thank Mr. Doo Wan Boo, a second year student who is now Czar of the machine, for his hard work and lessons in Zen.

Two other Lee group members, Jim Myers (driver of the battlewagon of science) and Dr. Matthew J. Côté (cofounder of UGI enterprises) deserve recognition for both their scientific suggestions, and friendship. I am grateful to them for long conversations over pitchers about life after graduate school.

The rest of the Lee group, and Ann Weightman in particular, deserve a special note of thanks. The group in general for the friendly environment, and Ann for her help in navigating the sea of bureaucracy.

Outside the Lee group there are three men who have become my friends in the time I have been here. They are, presented in alphabetical

order: Joel S. Bader, Dr. Jack B. Hartung and Charles E. Miller. Their friendship is "perhaps not unlike the most"[2] important thing I take from this place.

Finally, I would like to thank my parents and my wife, Laura. Their constant love and support has been a great source of strength for me. It is to them that this work is dedicated, for without them, it never would have come to pass.

This work was supported by the Director, Office of Energy Research, Office of Basic Energy Sciences, Chemical Sciences Division, of the U.S. Department of Energy under Contract No. DE-AC03-76SF00098.

REFERENCES:

1. J.B. Hartung, Jr., Personal Communication, (1987).
2. Copywrite, (c) 1986 C.E. Miller, All Rights Reserved.

TABLE OF CONTENTS

CHAPTER I.

Introduction to Cluster Ion Spectroscopy

"[N]o rest is given to the atoms in their course through the depths of space. Driven along in an incessant but variable movement, some of them bounce far apart after collision while others recoil only a short distance from the impact. From those that do not recoil far, being driven into a closer union and held there by the entanglement of their own interlocking shapes, are composed firmly rooted rock, the stubborn strength of steel and the like..."

-Titus Lucretius Carus, "On the Nature of the Universe",
55 B.C.[1]

1.1 CLUSTERS, IONIC CLUSTERS, AND MOTIVATION:

The above reference demonstrates that our interest in the forces that hold groups of atoms together is nearly as old as the concept of atoms themselves. Progress in our understanding of the strong interactions that constitute chemical bonds has been considerable, but it has not been until relatively recently that it has been possible to probe the much weaker forces between molecules that give rise to many of the interesting properties of bulk matter. One important approach in the investigation of these forces has been to study cluster systems.[2]

As weakly bound groups of molecules, clusters represent a fascinating "intermediate case" between isolated molecules, whose properties are dominated by strong chemical bonds, and molecules in the condensed phases, whose properties are largely defined by the interactions between molecules.[3] Significant insight can be gained into the nature of the liquid and solid phases of matter by observing the onset of bulk properties in large clusters. Clusters, in a sense, provide the experimentalist with the capacity to build up matter in the condensed phases one molecule at a time.

In addition to providing an opportunity to learn more about the bulk, clusters possess properties unique to themselves. Novel chemical species have been observed in the mass spectra of clusters that have not been found elsewhere.[4] Strong enhancements and diminutions in chemical reactivity and stability have been observed between cluster species differing by only a

few members. Such effects have been explained in terms of novel geometries that particular "magic numbers" of clustering species are able to assume.[5] The hydrated hydronium ion, $H_3O^+(H_2O)_{21}$, for example has been found to be particularly stable. This has been ascribed to the closed clathrate structure that the water molecules can assume about the hydronium ion for this particular sized cluster, forming a distorted dodecahedral cage about the hydronium ion[6].

Ionic clusters like the hydrated hydronium ions are the subject of this thesis, and constitute an important class about which little structrural or dynamical information has been measured so far in the gas phase. These species are represented by the generic formula: $A^{\pm}(M)_n$, where $A^{\pm}$ is the ionic core of the cluster and may be either a molecular or atomic ion (of either positive or negative charge) and $(M)_n$ are the surrounding n neutral ligands. In contrast to the more weakly bound neutral clusters, these species may have binding energies of nearly "chemical" strengths: on the order of 30-40 Kcals/mole. (See Table I.)[7]

In the gas phase, these ionic clusters are formed through a series of association reactions between the ion and neutral molecules:

$$A^{\pm}(M)_{n-1} + M + N \rightleftharpoons A^{\pm}(M)_n + N \qquad (1)$$

Here N is a third body which serves to stablize the cluster during its formation.

Due to their ease of production and detection in a molecular beam environment, ionic clusters lend themselves to thermodynamic and kinetic measurements. A large body of data of this type is available, and careful measurements of the enthalply, entropy and energy (ΔH°, ΔS° and ΔG°) of formation for individual clustering steps has been obtained for a wide range of ions. Castleman has assembled the results of a large number of workers into an atlas, listing this information for both molecular ions and ionic clusters.[8]

Structural information about charged clusters can sometimes be found by mapping ΔH° as a function of cluster size. Performing this operation can yield a curve with discontinuities at cluster sizes where the ion's first solvation shell is expected to fill.[9] Given the geometry of the ion, one is usually able to make reasonable guesses about the geometry of the smaller clusters from this data, as there are often intuitive binding sites for the solvent molecules. Discontinuities of this type are observed for the ammoniated ammonium ions, $NH_4^+(NH_3)_n$, where a strong discontinuity is observed between n=4, the complete first solvation shell, and n=5. (See Table I and Figure 5.) There is no obvious discontinuity in the analogous plot for the hydrated hydronium ions however, which have quite high binding energies even for second shell ligands. (The first shell of the

hydrated hydronium ions is expected to fill at n=3. --See Table I and Figure 5.) Although these measurements can give qualitative information about the location of the solvent molecules around the ion, and consistent geometries can be calculated from ab initio methods[10], the accurate equilibrium geometry of a given cluster can still only be obtained from spectroscopic measurements.

In spite of the wealth of thermodynamic data, very few spectroscopic investigations have been performed on ionic clusters due to the poor number densities of clusters that can be obtained with conventional cluster ion sources. In those cases where sufficient number densities to measure absorptions directly can be obtained, the source conditions needed to produce enough cluster ions for a measurable absorption have yielded samples with large amounts of vibrational and rotational excitation from the violent ionization conditions.[11] The more successful attempts to gain spectroscopic information about ionic clusters have made use of "consequence" techniques rather than direct absorption methods. Consequence techniques use a direct consequence of photon absorption rather than attenuation of the incident radiation as the signal that an absorption event has taken place. Such methods include, among others, fluorescence spectroscopy and vibrational predissociation spectroscopy.

1.2 EXPERIMENTAL TECHNIQUE:

1.2.1 Method: Vibrational Predissociation Spectroscopy

This work employs the consequence technique of vibrational predissociation spectroscopy. Cluster ions are generated by one of a number of sources. Of the distribution of cluster ions created by the source, a population of equal sized ions is selected for study by means of a sector-type mass analyzer. The mass selected beam is then directed into a radio frequency ion trap which holds the cluster ions of interest under collision free conditions while they interact with a tunable infrared laser, either alone or in conjunction with a high power line tunable CO_2 laser. If sufficient energy is absorbed from the lasers, the weakly bound clusters may undergo vibrational predissociation along a channel involving the loss of one or more solvent molecules.

The vibrational predissociation reaction is represented in its most general form for positive ionic clusters by the following:

$$A^+(M)_n + l(h\nu_1) + m(h\nu_2) \rightarrow A^+(M)_{n-i} + iM \qquad (2)$$

In this case, $l(h\nu_1)$ represents l (number of) tunable infrared photons of frequency ν_1 and $m(h\nu_2)$ represents m (number of) fixed frequency photons of frequency ν_2. The parent cluster in this case has absorbed sufficient

energy from the two lasers to result in the evaporation of i (number of) solvent molecules to produce a smaller mass daughter ion.

After excitation, the contents of the trap are then directed into a second mass spectrometer tuned to pass one of the smaller massed products. Since the appearance of mass selected product is a direct result (or consequence) of the absorption of one of the tunable infrared photons by the larger parent cluster ions, the smaller mass daughter ions can be used as a signal that an absorption has taken place. Plotting the number of daughter ions produced as a function of the tunable infrared wavelength yields, to a first approximation, the absorption spectrum of the parent ion. More details of the excitation scheme and the approximations involved in this technique are found below.

In contrast to direct absorption methods, the sensitivity of this technique is extremely high. Ion counting permits the detection of single absorption events with essentially zero background at the mass of interest. For typical conditions in the experiments described below, we have an infrared absorption cross section $\sigma \approx 10^{-17}$ cm^2, an absorption pathlength $l \approx 100$ cm, and an ion beam density $n \approx 10^3$/cm^3. The fractional absorption, given by $n\sigma l$, is then on the order of 10^{-12}, at least five orders of magnitude more sensitive than the detection limit of the best direct absorption experiments.

1.2.2 Excitation Scheme: The Quasi-Continuum of States

For neutral clusters or weakly bound ionic clusters such as the hydrogen cluster ions (see Table I), a single photon of tunable infrared light in the 4000 cm^{-1} region provides sufficient energy to promote the system over the dissociation threshold along the solvent molecule channel. Absorption of a photon into one of the high frequency stretching modes of the ion core in $H_3^+(H_2)_3$ results in the loss of up to two of the three available H_2 ligands.[12] For weakly bound systems, excitation of a single quanta of a high frequency vibrational stretch can couple to the continuum of levels of the dissociating products.

This situation is illustrated schematically in Figure 4. Two orthogonal Morse potentials are plotted, one representing a high frequency stretching coordinate and another representing a low frequency ligand-cluster coordinate. Excitation of a fundamental vibration in the high frequency coordinate (represented by E) can put more energy into the system than the D°_2 dissociation energy along the other coordinate.

For weakly bound systems like these, the absorption spectrum of the parent cluster ion should be well represented by the number of daughter ions produced as a function of the tunable infrared light. The frequency dependence of the reaction cross section for the photodissociation reaction:

$$H_3^+(H_2)_n + h\nu_1 \rightarrow H_3^+(H_2)_{n-1..2} + (1..2)H_2 \quad (3)$$

comes only from the frequency dependence of the absorption cross section of the parent cluster and whatever frequency dependence there is for the coupling between the two states. It is our approximation that this later term changes little over the energy ranges of the present work.

The situation becomes somewhat more complicated when the ionic cluster in question has a binding energy larger than the energy of a single tunable infrared photon. Under these circumstances, more energy must be deposited in the system to induce dissociation unless there are large amounts of internal excitation already present. Virtually all of the systems studied in this work fall under this category. An examination of Table I reveals that for the hydrated hydronium and ammoniated ammonium ion dimer species (either a hydronium or an ammonium ion solvated by a single ligand) the ΔH° of formations are roughly a factor of three larger than the energy of a 3000 cm^{-1} photon. Only for the largest clusters is the binding energy small enough for a single photon to be effective in removing a solvent molecule. To put the required extra energy into the system we have turned to a multiphoton excitation scheme.

Multi-photon excitation has been widely used in the study of neutral polyatomic molecules as a probe of both reaction dynamics and spectroscopy.[13] Although exact quantitative theories to describe the behavior of a molecule in a strong IR field are not yet available, a generally

accepted qualitative picture exists which describes many of the observed phenomena. Illustrated graphically for a generic ionic cluster in Figure 3, the behavior of a molecule in a moderately strong infrared field may be divided into the four regimes discussed below.

In regime (I), the system undergoes stepwise resonant excitation between well separated vibrational levels. The fact that a molecule can undergo this kind of stepwise excitation with a fixed frequency laser was particularly surprising in early experiments as it was thought that the vibrational anharmonicities would quickly tune the levels out of resonance with the laser.[14] However, it was found that the myrad of rotational levels accessible to even a modestly sized polyatomic molecule serves to compensate, in many cases, for the relative shift of the energy levels. Further compensation for the anharmonicities comes from the presence of energy levels resulting from the splitting of degenerate or near degenerate excited vibrational states. An important feature, for the purposes of our discussion, is that the first photon absorbed is through a resonant excitation to a well defined vibrational level and that in the lowest part of the energy level diagram the separation between levels is large compared to the bandwidth of the excitation source. All subsequent excitation hinges on the resonant absorption of the first photon.

The density of levels increases quite rapidly with energy, and as more photons are absorbed, the number of possible vibration-rotation levels

accessible to the laser at a given frequency goes up astronomically.[15] Transitions between levels in this region of high state density, known as the vibrational "quasi-continuum" have much lower absorption cross sections than for the sharp resonances at lower energies. This regime is labled in the figure as region (II). While the cross section for absorption beween levels in the quasi-continuum is much lower than for the lower state levels, so is the frequency dependence of the absorption cross section. At high enough state densities, the absorption spectrum of the quasi-continuum is undifferentiated, having little or no sharp structure.

It is quite possible for an ionic cluster to accumulate enough energy by multi-photon absorption through the quasi-continuum to be excited to an energy greater than that of the weakest bond in the system. Redistribution of the energy throughout the system quickly accumulates the energy into this bond, and dissociation along that channel can take place. Labled (III) in the above figure, this process is illustrated by the highly excited cluster ion dissociating into the next smaller cluster through the loss of a solvent molecule. (For ionic cluster systems, the weakest bond will undoubtedly be one of the bonds between the neutral ligands and the rest of the cluster.) Should there be sufficient laser fluence, the product of the dissociation can itself be excited by multi-photon absorption. This possibility is illustrated in region (IV) of the figure.

In our experiments, the excitation of the clusters is generally separated into two phases. First, the absorption of a single photon of tunable infrared light to one of the discrete energy levels in region (I) described above. From here, a fixed frequency, high power laser is used to drive the excited clusters up through the vibrational quasi-continuum of region (II) and over the dissociation threshold to products via region (III). Since the fixed frequency laser is not in resonance with any of the low lying vibrational levels, there is very little product generated without the presence of the tunable laser. As stated above, the infrared spectra are obtained by monitoring the number of daughter ions produced as a function of the tunable infrared frequency.

In order for the number of product ions produced to accurately represent the intensity of the initial absorption, the transitions through the quasi-continuum must contain little in the way of sharp structure. This requires that the density of states in the quasi-continuum be high enough that no isolated pockets of low state density exist. A number of approximations have been developed to calculate the density of states for polyatomic molecules as a function of energy. Perhaps the most often used is the Witten-Rabinovich approximation for $\rho(E)$ (State density as a function of energy) which has the following form.[16]

$$\rho(E) = \frac{[E + E_0 - \beta W(n)]^{(s-1)}}{(s-1)!\prod_{i=0}^{s}\omega_i}[1 - \beta w(n)], \tag{4}$$

Here, S is the number of vibrational degrees of freedom, and the vibrational energy E is measured relative to the zero point energy:

$$E_0 = \frac{1}{2}\sum_{i=1}^{s}\omega_i \tag{5}$$

The parameter β is expressed by

$$\beta = \frac{S-1}{S}\frac{\langle\omega^2\rangle}{\langle\omega\rangle^2} \tag{6}$$

W(n) is a numerical parameter which depends on the degree of excitation above the zero point level. It is a function of the variable $\eta = E/E_0$ and may assume the values:

$$\begin{cases} (5\eta + 2.73\eta^{\frac{1}{2}} + 3.5)^{-1}, & 0 < \eta < 1 \\ Exp(-2.42\eta^{\frac{1}{4}}), & 1 < \eta < 8 \\ 0, & \eta > 8 \end{cases} \tag{7}$$

The strong dependence of the above expression for the density of states upon the number of vibrational degrees of freedom suggests that clusters, with their large number of such modes, should have low lying, dense quasi-continuua. Table II compares the density of states calculated using the above expression for a number of polyatomic molecules, and several of the ionic clusters from this work. The cluster ions have

significally higher densities of states than most of the neutral molecules. Notice that the density of states is also dependent upon the relative number of low frequency modes since sum and difference frequency bands incorporating low frequency modes will be spaced more closely than those involving higher frequency motions. UF_6 for example, has a substantially higher density of states than the structurally similar SF_6. The large ionic clusters are expected to have a great number of low frequency bending modes accessible to them. These results serve to support the a priori notion that in the case of the ionic clusters presented in this study, the quasi-continuum is dense and low lying and that excitation of the system by a single photon of tunable infrared light near 3000 cm^{-1} should place most, if not all, the systems presented here into the quasi-continuum.

1.3 THE EXPERIMENTAL APPARATUS:

The experimental apparatus used in this work has been well described in previous publications.[17] Some of the salient components will be described below. Details regarding the conditions during the aquisition of the spectra will be discussed in the following chapters. Modifications made to the experimental apparatus during my tenure will be disscussed in the appendicies. Schematic diagrams of the apparatus and the ion source appear in Figures 1 and 2, respectively.

The Corona Discharge Ion Source:

The cluster ions studied in this work were produced in several corona discharge ion sources shown schematically in Figure 2. Unlike conventional ion sources, the corona discharge produces comparatively cold species at the expense of number density. Ionization takes place in a high pressure, low current discharge between the source body (the anode) and a nickel coated sewing needle (the cathode). Typical discharge currents used were in the 10-100 microamp range and pressures inside the source were usually held at or near 200 torr.

In contrast to low pressure ion sources, the ions produced in the corona discharge undergo a large number of collisions with the carrier gas before they find their way out of the source. Typically, an ion undergoes some 10^5 collisions during the time it takes it to make its way out of the ionization region and through the 0.5 cm drift region to the 75 micron

nozzle. Since the source body can be maintained at a given temperature through contact with a liquified gas reservoir, the ions are expected to be at a resonably cool vibrational temperature (<300K).

Expansion of the weakly ionized gas through the nozzle results in rotational cooling of the ions due to the thermodynamic properties of the supersonic expansion.[18] Clustering of neutral solvent molecules around the ionized species also takes place, for the most part, in this region. Fits of the rotational band contours for a number of different cluster ion systems have consistently shown that the cluster ions have rotational temperatures less than 50K under normal operating conditions.

Mass Selection and Ion Storage:

The distribution of clusters produced by the corona discharge source is directed onto the entrance slits of a 60-degree sector type mass spectrometer with a mass resolution of $M/\Delta M = 250$ (See fig. 1.). This level of resolution is routinely achieved by the experimental apparatus, but relies strongly upon the monochromaticity of the ion beam. Variations in the energy of the ions must be minimized, and to some extent, the resolution is dependent upon the conditions of the ion source. Large voltage differences between the nozzle of the source and the skimmer shown in Figure 2 lead to degradation of the mass resolution due to fringing field effects.

Following the mass selection, ions of the desired mass are deflected 90° by a dc quadrupole bending field, then decelerated and focused into the

octupole ion guide whose axis is that of the infrared laser beam. The octopole consists of eight molybdenum rods, equally spaced on a 1.5 cm radius. The rods of the octapole carry approximately 350 volts dc, with applied radio frequency voltages of typically 300 volts peak to peak. Adjacent rods are maintained 180° out of phase. The capacitance of the rods together with the inductance of a copper coil atop the machine form an LC tank circuit which is made resonant in the range 5-20 MHz by the choice of the coil. Smaller ions such as H_5^+ are trapped most efficiently at frequencies toward the high end of the range.

Trapping is accomplished by means of entrance and exit repellers, each of which carries a positive ≈350 volts dc. Upon these a negative 12 volt pulse may be applied to allow the entrance and exit, respectively, of ions into and out of the octopole. The relative timing is adjustable to vary the storage time and the ions can be easily stored for $t < 1$ minute with only about 50% losses. The upper limit to our trapping time is determined by the $\approx 10^{-9}$ torr background pressure in the UHV region of the octapole. The number of trapped ions is optimized by adjusting the DC voltage on the rods of the octapole: the dependence is rather sharp. One thousand ions are routinely trapped at a time, with a repeat frequency of 40 Hz. The major limitation in the number of stored ions is the low ion flux from the source. The trapped ion energy in the longitudinal direction is < 0.5 eV.

The choice of an octopole ion trap over the simpler quadrupole design stems from the superior shape of the effective potential that an octopole field generates. For the present case of a rapidly oscillating field, the effective potential governing the motion of a slow moving charged particle in an ideal electric multipole field with 2n poles is given by:

$$U_{eff}(r) = n^2 K \left(\frac{r}{r_0}\right)^{2n-2} \tag{8}$$

where K is described by:

$$K = \frac{q^2 V_0^2}{4m\omega^2 r_0^2} \tag{9}$$

For an octapole, the effective potential varies as $(r/r_0)^6$.[19] This dependence is $(r/r_0)^2$ for a quadrapole, with a well depth only 25% of the octapole depth for a given voltage, mass, and frequency.

Laser Excitation:

The trapped, mass-selected, ionic clusters are vibrationally excited by a pulsed infrared laser derived from the difference frequency mixing, in a $LiNbO_3$ crystal (Quanta Ray IR WEX), of a Nd:YAG laser fundamental (1064, nm Quanta Ray DCR 1A) and tunable dye laser radiation (typically 740-835 nm Quanta Ray PDL 1). With the aid of a feedback loop, this commercial unit automatically adjusts the tilt of the crystal to maintain the phase matched condition for difference frequency generation as the dye

laser is scanned. Typical laser power is 3.5mj/pulse at 4000cm^{-1} with a pulse length of approximately 10ns.

For the more strongly bound species, a high power CO_2 laser was employed (MBP Technologies, 8 Watts CW at 10.6um TEM) as well to drive the vibrationally excited molecules over the dissociation threshold. Excitation times for this source were equal to the trapping time of the species of interest, as the laser was run in a continuous wave mode. Typical trapping times were on the order of a few milliseconds.

Detection:

A quadrupole mass spectrometer is used to separate the product ions produced by the excitaton from the parent clusters. A Daly-type ion detector is used to monitor the number of fragment ions produced as a function of laser wavelength. Spectra were normalized for tunable infrared power using a simple linear power dependence.

1.4 ASSIGNMENT OF SPECTRAL FEATURES: NOTATION.

Traditionally, the interpretation of liquid and solid phase spectra relies upon measurments from the gas phase. Assignment of spectral features begins with a search for correlations between observed liquid phase transistions and those from measurements of the isolated molecules. Although many assignments can be made this way, the relative transition strengths can vary widely between the gas phase and the bulk, and new features are often observed in bulk spectra that have no correspondence with the gas phase. This phenomenon manifests itself strongly in those cases where hydrogen bonding is involved between the molecules.

Says Herzburg (speaking of formic acid):

"Here the vapor shows the characteristic O-H vibration (3570 cm^{-1}) only at higher temperatures, when it certainly is monomeric. At lower temperatures and in the liquid state this O-H vibration does not occur, but instead a new band at 3080 cm^{-1} is observed which must be ascribed to the O-H vibration in the dimer. The reason for the great change of the O-H vibration frequency in the dimer is now genrally agreed to be hydrogen bonding, which is also responsible for the considerable stability of the dimer..."[20]

These studies involving ionic clusters are a special case of this strong hydrogen bonding situation. As stated earlier, the strength of the ion-solvent bonds in an ionic cluster is very large compared to that of neutral clusters. Consequently, the influence of the hydrogen bonds upon the vibrational motions of the absorbing species can be particularly large. Exactly which vibrational transistions are perturbed, and the extent of the perturbation, depends to a large degree upon the geometry of the cluster.

Of the vibrational motions that take place within the cluster ions presented here, the only fundamental vibrational transitions accessible to the present laser system involve the high frequency N-H or O-H stretching motions. The numerous low frequency bending motions available to the clusters are, in the case of this work, observed only as overtone absorptions or in combination with a high frequency stretch. The higher frequency stretches we have assigned involve two types of oscillators: those associated with the ion core of the clusters and those of the solvent molecules.

For each of these, the frequency of a given transition for a particular subunit (H_3O^+, H_2O, NH_4^+ or NH_3) will be shifted from that of the free molecule (or ion) by an amount determined by the local environment around the absorbing species. The normal modes of the NH_4^+ ion in the $NH_4^+(NH_3)$ system for example, will be split into lower and higher frequency components due to the influence of the NH_3 ligand. Components of a normal vibration involving N-H bonds of the ion in a hydrogen bond with the NH_3 molecule will be shifted to lower frequencies than components of the motion that are not involved. Similarly, for large ammoniated ammonium ion clusters, the NH_3 solvent molecules in the first solvation shell ($n<=4$) will be strongly influenced by NH_3 molecules in the second solvation shell and beyond ($n>4$).

Because of the lengthy descriptions required to indicate the assignment of many of the vibrational bands, I introduce a short-hand

notation: $^{y}X^{o}N\text{-}H^{z}_{p}$ to designate the subgroup involved in a particular transition and to describe the type of vibrational motion the subgroup undergoes. Under this notation, X takes on the values 0,1,2,... and indicates whether the subgroup is in the core, first solvation shell, second solvation shell, etc., y is the number of equivalent N-H oscillators of a particular bond type in the local subunit, z is either b (bound) or f (free) to indicate whether the H of the N-H bond is involved in hydrogen bonding, and p is s, a or b depending upon whether the vibration can be considered as a symmetric or antisymmetric stretch, or a bending mode, respectively, in the local subunit. If the symmetry of the stretch is not determined, but we still consider the transition a stretching type vibration we omit the "s" or the "a" in the notation. If a bond is directly affected by two attached subunits, where one of the subunits attaches to the other, z takes the form b,b. Our notational system can be used for spectra of other ion clusters as well, by adapting the N-H designation to indicate the appropriate bond type.

This system treats the vibrational modes of each subunit separately from the rest of the complex. This "local subunit" approximation seems to work well for labeling spectra of weakly bound clusters, at least for the present spectral resolution. I will also use more conventional labels and full descriptions in many cases, reserving the most extensive use of the new notation for the tables of assignments in the following chapters.

Table I: The Stepwise Heats of Formation for a Number of Different Ion-Neutral Pairs.

Ref	Ion A^+	Neut. (M)	ΔH° : $A^+(M)_{n-1} + M \rightarrow A^+(M)_n$ (Kcals/Mol) at 298K						
			n=1	2	3	4	5	6	7
[21]	H_3^+	H_2	9.6	4.1	3.8	2.4			
[22]	H_3O^+	H_2O	36	22.3	17	15.3	13	11.7	10.3
[23]	NH_4^+	H_2O	19.9	14.8	12.2	10.8	10.6	9.1	8.4
[24]	$NH_4^+(NH_3)$	H_2O	12.9	12.7	12.2				
[25]	$NH_4^+(NH_3)_2$	H_2O	12.4	11.7					
[26]	$NH_4^+(NH_3)_3$	H_2O	11.7						
[27]	NH_4^+	NH_3	27	17	16.5	14.5	7.5		
[28]	NH_4^+	NH_3	21.5	16.2	13.5	11.7	7.0	6.5	

Table II. Density of States Calculated Using Equation (4) for Several Neutral Molecules and Cluster Ions at 3500 to 15000 cm^{-1}.

Molecule, Ion or Cluster	Frequency Groups Used:	ρ at 3500 cm^{-1}	ρ at 7000 cm^{-1}	ρ at 15000 cm^{-1}
H_2O	ν_1: 3825 (1) ν_2: 1654 (1) ν_3: 3936 (1)	1.25×10^{-3}	2.61×10^{-3}	7.57×10^{-3}
NH_3	ν_1: 3336 (1) ν_2: 955 (1) ν_3: 3414 (2) ν_4: 1628 (2)	1.03×10^{-2}	4.43×10^{-2}	4.31×10^{-1}
NH_4^+	ν_1: 3270 (1) ν_2: 1669 (2) ν_3: 3343 (3) ν_4: 1447 (3)	2.99×10^{-2}	1.87×10^{-1}	3.98
$NH_4^+(NH_3)$	ν_1: 3000 (6) ν_2: 1676 (1) ν_3: 1578 (4) ν_4: 1434 (2) ν_5: 954 (4) ν_6: 668 (1) ν_7: 105 (2)	$4.59 \times 10^{+2}$	$1.00 \times 10^{+4}$	$2.64 \times 10^{+6}$
$H_3O^+(H_2O)$	ν_1: 3100 (2) ν_2: 2800 (2) ν_3: 1500 (2) ν_4: 1050 (4) ν_5: 1000 (1) ν_6: 670 (1) ν_7: 180 (2)	$2.32 \times 10^{+1}$	$4.47 \times 10^{+2}$	$3.59 \times 10^{+3}$

Molecule, Ion or Cluster	Frequency Groups Used:	ρ at 3500 cm^{-1}	ρ at 7000 cm^{-1}	ρ at 15000 cm^{-1}
SF_6	ν_1: 965 (3) ν_2: 772 (1) ν_3: 642 (2) ν_4: 617 (3) ν_5: 525 (3) ν_6: 370 (3)	$1.39 \times 10^{+2}$	$2.05 \times 10^{+4}$	$3.06 \times 10^{+7}$

FIGURE CAPTIONS:

1. Schematic diagram of the experimental apparatus. Showing the ion source, the two stages of mass selection, and the ion trap.

2. Schematic diagram of the ion source, which consists of a corona discharge and supersonic expansion.

3. The stepwise multiphoton dissociation scheme for a generic ionic cluster showing the four regimes with different densities of states (Ater Letokhov. See ref.14.). Regime I: Low state density, strongly resonant excitation. Regime II: High state density, excitation through the "quasi-continuum" of states. Regime III: Excitation through the continuum of states, leading to highly excited species and dissociation. Regime IV: Excitation of the smaller massed product of the original reaction by additional laser fluence.

4. Morse Potentials showing two orthogonal potential energy surfaces. Excitation of a vibration on one surface may exceed the D^0 dissociation energy on another surface. This is analogous to the situation found in the weakly bound hydrogen cluster ions.

5. Graph showing the stepwise heat of formation for the ammoniated ammonium ions, $NH_4^+(NH_3)_n$ (A.A.) and the hydrated hydronium ions, $H_3O^+(H_2O)_n$ (H.H.). The A.A. curve shows a strong discontinuity at the n=5 step. -- The first solvation shell of this cluster is expected to fill at n=4. Molecules in the second solvation shell are bound more weakly in this case.

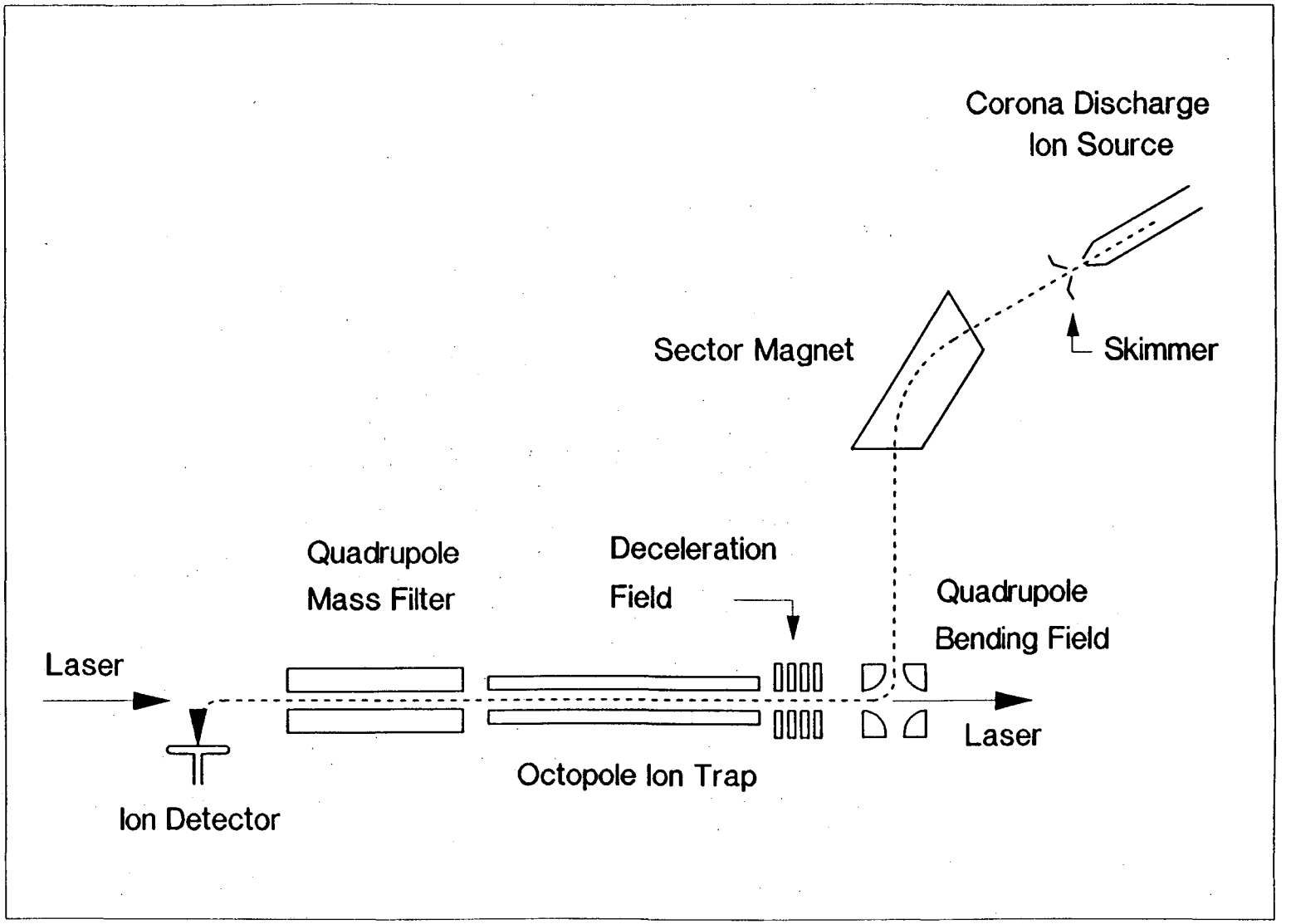
Corona Discharge
Ion Source
Sector Magnet
Skimmer
Quadrupole
Mass Filter
Deceleration
Field
Quadrupole
Bending Field
Laser
Laser
Octopole Ion Trap
Ion Detector

Figure 1.

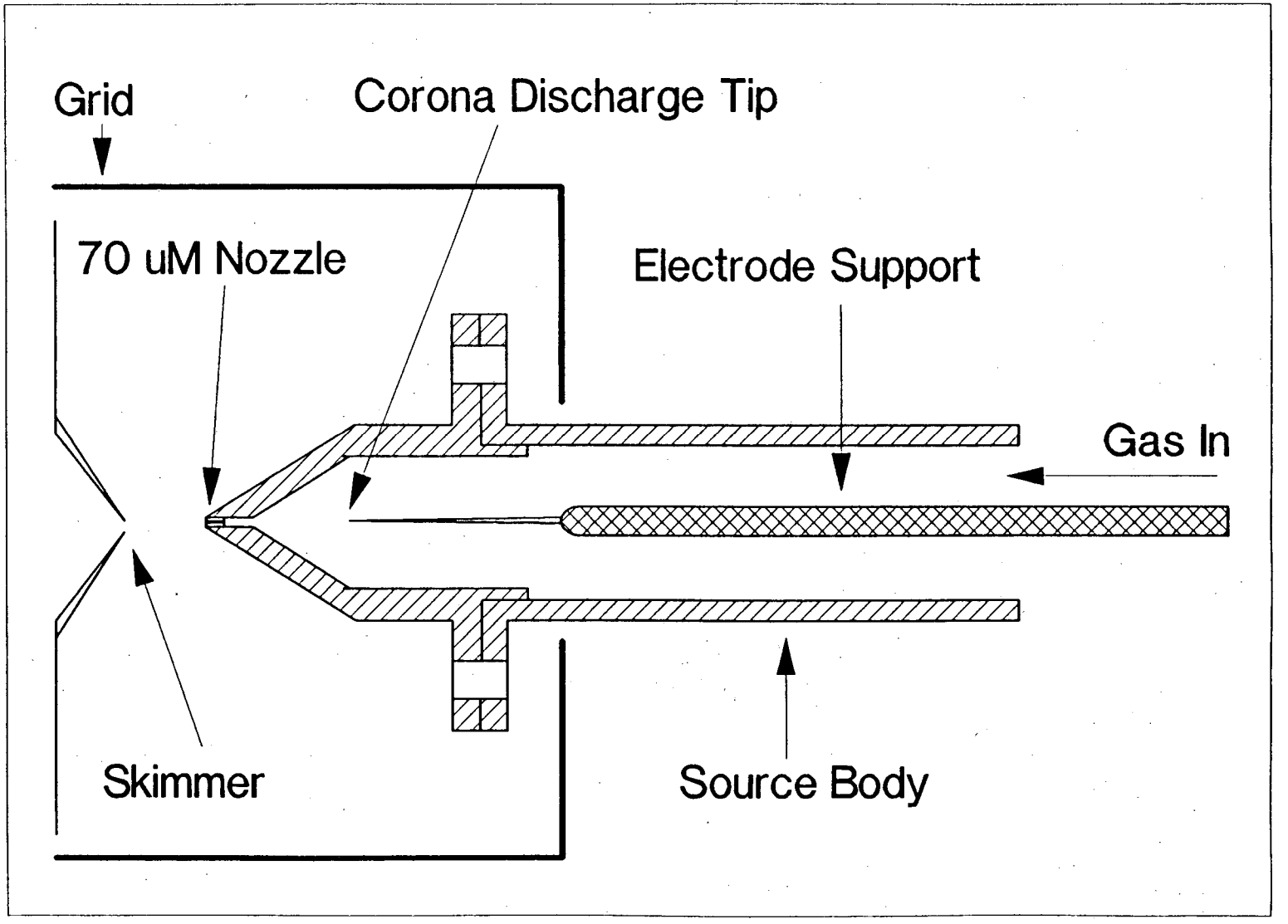
Grid
Corona Discharge Tip
70 uM Nozzle
Electrode Support
Gas In
Skimmer
Source Body

Figure 2.

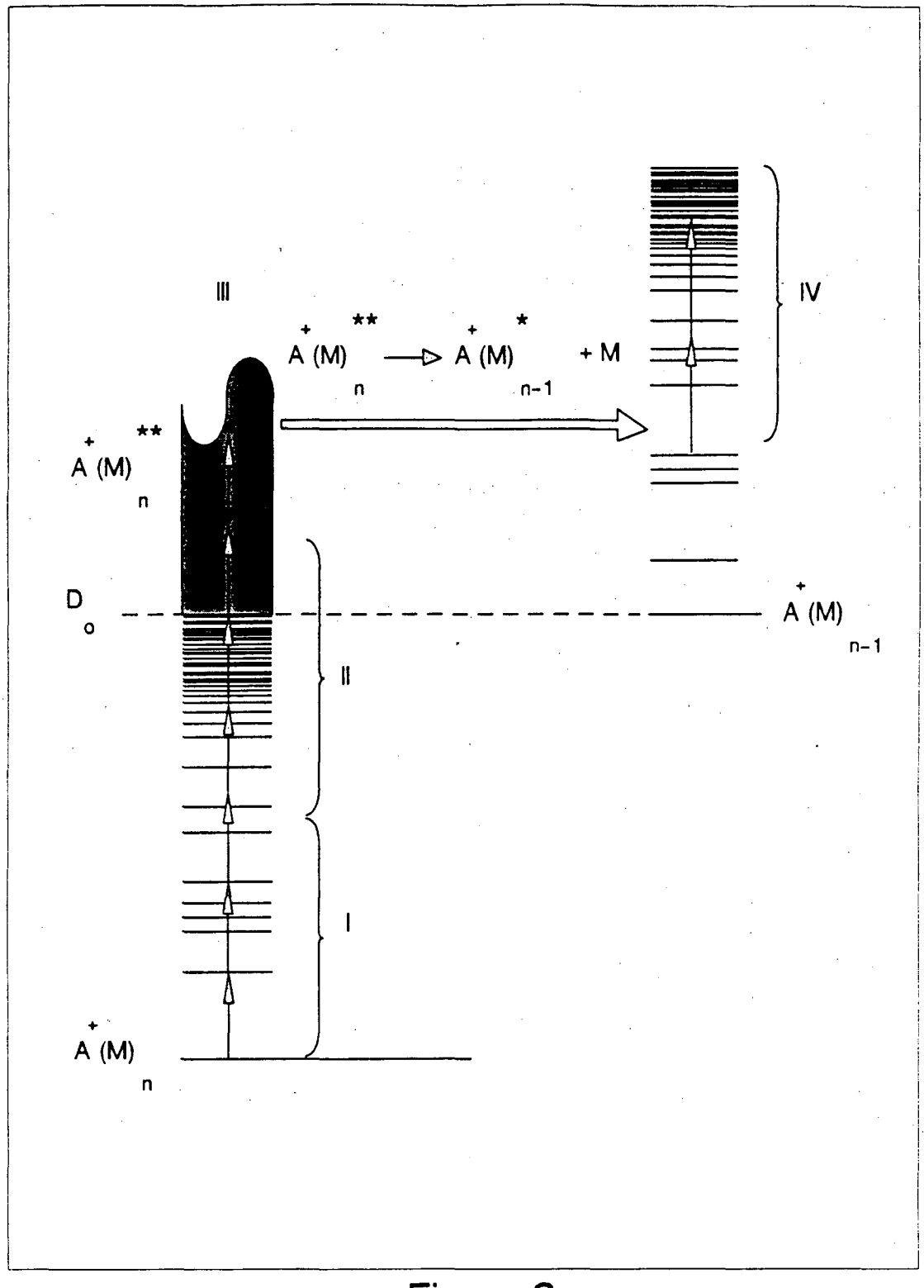

Figure 3.

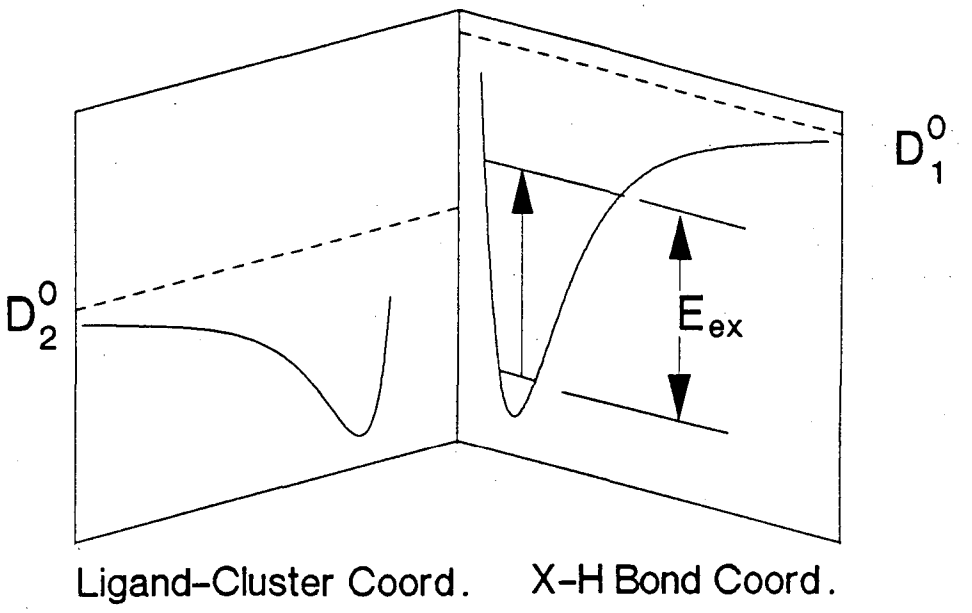

Figure 4.

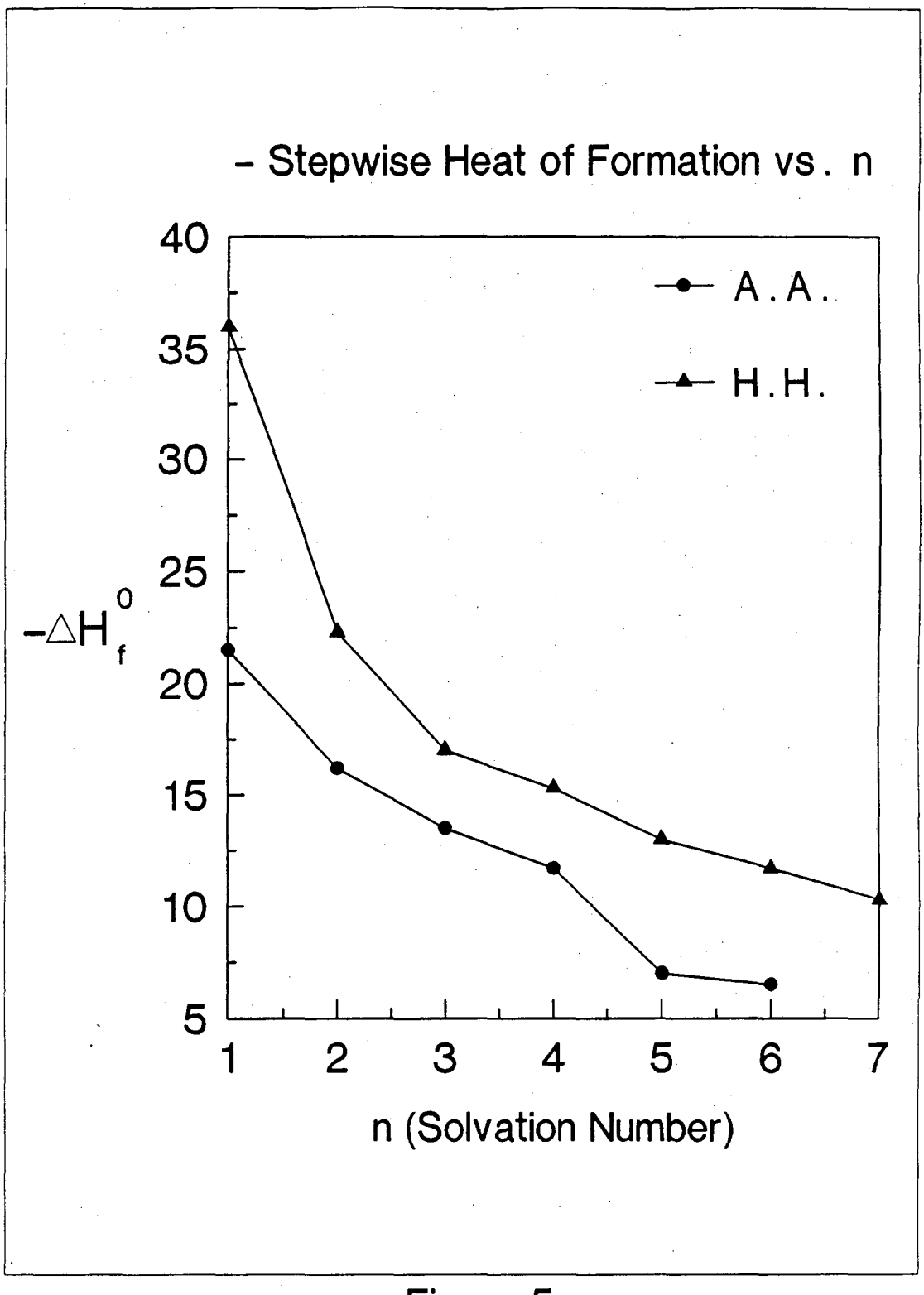
- Stepwise Heat of Formation vs. n
40
35
30
25
20
15
10
5
$-\Delta H_f^0$
A.A.
H.H.
1
2
3
4
5
6
7
n (Solvation Number)

Figure 5.

REFERENCES:

1. T.L. Carus, On the Nature of the Universe, trans. R.E. Lantham, Ed. B. Radice (New York: Penguin Books, 1956).

2. For recent reviews on clusters, and ionic clusters see:
A.W. Castleman, Jr., and R.G. Keesee Chem. Rev. **86**, 589 (1986); A.W. Castleman, Jr., and R.G. Keesee, Acc. Chem. Res. **19**, 413 (1986); T.D. Mark, and W.W. Castleman, Jr., Adv. in Atomic and Mol. Phys. **20**, 65 (1985).

3. R. Pool, Science **248**, 1186 (1990).

4. M.T. Coolbaugh, W.R. Peifer and J. Garvey, Chem. Phys. Lett. **156**(1), 19 (1989); W.R. Peifer, M.T. Coolbaugh, and J. Garvey, J. Phys. Chem. **93**, 4700 (1989).

5. W.R. Peifer, M.T. Coolbaugh and J.F. Garvey, J. Chem. Phys. **91**(11), (1989).

6. P.M. Holland, and A.W. Castleman Jr., J. Chem. Phys., **72**, 5984 (1980); U. Nagashima, H. Shinohara, N. Nishi, and H. Tanaka, J. Chem. Phys. **84**, 209 (1986).

7. A.W. Castleman Jr., K.I. Peterson, B.L. Upschute, F.J. Schelling, Int. J. Mass Spectrom. Ion Phys. **47**, 199 (1983).

8. R.G. Keesee, A.W. Castleman, Jr., J. Phys. Chem. Ref. Data, Vol. 15, No. 8, (1986).

9. N. Lee, R.G. Keesee, and W.W. Castleman Jr., J. Chem. Phys. **72**, 1089 (1980).

10. Articles in: The Hydrogen Bond: Recent Developments in Theory and Experiment Vol. I. (Theory), ed., P. Schuster, G. Zundel, and C. Sandorfy.

11. H.A. Schwarz J. Chem. Phys. **72**, 284 (1980). C.S. Gudeman and R.J. Saykally, Ann. Rev. Phys. Chem. **35**, 387(1984).

12. M. Okumura, L.I. Yeh, and Y.T. Lee, J. Chem. Phys. **88**, 79 (1988).

13. P.A. Schulz, A.S. Sudbo, D.J. Krajnovich, H.S. Kwok, Y.R. Shen, and Y.T. Lee, Ann. Rev. Phys. Chem. **30**, 379 (1979).

14. V.S. Letokhov Nonlinear Laser Chemistry: Multiple Photon Excitation (Springer-Verlag, New York 1983). See also ref. 13 and references therein.

15. P. J. Robinson and K. A. Holbrook, Unimolecular Reactions, (Wiley-Interscience, New York, 1972).

16. M. J. Pearson, B.S. Rabinovitch and G.Z. Whitten, J. Chem. Phys., **48**, 1427 (1968).

17. S.W. Bustamente, Ph.D. Thesis, University of Califonia at Berkeley, (1983); M. Okumura, Ph.D. Thesis, University of California at Berkeley, (1986); L.I-C. Yeh, Ph.D. Thesis, University of California at Berkeley, (1988).

18. ed., S. Scoles Atomic and Molecular Beam Methods Vol. I, (Oxford University Press, New York, 1988).

19. E. Teloy and D. Gerlich, Chem. Phys. **4**, 417 (1974); D. Gerlich in, Electronic and Atomic Collisions ed. D.C. Lorents, W.E. Meyerhof and J.R. Peterson, (North-Holland press, Amsterdam 1985).

20. G. Herzburg, Infrared and Raman Spectra of Polyatomic Molecules, (Van Nostrand Reinhold Co. New York, 1945).

21. K. Hiraoka and P. Kebarle, J. Chem. Phys. **62**, 2267 (1975).

22. P. Kebarle, S.K. Searles, A. Zolla, J. Scarborough, and M. Arshadi, J. Am. Chem. Soc. **89**, 6393 (1967).

23. M. Meot-Ner, J. Am. Chem. Soc. **106**, 1265 (1984).

24. J.D. Payzant, A.J. Cunningham, and P. Kebarle, Can. J. Chem. **51**, 3242 (1982).

25. Ibid.

26. Ibid.

27. S.K. Searles and P. Kebarle, J. Phys. Chem **72**, 742 (1968).

28. M. R. Arshadi and J. H. Futrell, J. Phys. Chem. **78**, 1482 (1974).

CHAPTER II.

The Hydrated Hydronium Ion Clusters:

$H_3O^+(H_2O)_m$ (m=3 to 8)

"Clouds may be produced and formed both by the condensation of the atmosphere owing to compression by winds and by the interlacing of atoms clinging to one another and suitable for producing this result..."

-Epicurus, "Letter to Pythocles"
c.a. 200 B.C.[1]

2.1 INTRODUCTION:

In nature, gas phase ionic clusters are abundant in cold environments with ionizing particles or photons present, including interstellar space and the earth's atmosphere.[2,3] It is known from mass spectrometer studies, for example, that the hydrated hydronium ($H_3O^+(H_2O)_m$) species are the dominant ions in some regions of the atmosphere.[4,5] Hydrated hydronium ion clusters also play essential roles in atmospheric chemistry,[6] nucleation[7] and biology,[8] and are important components of many solutions and crystalline materials. The hydronium ion in solution can be thought of at some level of approximation as an extremely large ionic cluster.

Charged clusters, as stated in the first chapter, generally have a higher binding energy than their neutral counterparts. For the small species with n=1, binding energies similar to those of weak covalent chemical bonds are not uncommon:[2] ΔH° is ≈ -36 kcal/mole for the reaction $H_3O^+ + H_2O \rightarrow H_5O_2^+$ [9,10] and ≈ -27 kcal/mole for the reaction $OH^- + H_2O \rightarrow HOHOH^-$.[11,12] For Li^+ ions solvated by H_2O and a variety of basic ligands, the binding energy is extremely high, often 60 kcal/mole or even more.[2,13,14] Because of the small size of the Li^+, the ion dipole interaction energy is unusually large, and interactions arising from polarization effects can play a considerable role as well. Binding energies for a number of the ionic clusters discussed in this chapter appear in Table I of Chapter 1.

Among charged clusters, those species like the hydrated hydronium

ions containing hydrogen bonds are of particular importance. Hydrogen bonded species are among the most strongly bound ionic clusters. The strongest hydrogen bond measured in nature, that of FHF^-, has a dissociation energy of 58 kcal/mole[15] or 2.5 eV, weaker than the average covalent bond but well within the range of covalent bond energies. As one of the most ubiquitous interactions in chemistry, the hydrogen bond is profoundly influential in determining the structural organization and processes that occur in a variety of environments, from hydrogen bonding solvents to entire living organisms. The proton transfer reaction, [16,17,18,19,20,21] perhaps the most general and important reaction in chemistry, is governed in hydrogen bonding solvents by hydrogen bonded "cluster" species.

A great many studies have been made of the solvated proton in the liquid and solid phases, using x-ray and neutron diffraction, infrared and nuclear magnetic resonance (NMR) spectroscopy and other techniques.[18,23] While much has been learned from these studies, the presence of a distribution of species in the sample, the impossibility of studying most samples at very low temperatures and other problems, often result in serious ambiguities in data interpretation. Particularly in solution, the structures of $H_3O^+(H_2O)_m$ have not been well understood. In the solid phase, convincing evidence for $H_5O_2^+$ with a centralized bridging proton and $H_9O_4^+$ with C_{3v} symmetry have been found. Many ammonium salts such as the

series $NH_4^+X^-$ and $NH_4^+(NH_3)_nX^-$, where X = Cl^-, Br^-, I^- have well-characterized vibrational spectra.[22] The solid phase results, however, are difficult to extrapolate to the liquid or gas phase.

In spite of the substantial effort devoted to the study of the solvated proton in the bulk phases, predictions of the structures and dynamical processes relating to hydrogen bonded systems are often unreliable or computationally intractable.[23,24] For larger systems, it is usually impractical to attempt any detailed predictions. Hydrogen bond lengths, the distance between the X atoms in X-H···X, and stretching frequencies are in general far less accurately determined for cluster systems than for molecules of similar size and type but containing only covalent bonds. This is due in part to the flatness of the potential well even near the bottom, and the greater anharmonicity of the potential surface associated with the hydrogen bond. There is a need for experimental data from which accurate potential surfaces can be derived, in order to guide theoretical efforts.

The understanding of neutral hydrogen bonded systems has been considerably enhanced recently by the detailed spectroscopic studies of species such as $(H_2O)_2$,[25,26,27] $(NH_3)_2$,[25] and a host of van der Waals complexes.[28,29] From these, accurate equilibrium geometries can be determined. While some low resolution data exists for a few of the larger clusters of $(NH_3)_n$[30] and $(H_2O)_n$,[31,32,33] which are of direct interest to the question of the onset of the liquid state, these systems have resisted

detailed analysis. The study of these neutral cluster species is complicated experimentally by difficulties in obtaining the spectrum for a given solvation number n without contributions from clusters of different sizes.[32,34] This is due to the lack of an unambiguous technique for mass selection, which is not a problem for charged clusters. The spectroscopic study of hydrated hydronium ion can answer many of the same questions about hydrogen bonding as similar studies of neutral clusters and further sheds light on the topics of proton transfer and the solvation of ions in solution.

From the discussion above it is obvious that there is a wealth of information concerning the hydronium ion in a condensed phase environment. Gas phase investigations of ionic clusters containing the hydronium ion have primarily been limited to thermodynamic measurements of the entropy, enthalpy and energies for the reactions:

$$H_3O^+(H_2O)_{m-1} + H_2O + N \rightleftharpoons H_3O^+(H_2O)_m + N$$

Where N is a third body used to stablize the cluster during the reaction. (The reader is refered to table I of Chapter one, and the references therein for more information.) Spectroscopic studies of the hydrated hydronium ions ($H_3O^+(H_2O)_m$) have been limited however, to the pioneering direct absorption measurements of Schwarz for m=0 to 4, made in 1977,[35] and the more recent results from this laboratory employing both the two-color consequence technique described in the first chapter for m=1 to 3, and a messsenger technique employing a weakly bound H_2 molecule.[36] These

results served to show that the structure of the smallest cluster, $H_3O^+(H_2O)$, is symmetric with respect to the position of the central proton, and that the first solvation shell of the hydronium ion is filled by m=3. The present work extends these earlier measurements, and probes the spectroscopy of the larger species ($m \geq 3$).

2.2 EXPERIMENTAL DETAILS:

The experimental conditions used in the acquisition of the spectra presented in the following section are essentially the same as those listed in the first chapter. The hydrated hydronium ions were produced by the corona discharge source. Typical operating conditions involved 60 to 190 microamps of discharge current in 150 to 200 torr of Matheson UHP neon or hydrogen. The source body temperature was maintained at either liquid nitrogen, or freon temperatures, depending upon the peak of the cluster ion distribution desired for the study. The source of water for these experiments came from a trap of Linde molecular sieve material that that the gas passed over prior to entering the source region. The seive material was allowed to reach equilibrium with the ambient water in the air of the laboratory prior to being placed in the inlet line and subesquently evacuated. If the trap was not baked after being pumped upon, sufficient water could be introduced into the system such that the only ions observed from the source were the large mass hydrated hydronium ion series ($m>6$). Cooling the trap to liquid nitrogen or dry ice-acetone bath temperatures could effectively remove most of the water. Under these conditions, for the same backing pressure and discharge current, the smaller cluster ions were favored ($m<3$).

2.3 RESULTS AND ANALYSIS:

The early studies of the hydrated hydronium ions performed in this laboratory have been extended to the larger cluster ions where m is greater than 3 and the second solvation shell is formed.[37] Figure 1 contains the spectra of the hydrated hydronium ions for m=3-8 in the 2600-4000 cm^{-1} region (with the exception of m=7 and 8 where only the region 3200-4000 cm^{-1} was obtained). A list of observed transition maxima and assignments of the spectral features for the m=3 to 8 species is given in Table II. A comparison is made with previous experimental measurements when possible. Table I contains the spectroscopic constants for the hydronium ion and water. Where available empirical data have been used, otherwise, the most recent high level theoretical calculation for the constant is given. Figure 2 shows the prefered schematic structures for the m=3 to 6 ions derived from the assignments.

It is instructive to compare some of the general features of these data, and the data for the ammoniated ammonium ions discussed in the following chapter. The spectra of $H_3O^+(H_2O)_m$ are similar to those of $NH_4^+(NH_3)_n$ in several respects, including a) the presence of band series decreasing in $\Delta\nu/\Delta n$ as n increases, b) a clear separation between those bands associated with non-bonded oscillators, 1° or 2° ligand bonded oscillators, and hydrogen bonded oscillators of the ion core, and c) agreement with the rough empirical correlation of width and frequency of

the bands with the strength of the hydrogen bond.[38]

Previously, theorists and experimentalists collaborated heavily to determine that $H_5O_2^+$ (n=1) has a single minimum potential with respect to the proton involved in the hydrogen bond.[39] The minimum energy position was found to be midway between the oxygen atoms. The Schaefer group has calculated geometries, vibrational frequencies and intensities for $H_3O^+(H_2O)_m$ ($m \leq 3$) using full configuration-interaction with single and double excitations in the simulation.[40] These are the highest level ab initio calculations yet performed for ionic clusters.

For larger systems, due to the expense of the Schaefer-type calculations, other methods have been used such as Monte Carlo (MC) and Molecular Dynamics (MD) simulations. These methods assume that the summation of pairwise interaction potentials between molecular groups will give an accurate description of the potential energy surface. The MC method has given predictions concerning the structure and thermodynamic properties of solvated ions in solution and in the gas phase.[41,42,43] For example, Kochanski has predicted that the presence of four water molecules in the first solvent shell has a significant probability in the $H_3O^+(H_2O)_m$ species if m is considerably larger than 4, and that successive shells will tend to begin filling before the previous one is full.[63] When the pairwise potentials are well known, the results tend to be reliable. Recent MD simulations have been conducted on ion-water systems.[44,45]

The m=3 spectrum (figure 1a) is the only one in this set of data for which vibrational frequencies have been calculated at a high level of theory. The vibrational transition of the H_3O^+ core with the largest predicted intensity is the antisymmetric stretch of the three O-H oscillators. The ab initio frequency for this mode was 2997 cm^{-1} for a C_{3v} structure, with the symmetric stretch 23 cm^{-1} higher and a factor of 40 less intense.[46] The experimental spectra from Schwarz's previous direct absorption measurements and our own consequence technique show a rather broad band centered at 2670 cm^{-1} and a weaker one at 3050 cm^{-1}. Schwarz assigned the 2670 cm^{-1} feature to the core antisymmetric stretch. This feature and its analogous counterparts in the spectra of the larger clusters is designated by series A of figure 1. If this assignment is correct (the antisymmetric stretch band is expected to be the most intense feature of the spectrum below 3000 cm^{-1}, which this band is), it means that the theoretical calculation is wrong by more than 300 cm^{-1} for the frequency of this vibration, or more than 10%. The usual accuracy for small, polyatomic molecules is better than 2 or 3%. The poor accuracy for the cluster systems results from an inadequate treatment of the effect of hydrogen bonding. One obvious difficulty is that the most sophisticated calculations still do not consider the influence of anharmonicity directly, and instead apply a semi-empirical scaling factor to a calculated harmonic frequency. The scaling factor is often taken to be the same for all modes.

The symmetric stretch of the m=3 core has been a source of some controversy, especially since Schwarz and Newton[47] identified it with the weak band at ≈ 3000 cm^{-1} but the recent ab initio calculation placed it only 23 cm^{-1} above the antisymmetric stretch.[68] We believe the 3050 cm^{-1} band to be the same feature Schwarz observed, but assign it to either a bending overtone, most probably of the solvent molecules, or a combination band which would likely involve the core antisymmetric stretch and a hydrogen bond stretching vibration (the harmonic frequency of the antisymmetric stretch involving $\nu_{O\text{-}H\text{-}O}$ in the m=3 C_{3v} structure is of the order of 300 cm^{-1})[68]. In figure 1b, the band of series A has a less intense companion about 70 cm^{-1} to the blue: this is probably the core symmetric stretch. For a structure of type similar to the ammoniated ammonium case but with 3 instead of 4 solvent molecules in the first and second shells, series A should consist of a single band for m=5 (it does), probably with significantly reduced intensity since stretches of the core will only carry high intensity for antisymmetric stretches of two or more equivalent oscillators. Indeed, the intensity is low, as it was for the analogous band of n=7 ammoniated ammonium.

Series B, which begins at m=4, and continues through m=8, can be identified quite readily with the stretch of O-H oscillators of 1° H_2O which are hydrogen bonded to 2° H_2O. The width of the m=4 peak seems a bit large compared to the rest of the series, and might arise from an

overlapping band on the low frequency side; m=5 also has a broad feature in this region. A comparison of m=5 with m=4 and 6, however, after mentally removing the presence of series B, suggests that the m=5 spectrum might be anomalous. It has broad absorption in the 3150 - 3450 cm^{-1} region which appears similar to the m=4 spectrum if the series A band of m=4 is included, but bears little resemblance to the m=6 case with or without the series A band. One possible explanation is the presence of a second isomer of m=5.

According to Newton, a structure for the m=5 ion involving an $H_5O_2^+$ ion core should exist.[48] Designated $H_5O_2^+(H_2O)_4$, this species should have a global minimum energy only 2.5 kcal/mole above that of the $H_3O^+(H_2O)_5$ structure. Newton proposed this structure to be an important intermediate in the proton transfer mechanism in aqueous acid solution, with the symmetry of the $H_5O_2^+(H_2O)_4$ complex being essential to the mechanism. The expected stretching frequencies of the four equivalent O-H oscillators in the $H_5O_2^+$ core are, of course, unknown, but should certainly fall somewhere between 3000 and 3400 cm^{-1} and carry a large intensity. The low relative intensity of the series B band in the m=5 spectrum, compared to the trend of m=4-8, may offer some small support for the $H_5O_2^+(H_2O)_4$ hypothesis. If the hypothesis is correct, a very intense, very broad band should exist somewhere in the 500-2000 cm^{-1} region, arising from the vibration of the central $H_5O_2^+$ proton.

Series C and E arise, respectively, from the symmetric and antisymmetric stretching modes of the ligands which have none of their O-H bonds involved in a hydrogen bond. As solvent molecules with all O-H oscillators free, the O-H stretching frequencies are shifted very little from their isolated gas phase values. In n=5, for example, the shifts are ≈ 4 and ≈ 15 cm^{-1} to the red for symmetric and antisymmetric stretch, respectively (see table I). Because of the small shifts, contributions from ligands in more than one shell tend to overlap. The decreasing relative intensity from m=3-8 suggests, however, that the absorption cross section decreases in the order 1°>2°>3° for these oscillator types.

The assignment of a given spectral feature is made primarily on the basis of the lowest solvation number for which it is present, the frequency at which it appears, and the change in relative intensity with solvation number. Series D begins as the second solvation shell begins to form with the m=4 cluster and increases in relative intensity as a function of cluster size to dominate the spectrum by m=6. This feature has been assigned to the free O-H stretch of an H_2O that has one of its O-H oscillators involved in a hydrogen bond with another solvent molecule. Since molecular species tend to carry a transition dipole moment which increases with partial charge, a general trend with respect to absorption cross section of core>1° is expected when similar oscillators are compared. Theoretical calculations show that the partial charge decreases in the order core>1°>2° so we would

expect that most of the intensity associated with this peak is due to transitions involving the H_2O's in the 1° shell bound by 2° H_2O's.

A similar series begins very weakly at m=6 and is very apparent at m=7, where the third solvation shell is expected to begin filling. This feature is attributed to the free O-H stretch of species involved in hydrogen bonding to <u>both</u> 2° and 3° H_2O's. It is labeled F in the figure. If this assignment is correct it confirms the Monte Carlo prediction mentioned above, that the higher solvation shells may begin to fill before the lower shells have been completely occupied.

While the vibrational predissociation spectra of $NH_4^+(NH_3)_n$ become somewhat indifferent to an increase in n above n=7, the spectra of $H_3O^+(H_2O)_m$ evolve considerably from m=6 to 7 and 7 to 8, in spite of the fact that each shell is thought to contain only three ligands instead of four. This can be attributed to at least two factors: 1) the larger intrinsic hydrogen bonding interaction of H_2O as compared to NH_3, and 2) a larger absorption cross section for H_2O than for NH_3 in the secondary and tertiary solvation shells. Even the spectrum of the gas phase cluster $(H_2O)_{17}$ is known to have a sharp feature at about 3710 cm^{-1},[49] corresponding to the non-bonded O-H stretch of H_2O ligands where the other O-H is part of the hydrogen bonded network. The $(H_2O)_{17}$ spectrum is more reminiscent of liquid water in the 3100-3600 cm^{-1} region, however, which consists of a very broad, featureless absorption. It is not really difficult to imagine that the

spectrum even of $H_3O^+(H_2O)_{17}$ is similar in this region.

The spectrum by m=8 has several broad peaks, arising from various hydrogen bonded O-H oscillator stretching vibrations. These could include 1° O-H to 2° H_2O, 1° O-H to 2° H_2O to 3° H_2O, and 2° O-H to 3° H_2O. Bending overtones may appear in the 3100-3300 cm^{-1} region as well. As the cluster size grows, the number of possible types of hydrogen bonds increases further, with a resultant filling effect in the 3100-3500 cm^{-1} spectral region. Further, the ratio of hydrogen bonded to free O-H oscillators is certain to rise, with a resultant decrease in the relative intensity contribution of free O-H oscillators in the 3600-3800 cm^{-1} region. The difference between spectra of hydrated hydronium and neutral water clusters should become small when the size of the clusters is very large (hundreds or thousands of H_2O subunits). For the intermediate case, vibrations of the ion core and the inner shell(s) account for most of the difference.

TABLE I: Molecular Constants for H_3O^+ and H_2O.
(All units are in cm^{-1} except ζ which is dimensionless. Rotational constants are for the ground vibrational state.)

Molecule or Ion:	Symmetry	Molecular Constants:	Reference
H_3O^+	C_{3v}	ν_1: 3570	a
		ν_2: 954.40 ($1^- \leftarrow 0$)	b
		ν_2: 525.83 ($1^+ \leftarrow 0$)	b
		ν_3: 3530.17, 3513.84	c
		ν_4: 1564	a
		$A_o=B_o$: 11.2540 (0^+)	b
		C_o: 6.1	c
H_2O	C_{2v}	ν_1: 3656.7	d
		ν_2: 1594.6	d
		ν_3: 3755.8	d
		A: 27.877	e
		B: 14.512	e
		C: 9.285	e

[a] P.R. Bunker, W.P. Kraemer and V. Špirko, J.Molec. Spec. **101**, 180 (1983). -- Scaled ab initio value.

[b] D-J. Liu, T. Oka, and T.J. Sears, J. Chem. Phys. **84**, 1312 (1986); and references therein.

[c] M.H. Begemann, G.S Gudeman, J. Pfaff, and R.J. Saykally, Phys. Rev. Lett. Vol. 51, 554 (1983); M.H. Begemann and R.J. Saykally: J. Chem. Phys. **82**, 3570 (1985).

[d] W.S. Benedict, N. Gailar, and E.K. Plyler, J. Chem. Phys. **24**, 1139 (1956).

[e] G. Herzberg, Electronic spectra of Polyatomic Molecules (Van Nostrand, Princeton, N.J., 1967).

TABLE II. Vibrational frequencies for the hydrated hydronium ions. Experimental frequencies from this work were found using the IRMPD technique. Units are in cm^{-1}.

This Work	Previous Work[a]	Assignment
$H_3O^+(H_2O)_3$		
2670	2660(S)	H_3O^+ ν_3 asym stretch
3050	3000(S)	H_3O^+ bending overtone or combination band
3639 3647	3644.9(Y)	1° H_2O ν_1 sym stretch (^{1}1°O-H^f_s)
3732	3730.4(Y)	1° H_2O ν_3 asym stretch (^{1}1°O-H^f_a)
$H_3O^+(H_2O)_4$		
	2860(S)	H_3O^+ ν_3 asym stretch
		H_3O^+ ν_1 sym stretch
3213	3200(S)	1° H_2O H-bonded stretch (^{1}1°O-H^b)
3645 3650	3620(S)	1° H_2O ν_1 sym stretch (^{1}1°O-H^f_s)
3708	3710(S)	1° H_2O free O-H stretch bound by 2° H_2O (^{1}1°O-H^f)
3733		1° H_2O ν_3 asym stretch (^{1}1°O-H^f_a)
$H_3O^+(H_2O)_5$		
2990 3165		H_3O^+ ν_3 asym stretch
3311		1° H_2O H-bonded stretch (^{1}1°O-H^b)
3651		1° H_2O ν_1 sym stretch (^{1}1°O-H^f_s)
3711		1° H_2O free O-H stretch bound by 2° H_2O (^{1}1°O-H^f)
3738		1° H_2O ν_3 asym stretch (^{1}1°O-H^f_a)
$H_3O^+(H_2O)_6$		

3357		1° H_2O free O-H stretch bound by 2° H_2O (^{1}1°O-H^f)
3653		1° H_2O ν_1 sym stretch (^{1}1°O-H^f_s)
3678		1° H_2O free O-H stretch bound by 2° and 3° H_2O (^{1}1°O-H^f)
3713		1° H_2O free O-H stretch bound by 2° H_2O (^{1}1°O-H^f)
3741		1° H_2O ν_3 asym stretch (^{1}1°O-H^f_a)
$H_3O^+(H_2O)_7$		
3371		1° H_2O free O-H stretch bound by 2° H_2O (^{1}1°O-H^f)
3651		1° H_2O ν_1 sym stretch (^{1}1°O-H^f_s)
3681		1° H_2O free O-H stretch bound by 2° and 3° H_2O (^{1}1°O-H^f)
3716		1° H_2O free O-H stretch bound by 2° H_2O (^{1}1°O-H^f)
3741		1° H_2O ν_3 asym stretch (^{1}1°O-H^f_a)
$H_3O^+(H_2O)_8$		
3650		1° H_2O ν_1 sym stretch (^{1}1°O-H^f_s)
3683		1° H_2O free O-H stretch bound by 2° and 3° H_2O (^{1}1°O-H^f)
3716		1° H_2O free O-H stretch bound by 2° H_2O (^{1}1°O-H^f)
3738		1° H_2O ν_3 asym stretch (^{1}1°O-H^f_a)

[a] Previous measurements made by Schwarz (See ref. 35.) are denoted by (S). Previous measurements by Yeh et. al. (See ref. 36.) are denoted by (Y).

FIGURE CAPTIONS:

1. Vibrational predissociation spectra of $H_3O^+(H_2O)_m$ (m=3-8) in the 2600-4000 cm^{-1} region. Bands forming clear series are connected by dashed lines. Evidence is seen for the filling of solvation shells at m=3 and 6. See text for discussion.

2. Prefered structures for the $H_3O^+(H_2O)_m$ (m=3-8) complexes. For the m=6 species, there is evidence from the infrared spectrum that the third solvation shell may begin to fill before the second is complete.

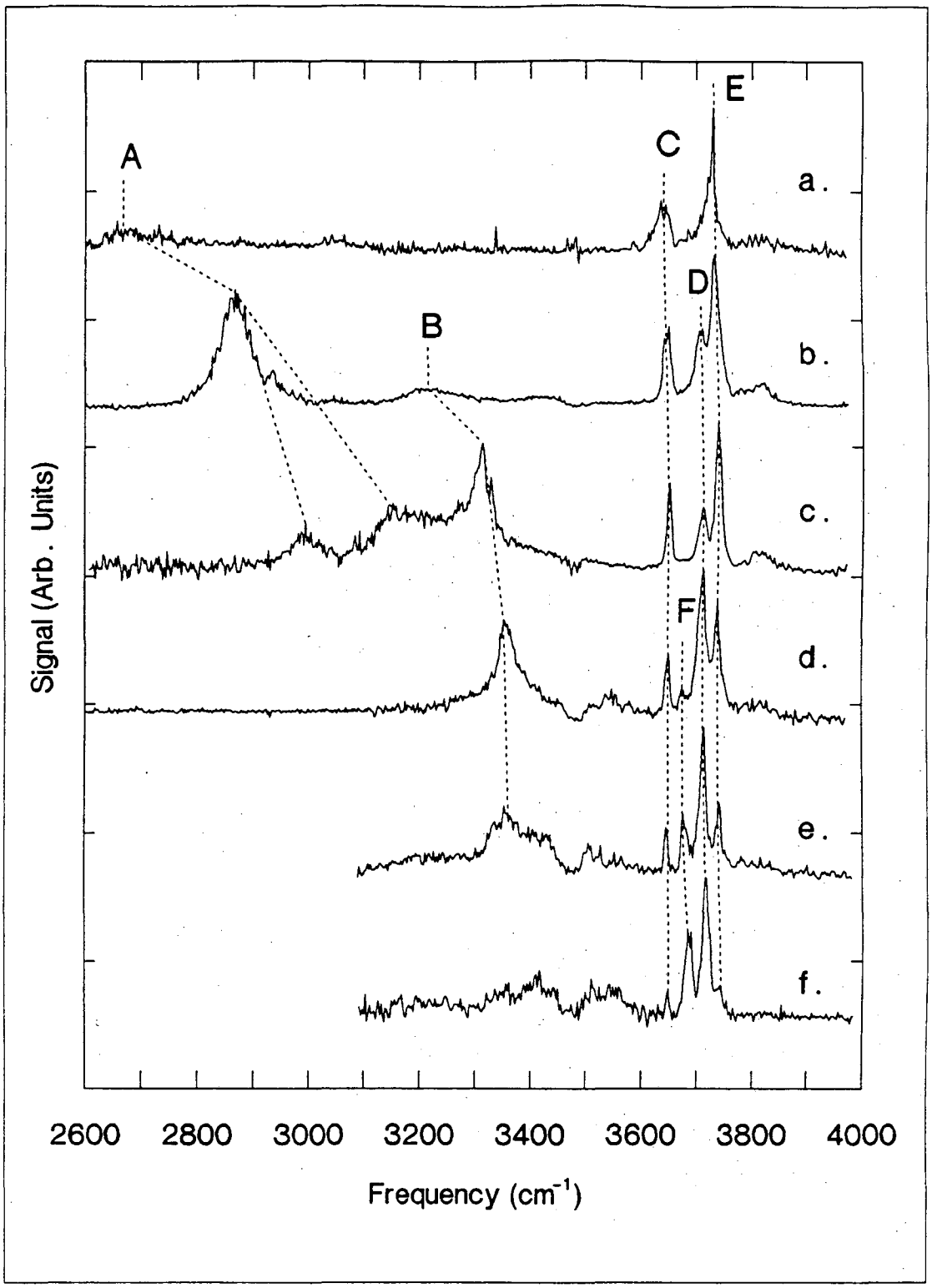
A
B
C
D
E
F
a.
b.
c.
d.
e.
f.
Signal (Arb. Units)
2600
2800
3000
3200
3400
3600
3800
4000
Frequency (cm-1)

Figure 1.

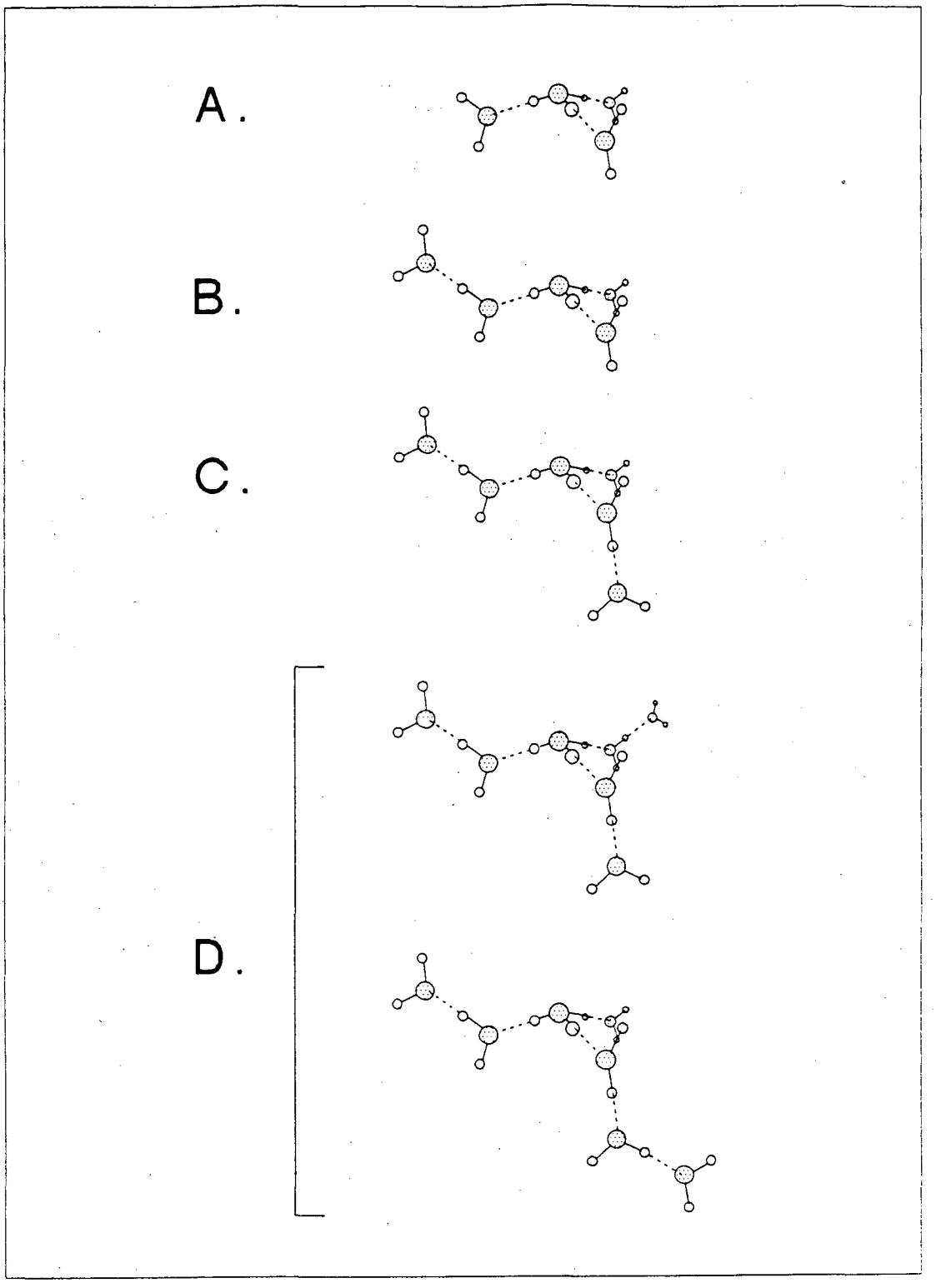

Figure 2.

REFERENCES:

1. Epicurus, "Letter to Pythocles", Trans. C. Bailey, in The Stoic and Epicurean Philosophers, Ed. W.J. Oates (New York: Random House, 1940).

2. J.V. Coe, and R.J. Saykally, " Infrared Laser Spectroscopy of Molecular Ions" in Ion and Cluster Ion Spectroscopy and Structure, ed. J.P. Maier (Elsevier, Amsterdam, 1989).

3. H. Heitmann, and F. Arnold, Nature **306**, 747 (1983).

4. R.S. Narcisi and A.D. Bailey, J. Geophys. Res. **70**, 3687 (1965).

5. E.E. Ferguson, F.C. Fehsenfeld, and D.L. Albritton, in Gas Phase Ion Chemistry, vol. 1, M.T. Bowers, ed. (Academic Press, New York, 1979).

6. Smith, D.S. and Adams, N.G., Top. Curr. Chem. **89**, 1 (1980); Keesee, R.G. and Castleman, A.W. Jr., J. Geophys. Res. **90**, 5885 (1985).

7. Castleman, A.W. Jr., Holland, P.M., and Keesee, R.G., J. Chem. Phys. **68**, 1760 (1978); Castleman, A.W. Jr., Adv. Colloid and Interface Science **10**, 73 (1979).

8. Heinis, T., Chowdhury, S., Scott, S.L., and Kebarle, P., J. Am. Chem. Soc. **110**, 400 (1988); Grese, R.P., Cerny, R.L., and Gross, M.L.,: **111**, 2835 (1989).

9. Y.K. Lau, S. Ikuta, and P. Kebarle, J. Am. Chem. Soc. **104**, 1462 (1982); A.J. Cunningham, J.D. Payzant, and P. Kebarle **94**, 7627 (1972); P. Kebarle, S.K. Searles, A. Zolla, J. Scarborough, and M. Arshadi, **89**, 6393 (1967).

10. M. Meot-Ner and F.H. Field, J. Am. Chem. Soc. **99**, 998 (1977).

11. J.C. Gary and P. Kebarle, J. Phys. Chem. **94**, 5184 (1990).

12. M. Meot-Ner, L.W. Sieck, J. Phys. Chem. **90**, 6687 (1986); L.W. Sieck, J. Phys. Chem. **89**, 5552 (1985).

13. I. Dzidic and P. Kebarle, J. Phys. Chem. **74**, 1466 (1970).

14. Alcami, M., Mo, O., Yanez, M., Anvia, F., and Taft, R.W.: J. Phys. Chem. 94, 4796 (1990).

15. "Calculated Vibrational Spectra of Hydrogen Bonded Systems" by P. Janoschek in The Hydrogen Bond, vol. I, ed. by P. Schuster, G. Zundel and C. Sandorfy (North-Holland, New York), 1976, p.183.

16. The Hydrogen Bond Vols. I, II, and III, ed., P. Schuster, G. Zundel and C. Sandorfy, (North-Holland Publishing, Amsterdam 1976).

17. S. Scheiner, Acc. Chem. Res. **18**, 174 (1985), and references therein.

18. R.A. Copeland, and S.I. Chan, Annu. Rev. Phys. Chem. **40**, 671 (1989); F.M. Koswer and D. Huppert, Annu. Rev. Phys. Chem. **37**, 127 (1986).

19. G.C. Pimentel M.O. Bulanin and M. Van Theil, J. Chem. Phys. **36**, 500 (1962).

20. Caldin, E.F., Gold, V., eds.: Proton Transfer Reactions (Chapman and Hall, London), 1975.

21. C.I. Ratcliffe and D.E. Irish, in Water Science Reviews 2, ed. by F. Franks (Cambridge University Press, Cambridge 1986).

22. J. Corset, P.V. Huong and J. Lascombe, Spectrochim. Acta A **24**, 2045 (1968).

23. D.D. Nelson, Jr., G.T. Fraser and W. Klemperer, J. Chem. Phys. **83**, 6201 (1985).

24. Water Science Reviews 3 , F. Franks, ed. (Cambridge University Press, Cambridge 1988).

25. T.R. Dyke and J.S. Muenter, J. Chem. Phys. **57**, 5011 (1972); Z.S. Hyang and R.E. Miller, J. Chem. Phys. **88**, 8008 (1988).

26. K.L. Busarow, R.C. Cohen, G.A. Blake, K.B. Laughlin, Y.T. Lee, and R.J. Saykally, J. Chem. Phys. **90**, 3937 (1989).

27. L.H. Coudert, and J.T. Hougen, J. Mol. Spectr. **130**, 86 (1988); L.H. Coudert, F.J. Lovas, R.D. Suenram and J.T. Hougen, J. Chem. Phys. **87**, 6290 (1987); J.T. Hougen, J. Mol. Spectr. **114**, 395 (1985).

28. S.E. Novick, K.R. Leopold, and W. Klemperer, The Structures of Weakly Bound Complexes as Elucidated by Microwave and Infrared Spectroscopy, ed. by E.R. Bernstein (Elsevier, New York, 1989).

29. R.E. Miller, J. Phys. Chem. **90**, 3301 (1986); Structure and Dynamics of Weakly Bound Molecular Clusters, ed. by A. Weber, NATO ASI Series (Reidel, Dordrecht, 1987); D.J. Nesbitt, Chem. Rev. **88**, 843 (1988); M.A. Duncan and D.H. Rouvray, Sci. Am. **261**, 110 (1989).

30. M.F. Vernon, Ph.D. Thesis, University of California, Berkeley, 1982.

31. M.F. Vernon, D.J. Krajnovigh, H.S. Kwok, L.M. Lisy, Y.R. Shen, and Y.T. Lee, J. Chem. Phys. **77**, 47 (1982).

32. R.H. Page, M.F. Vernon, Y.R. Shen and Y.T. Lee, Chem. Phys. Lett. Vol. 141, No. 1,2, 1 (1987).

33. D.F. Coker, R.E. Miller, and R.O. Watts, J. Chem. Phys. **82**, 3554 (1984).

34. Buck, U.; and Lauenstein, C.: J. Chem. Phys. 92, 4250 (1990).

35. H.A. Schwarz, J. Chem. Phys., **67**, 5525 (1977).

36. L. I-C. Yeh, M. Okumura, J.D. Myers, J.M. Price, and Y.T. Lee, J. Chem. Phys **91**, 7319 (1989).

37. M.W. Crofton, J.M. Price, and Y.T. Lee, "Infrared Spectroscopy of the Hydrated Hydronium Ions, $H_3O^+(H_2O)_m$ (m=3-8)", to be submitted to J. Chem. Phys. (1990).

38. G. Herzburg, Infrared and Raman Spectra of Polyatomic Molecules (Van Nostrand Reinhold Company, New York 1945).

39. L. I-C. Yeh, Ph.D. Thesis, University of California at Berkeley, (1988); L. I-C. Yeh, M. Okumura, J.D. Myers, J.M. Price, and Y.T. Lee, J. Chem. Phys., (1988).

40. R. Remmington and H.F. Scheafer III, unpublished results.

41. Jorgensen, W.L.,: J. Am. Chem. Soc. **103**, 341 (1981); Chandrasekhar, J. and Jorgensen, W.L.,: J. Chem. Phys. **77**, 5080 (1982).

42. E. Kochanski,: J. Am. Chem. Soc. **107**, 7869 (1985).

43. Malenkov, G.G.: "The Chemical Physics of Solvation," in Studies in Physical and Theoretical Chemistry, ed. by R.R. Dogonadze, E. Kalman, A.A. Kornyshev, and J. Ulstrup (Elsevier, New York, 1984).

44. DeRaedt, B., Sprik, M., and Klein, M.L.,: J. Chem. Phys. **80**, 5719 (1984); Impey, R.W., Sprik, M., and Klein, M.L.,: J. Am. Chem. Soc. **109**, 5900 (1987).

45. Mezei, M. and Beveridge, D.L.,: J. Chem. Phys. **74**, 6902 (1981); Rao, M. and Berne, B.J.,: J. Phys. Chem. **85**, 1498 (1981).

46. R. Remington and H.F. Schaefer III., unpublished results.

47. M.D. Newton, J. Chem. Phys., **67**, 5535 (1977).

48. M.D. Newton, S. Ehrenson, J. Am. Chem. Soc. **93**, 4971 (1971).

49. See refs. 32-35.

CHAPTER III.

The Ammoniated Ammonium Ion Clusters:

$NH_4^+(NH_3)_{1\text{-}10}$.

"First of all then, we must not suppose that any other object is to be gained from the knowledge of the phenomena of the sky, whether they are dealt with in connexion with other doctrines or independently, than peace of mind and a sure confidence, just as in all other branches of study... For we must not conduct scientific investigation by means of empty assumptions and arbitrary principles, but follow the lead of phenomena: for our life has not now any place for irrational belief and groundless imaginings... Now all goes on without disturbance... when one admits, as we are bound to do, probable theories about them [the phenomena]. But when one accepts one theory and rejects another, which harmonizes just as well with the phenomenon, it is obvious that he altogether leaves the path of scientific inquiry and has recourse to myth."

-Epicurus, "Letter to Pythocles",
c.a. 200 B.C.[1]

3.1 INTRODUCTION:

3.1.1 Previous Experimental Studies

Early spectroscopic studies of the ammonium ion were confined to the condensed phases and employed direct IR absorption measurements of either crystals of ammonium salts, or ammonium salts dissolved in solution.[2,3,4] These measurements revealed spectral features that were assigned to vibrational modes of the perturbed NH_4^+ ion (T_d symmetry). Of these, the strongest in the 2000-4000 cm^{-1} region were found to involve the triply degenerate antisymmetric stretching motion ν_3, and the first overtone of the doubly degenerate bending motion $2\nu_4$. (See fig. 1.)

Gas phase studies which followed centered for the most part on the thermodynamics and kinetics of clustering reactions at relatively high pressures (< 100 torr). Many investigators contributed in the effort to determine the ΔH° of the solvated ammonium ion $NH_4^+(NH_3)_n$.[5,6,7,8,9,10,11] Kebarle and coworkers showed that in the larger clusters there was a discontinuity in the ΔH° for the n=4 -> n=5 clustering step. This result was consistent with the idea that there were four solvent molecules involved in the first solvation shell of the cluster, with the solvent ammonias probably oriented along the N-H bonds of the ammonium ion due to ion-dipole interaction. A summary of these results appears in Table I, of Chapter I, which lists the ΔH° of formation for each clustering step in the $NH_4^+(NH_3)_n + NH_3 \rightarrow NH_4^+(NH_3)_{n+1}$ reaction series.

3.1.2 Previous Theoretical Studies

A fairly extensive body of theoretical work also exists, investigating the structure and thermodynamics of these systems. Pullman and Armbruster examined the thermodynamics of the stepwise addition of H_2O or NH_3 to NH_4^+ for one to five solvent molecules and managed to reproduce the qualitative features of the experimental data.[12] The experimental change in preferential addition from NH_3 at low levels of solvation to H_2O at higher levels of solvation was reproduced. Errors in the energies calculated from the STO 3G basis set were found to decrease with increasing number of solvent molecules.

A more recent series of calculations on the thermodynamics of the $NH_4^+(NH_3)_n$ (n=1-5) ions as well as their detailed structures has been made by Hirao et al.[13] In this work, ab initio molecular orbital calculations determined the structure and binding energies of the series in reasonable agreement with high pressure equilibrium measurements. Values for the solvation energies obtained from this work, using 3-21G, 3-21G*, and 6-31G** basis sets yielded consistently higher values than experimentally obtained.

Gas phase spectroscopic measurements for the ammonium ion and the ammoniated ammonium clusters have only recently been carried out. The development of velocity modulation spectroscopy has yielded a great deal of information for a wide range of molecular ions, including the NH_4^+

ion.[14] The ν_3 band of the ammonium ion has been investigated at high resolution by both Crofton and Oka[15] and Schafer and Saykally[16] using this technique. From this data an accurate equilibrium geometry has been obtained.[14] Table II lists the measured rotational constants, and equilibrium geometry parameters for this ion and the NH_3 molecule. The only measurements of the spectra of the ammoniated ammonium ions (n=1 to 4) have been limited to the direct absorption measurements performed by Schwarz in 1980 in a pulsed radiolysis of a gas cell containing ammonia in a helium carrier.[17]

Schwarz's measurements made use of the known equilibrium constants for the clustering reactions to deconvolute the absorption signal obtained at various pressures into those of individual ammoniated ammonium ions. These pioneering measurements, discussed later in the context of the results of the present study, suffered from limited spectral resolution (40 cm^{-1} full-width-half-maximum (FWHM)), relatively high vibrational and rotational temperatures (> 300K), and some ambiguity regarding the distribution of cluster sizes present in the sample. Nevertheless, it was possible for Schwarz to observe the vibrational bands ν_3 and $2\nu_4$ of the ammonium ion core for the n=4 cluster, and to show that the n=3 spectrum was consistent with C_{3v} symmetry. Schwarz was able to prove by isotope substitution that the structure of the n=4 ion cluster is tetrahedral. No transitions were observed that could unambiguously be

assigned to the solvent molecules surrounding the ammonium ion.

Recently, the infrared vibrational predissociation spectroscopy of the tetra-ammoniated ammonium ion $NH_4^+(NH_3)_4$ were studied in this laboratory using an arrangement of tandem mass spectrometers, a radio frequency ion trap and a tunable infrared laser.[18] In addition to purely vibrational transitions, spectral features were observed which are due to nearly free internal rotation of the ammonia subgroups in $NH_4^+(NH_3)_4$, the first observation of such a phenomenon in an ionic cluster. This work also served to verify Schwarz's spectrum determined by deconvolution of the time dependent infrared absorbance based on equilibrium and rate constants, and his assignment of the ν_3 and $2\nu_4$ bands in the spectrum. The comparison with our spectra further indicates that the spectra we derive from vibrational predissociation are similar to those obtained by direct absorption for this system. In the present work we give a full account of our systematic investigation of a series of infrared vibrational predissociation (IRVPD) spectra of the ammoniated ammonium ions and present the absorption spectra for $NH_4^+(NH_3)_n$ (n=1-10) over the frequency range of 2600 to 3500 cm^{-1}.

It will be shown that correlation of spectral features with cluster size can provide information about solvation shell structure, the geometry of the clusters, and the onset of a condensed phase environment around the ion core. With sufficient laser resolution, rotational information about the

cluster should also be obtainable.

3.2 EXPERIMENTAL DETAILS:

The experimental apparatus used in this work has been described in Chapter I and in other publications.[19,20,21,22] Briefly, the ammoniated ammonium cluster ions were produced from a high pressure corona discharge source and subsequent supersonic expansion. Schematic diagrams of the source and the experimental apparatus are shown in figs. 1 and 2 of Chapter I. The corona discharge was maintained in 100-200 torr of gas (Matheson ultra high purity (UHP) neon typically seeded with 10% UHP H_2 and about 1% NH_3) flowing past a 1.2 KV potential from the discharge tip of the needle to the source body maintained at approximately 350 V above ground. The discharge current under these conditions ranged from 40-200 μamps. The source could be cooled from outside the machine by contact with a liquefied gas reservoir and was usually maintained at approximately -30° C. After passing through the discharge region, the ionized gas undergoes collisionally induced vibrational relaxation in the 1.0 mm long by 3.0 mm diameter drift region before expanding through the 70 μm expansion nozzle. It is estimated that an ion undergoes some 10^5 collisions in this region before leaving the source, resulting in the ion relaxing to a vibrational temperature near that of the source body by the time it reaches the nozzle.

Most of the clustering of the neutral gas around the ionic species and rotational cooling takes place during the supersonic expansion between the

nozzle and the skimmer. Typical pressures in the source chamber are 4 x 10^{-5} to 2 x 10^{-4} torr while running the experiment. To prevent internal excitation and dissociation of the ionic clusters through collisions with the background gas in the expansion, the potential of the skimmer was maintained within 5 volts of that of the source body. A shielding grid surrounding the expansion region maintained at 350 V prevented stray fields from affecting the ion trajectories in this region.

After the skimmer, the ion beam enters a second differential pumping region containing collimating and focusing optics. The pressure in this second region is typically an order of magnitude lower than that of the source region. The beam is then directed into a third differentially pumped region maintained at 10^{-8} torr and through the entrance slits of a 60° sector magnet mass analyzer (Resolution = $M/\Delta M$ = 200). To aid in transmission of the ion beam and to enhance mass resolution, a set of quadrupole lens pairs is placed before and after the magnet.[23,24]

The mass selected beam passes into the final differentially pumped region maintained at 10^{-9} torr. Here, the beam is bent 90° in a DC quadrupole field, decellerated to less than 0.5 eV, and focused into a radio frequency (RF) octopole ion trap through an entrance aperture lens. Ions are typically allowed into the trap for 1 ms before the potential of the entrance lens is raised, and the ions confined inside the octopole.

The confined, mass selected clusters are then vibrationally excited by

a pulsed, tunable infrared laser. (Quanta Ray, IR WEX 8 ns pulse, 0.3 - 1.2 cm^{-1} resolution, 0.7cm^{-1} absolute frequency accuracy, 0.2 - 1.0 mj/pulse in the 2600-4000 cm^{-1} region) The density of ionic clusters in the ion trap is not high enough to allow the measurement of photon absorptions directly. In order to detect the absorption of an IR photon by an ionic cluster, IR multiphoton dissociation processes were used to exclusively dissociate the vibrationally excited ionic clusters. Depending on the density of states and the dissociation energy of the species under study, one of two excitation schemes described below was employed.

Because of the large binding energies of the n=1 and 2 ammoniated ammonium ions, absorption of sufficient energy from the tunable infrared (IR) laser to cause predissociation is not a facile process. In these cases, a line tunable CO_2 laser is used (MPB Technologies Inc. 8 W cw on R(24) of the $00^0 1$-$02^0 0$ transition) to drive the clusters excited by the tunable IR laser over the dissociation limit through the absorption of multiple CO_2 laser photons. This process hinges on the initial absorption of the tunable IR photon, as the density of states 1000 cm^{-1} above the v=0 level is so low that multi-photon dissociation of the ionic clusters by the cw CO_2 laser alone is very unlikely even with tens of milliseconds of irradiation time. In the studies of the n=1 cluster, no vibrational predissociation signal was observed if the pulsed laser was not present. Further discussion of this technique may be found elsewhere.[21]

For the larger clusters, n=3-10, the energy required to predissociate one solvent molecule is exceeded by absorbing two photons in the usual tuning range of 2.5-3.8 μm. At an energy in the 2600-4000 cm^{-1} region, all of the ionic clusters (n=1-10) are literally in the "quasi-continuum" region[25] (See fig. 3, Chapter I and discussion.) after the absorption of one photon and an additional IR photon from the tunable laser may be absorbed to induce vibrational predissociation. For n=1 and 2, however, fragments were not detectable with the tunable laser only, presumably because the fluence was not sufficient for the absorption of more than two photons. For these ions, use of the CO_2 laser with an irradiation time of at least 10 msec at >10 watts/cm^2 was required to achieve a measurable degree of dissociation of vibrationally excited clusters. In those instances where spectra of a given ion were obtained by both one and two color schemes, they were found to be the same within experimental error, indicating that spectral features in the multiphoton dissociation spectra normally reflect the cross section for absorption of the first photon rather well.[21]

If the clusters absorb sufficient energy through one of the schemes described above, the loss of one or more solvent molecules from the parent cluster may occur. The potential on the exit aperture is lowered 1 msec after the laser pulse, extracting cluster ions of all masses from the trap. These ions are filtered by a second mass analyzer, a quadrupole mass spectrometer tuned to pass only the daughter ions smaller than the parent

cluster by one solvent molecule.

Daughter ions are counted using a Daly ion detector[26] for each laser shot. Background daughter ion counts resulting from the decay of metastable parent ions in the RF ion trap are monitored in a separate data cycle with the laser off at each wavelength, and subtracted from the laser on signal. Typical background count rates usually amount to no more than 1% of the signal at the stronger absorption maxima. The spontaneous decay of metastable parent ions to daughter ions in the trap was as high as 5 % for the largest ions and as low as 10^{-2} % for $NH_4^+(NH_3)$.

Laser power is monitored at each data point and spectra are normalized for the tunable infrared power using a simple linear power dependence. For a typical experiment, signals were averaged for about 400 laser shots at each wavelength in the 2600 to 3200 cm^{-1} region and longer, about 1000 laser shots at each wavelength, in the 3200 to 4000 cm^{-1} region where signals were typically much weaker. This extra averaging is reflected in the better signal to noise ratios in the higher frequency region for some of the traces shown in fig. 7. Relative intesities between the two frequency regions should be correct.

3.3 RESULTS AND ANALYSIS:

3.3.1 Mass Spectra

The distribution of ionic clusters produced by the corona discharge source could be shifted by altering the temperature of the source body, the backing pressure of the supersonic expansion, or the percentage of NH_3 in the H_2 carrier gas. Little dependence was observed between the peak of the cluster ion distribution and the magnitude of the current used in the discharge for a given value of the above parameters, indicating that the ions were at a reasonable equilibrium with the temperature of the source body before expansion through the nozzle.

The distribution of cluster sizes produced by the source could be easily monitored by sweeping the field of the 60 degree sector magnet and counting the ions that arrive at the Daly detector with the second mass filter set to transmit all ions. Two such mass spectra are shown in fig. 2. Spectrum 2a. was taken using a low concentration of ammonia in the H_2 carrier gas (<1%) , a backing pressure of 200 torr behind the nozzle and with the source body cooled to -30°C through contact with liquid freon 12. For these conditions the distribution shows a peak at the n=4 cluster. By cooling the source with liquid freon 22 (-40°C) instead of freon 12, and using a higher pressure behind the nozzle larger cluster ions could be favored as shown in 2c. Figure 2b. shows an intermediate condition. In this manner it was possible to produce in relatively high numbers the range

of ionic cluster sizes desired for this study.

3.3.2 Infrared Vibrational Predissociation Spectra:

In analyzing the infrared spectra of the ammoniated ammonium ion series, it is helpful to examine the general trends observed in the spectra before delving into a detailed investigation of individual cases. As implied by the notational scheme presented in the first chapter, the approach has been to treat the various subunits in the cluster as essentially isolated molecules (NH_3 or NH_4^+) perturbed by their particular environment. This approach is helpful from the standpoint of visualizing the types of vibrations involved in a given transition, and frees us from thinking of these large systems in terms of a normal-mode type of picture when the weak coupling between the subunits makes such an analysis difficult for all but the smallest clusters (e.g. n=1 and 2).

The spectra of the ammoniated ammonium ion series show a number of common features. Both absorptions due to the ammonium core stretches and those due to the ammonia solvent molecules can be assigned in every case. Features of the NH_4^+ core assigned to vibrations involved in hydrogen bonds with the solvent NH_3's are strongly red-shifted from the gas phase values obtained from velocity modulation spectroscopy[13-15] due to the strong interactions of the N-H bonds of the ion with the solvent molecules. Vibrational transitions involving the NH_3 molecules in the first solvation shell (1°) of the complex are significantly less perturbed from their gas

phase values, however because the N-H bonds of the ammonias are not themselves involved in the hydrogen bond. This situation is changed for an N-H bond of the 1° ammonia which is involved in a hydrogen bond with a second solvation shell (2°) ammonia. A larger red-shift will take place for that N-H bond of the 1° ammonia involved in the hydrogen bond than for the free 1° N-H's, although not as large as that for the ion.

The spectral features due to the ion core in particular and to a lesser extent the solvent molecules show some systematic trends with increasing cluster size. The ion core frequencies associated with extensive hydrogen bonding show a gradual blue shift. The amount of this shift is not constant with increasing solvation however, and in the extreme case of the largest clusters (n=9-10), the spectra change very little between the addition of one solvent molecule and the next, indicating that the core of the system is perhaps converging towards a liquid-like state.

The most striking feature of the spectra between 2600 and 3500 cm^{-1} for n=1-6 is a band originating at roughly 3400 cm^{-1} composed of a number of resolved subbands having a separation between adjacent components of about 12 cm^{-1}. This spacing is about twice the rotational constant for NH_3 about its C_3 symmetry axis and arises from the nearly free internal rotation of the 1° solvent molecules within the cluster. Observed previously in the $NH_4^+(NH_3)_4$ spectrum, and assigned to a perpendicular band corresponding to the ν_3 mode of free NH_3 (See fig. 3.), these transistions indicate that some

of the solvent molecules in the first solvation shell are relatively unhindered even when the second solvation shell has begun to fill.

The assignments of the internal rotation subbands were given for $NH_4^+(NH_3)_4$ and are analogous for the corresponding bands of the other cluster ions. We use the notation for a strongly prolate symmetric top rotor in the table of assignments (See Table II.) and in the text to describe the subbands. When the $^RQ_3$ and $^PQ_3$ transistions are observable, their intensities are consistent with the expected spin weight for transistions in NH_3 originating from the K=3 levels (here K is the quantum number for angular momentum about the NH_3 C_3 axis). The only vibrational transitions for which the internal rotor state of NH_3 will change are those involving modes of NH_3 with the $\Delta K=\pm 1$. (The use of K and the notation $^{R,P}Q_K$ as stated previously[27] is not strictly correct. It is used in this case for convenience, as it follows easily from the picture of NH_3 attached to a "wall", along its C_3 axis. In the standard treatment presented here for the internal rotation observed in $NH_4^+(NH_3)$, both K and K_i, the internal rotation quantum number must be used, and the symmetry and interaction of the rest of the molecule, must be included. There is no well developed theory for the treatment of the larger clusters.) No vibration of the ammonium core species carries this selection rule for angular momentum about one of the NH_3 C_3 axes; only a perpendicular vibration of the NH_3 subunit satisfies the condition. This includes the ν_3 type fundamental, but not the ν_1 (See

fig. 3.). It also inclueds the ν_4 type fundamental of NH_3 (The frequency is however, too low for the present work to observe.) and perpendicular components of overtone and combination bands. The overtone $2\nu_4$ could therefore have shown the characteristic 12 cm^{-1} spacing, but did not. The most intense component fo $2\nu_4$ is probably a parallel band. A detailed treatment of the internal rotation of the simpler n=1 cluster ion is given along more standard lines.

For n≥4, fundamental bands in the 3150-3500 cm^{-1} region derive entirely from perturbed ammonia subunits. In the region 2600-3150 cm^{-1}, only vibrations associated with the NH_4^+ core appear. NH_4^+ is strongly hydrogen bonded via its hydrogen atoms, resulting in a large redshift of the N-H stretching frequencies. The N-H vibrational frequencies in NH_3 shift relatively little when binding to the NH_4^+ core since the nitrogen atom of ammonia binds, rather than hydrogen. The hydrogen bonding between first shell (1°; primary) and second shell (2°; secondary) NH_3 is relatively weak, therefore the frequency shift of the bonded N-H stretch of 1° NH_3 is also relatively small. The separation of NH_3 and NH_4^+ vibrational bands for n≥4 in the 2600-3500 cm^{-1} region is therefore easily understandable. This separation of core and solvent bands, taken together with the way in which several bond types form well behaved series as a function of n, simplified the asssignment process considerably.

The infrared absorption spectra for $NH_4^+(NH_3)_n$ (n=1 to 10) are

discussed in detail below. Observed transistion frequencies and assignments of the vibrational and rovibrational transitions observed appear in Table III. Where available, observations from previous work are included in the table. Representative spectra for the n=1 to 8 ionic cluster series appear in figs. 4 and 7.

3.3.2.1 $NH_4^+(NH_3)$

The smallest ionic cluster studied in this work is the ammonium ion solvated by a single ammonia. Bound with a ΔH° of formation of -27 kcal/mole, it is the most strongly bound of the ammoniated ammonium cluster ion series. Due to its small number of low frequency vibrational modes, the densisty of states[28] is expected to be rather low at 3500 cm^{-1}. Like the analogous hydrated hydronium ion, it is important to know the equilibrium position of the proton between the two heavier nitrogen atoms. The two possible structures for this simplest cluster appear in fig. 5. In the C_{3v} structure, the proton is localized around one of the ammonias suggesting that the appropriate formulaic description of this system would by $NH_4^+(NH_3)$ whereas in the D_{3h} structure (D_{3d} is probably a more stable conformation by perhaps 10 cm^{-1}), it is equally shared suggesting that $(H_3N)H^+(NH_3)$ is the appropriate representation.

Ab initio calculations for the structure of the analogous $H_3O^+(H_2O)$ cluster ion suggested a double or single minimum for the potential energy surface for the proton position depending on the level of the calcuation. the

most sophisticated calculation to date is the as yet unpublished work of the Schaefer group in which the energies of the C_2 and C_s structures were found to have energies differing by no more than a few kcal/mole.[29] At the highest level of theory, (full CISD -- configuration interaction including single and double excitations) the single minimum potential (symmetric $(H_2O)H^+(OH_2)$ where the proton is at the midpoint of the oxygen atoms) was favored. At low levels of theory, the symmetric structure is usually favored also, but this order does not always hold.[30,31,32,33] Spectroscopic investigations performed in this laboratory concluded that in this case the proton is centrally located,[34,35] i.e., associated with a single minimum potential. Much evidence for the existence of such a structure in the solid an liquid phases has been presented previously in the literature.[36] One of the most plausible proposals for the mechanism of proton transfer in aqueous acid solutions requires the exsitence of the symmetric structure at least as a transition state. Knowledge of the function which describes the potential energy for the proton as a function of its position and the O-O separation, is critical to understand and evaluate such a mechanism.

Theoretical calculations on $NH_4^+(NH_3)$ are significantly more primitive than those used for $H_3O^+(H_2O)$, but predict $NH_4^+(NH_3)$ to have an asymmetric C_{3v} structure.[37,38] The calculated energy difference, once again, is only a few kcal/mole. Given the margin for error in such a calculation and the fact that $NH_4^+(NH_3)$ and $H_3O^+(H_2O)$ are isoelectronic and

obviously very similar molecules, such a conclusion cannot be accepted without verification. Both species have been theoretically studied extensively by Scheiner to determine the potential ennergy with respect to the proton position and the N-N and O-O separation[39]. His results show that the potential and its form depend much more strongly on the N-N or O-O separation than on the proton position, with respect to which the potential energy is extremely flat.

Assuming a symmetric structure (D_{3h}, see fig. 5b.) for this ion, the most intense absorption involving a high frequency N-H stretching motion would probably be the antisymmetric stretch of the NH_3 subunits. This motion, analogous to the ν_9, ν_{13} modes in 2-butyne (dimethylacetylene) would give rise to a degenerate perpendicular transition of E_{1d}, E_{2d} symmetry. From the standpoint of one of the ammonias, this motion is analogous to the doubly degenerate antisymmetric stretch, ν_3, of free ammonia, which occurs at 3444 cm^{-1} in the gas phase[40] (See fig. 3). The asymmetric structure for the dimer, in contrast, (C_{3v}, see fig. 5a.) would have at least two types of antisymmetric stretching vibrations, one associated with the H-bonded NH_4^+ ion and one associated with the NH_3 molecule.

Schwarz detected a weak absorption as a shoulder at 3420 cm^{-1} that he assigned to this cluster. Any band arising from a stretching motion involving the hydrogen bonded proton evidently occurs below 2000 cm^{-1}, and

was not observed. The transition we observed for this system appears in fig. 6a, and is centered at 3398.4 cm^{-1}, in reasonable agreement with the weak feature in Schwarz's spectrum at 3420 cm^{-1}. Schwarz assigned this to be ν_1 of the NH_3 subunit.

At the higher resolution available to this study, we found this band to be composed of a series of sub-bands spaced by 10.6 ± 0.3 cm^{-1}. For a prolate symmetric top molecule with the rotational constants A>>B=C, a strong Q-branch progression of this kind superimposed on vibrational transitions is commonly observed.[41] Spectra for molecules of this type, such as CH_3Br, have a characteristic separation between the Q-branch maxima of approximately 2(A-B).[42]

For the structure observed in the $N_2H_7^+$ spectrum to be due to a simple rotation of the dimer however, the spacing of the subbands should be ≈ 5.6 cm^{-1}, based on the ab initio equilibrium geometry.[12] The fact that the actual spacing is roughly twice as large and that similar structure is also observed in the much larger n=4 cluster (A=B=C ≈ 0.1 cm^{-1}) suggests that these bands are due to an internal rotation of the NH_3 subgroups about their local C_3 axes, similar to that observed in $NH_4^+(NH_3)_4$.[17]

3.3.2.1.1 Internal Rotation in $NH_4^+(NH_3)$:

Internal rotation of molecules containing C_3 subgroups has been given extensive theoretical treatment.[43] Theories developed by Longuet-Higgins and Bunker[44] and Papousek[45,46] have been used to explain the structure

in the antisymmetric stretching band, ν_9, ν_{13}, in 2-butyne attributed to internal rotation of the methyl subgroups. In these theories, the rotational motion of the methyls through the three-fold potential barrier is analyzed, taking into account the torsional barrier height, the degree of vibration-vibration coupling in the system, and the difference between upper and lower state rotational constants of the molecule. Using this approach, the ν_9, ν_{13} band is reproduced to nearly the limit of experimental resolution. For 2-butyne, it was found that the barrier to internal rotation was small, less than 10 cm^{-1}.[41-47] Microwave spectra later demonstrated that the barrier to internal rotation was 5.6 cm^{-1}.[48]

Exploiting the similarity between 2-butyne and the symmetric form of the $N_2H_7^+$ cluster ion, we have used the same formalism outlined by Papousek to simulate the antisymmetric stretching band, ν_3. For an ethane-like molecule, Papousek derived the expression for the fundamental band of a perpendicular transition involving E_{1d} and E_{2d} species. Frequencies for the fine structure transitions involved in the rotational Q branches of a transition from the ground vibrational state are given by the following:

$$\nu + \Theta + [\, A'(1-2\xi_r^z) - B' \,] \pm 2[\, A'(1-\xi_r^z) - B' \,]K \pm E(K_\rho). \qquad (1)$$

Where:

$$\Theta = [(A'-A'') + (B''-B')]K^2 + (A'-A'')K_i^2 + (B_i'-B'')J(J+1). \quad (2)$$

and

$$E(K_i) = 2A'(1-\xi_r^z)K_i + \frac{\Delta_\nu^2}{[16A'K_i(\xi_r^z-1)]}. \quad (3)$$

In these expressions, the vibrational band origin is denoted by ν. A and B are the rotational constants of the molecule, and the single and double primes denote the excited and ground state constants, respectively. K and J are the usual rotational quantum numbers of the molecule. K_i is the torsional quantum number for internal rotation and B_i is the rotational constant of one of the rotating subgroups around its local C_3 axis. ζ_r^z and Δν are the Coriolis coupling term and the vibration-vibration coupling term, respectively. Terms with the upper sign hold for ΔK = +1, the lower for ΔK = -1. For transitions from single-valued states, the quantum numbers K and K_i have the same parity, for transitions from the double-valued states, the opposite parity.

Selection rules for the perpendicular transition to the E_{1d} state should follow the selection rules: ΔJ = 0, ±1 , Δk = ±1 (K= |k|) and $\Delta k_i = 0$ (K_i = $|k_i|$). More details may be found in Papousek (See refs. 41 and 42.).

In fig. 6a, a simulated spectrum calculated using the above expressions for K = 0 to ± 1, K_i = -9 to +9, and J = K to K+9 is shown. The

relative intensities of the lines in the spectrum are calculated from the Boltzmann factors, statistical weights of nuclear spin states and orientation factors of the ground vibrational state. A Lorenzian convolution of the line spectrum so generated is employed with a FWHM of 1.0 cm^{-1} to simulate the resolution of the machine function.

For this simulation the only parameters that were systematically varied were the vibrational band origin of the transition, ν, the rotational temperature of the molecule and the vibration-vibration coupling constant Δν. Values for the A' and B' rotational constants were selected assuming a symmetric structure. The excited state vibrational constant A" was set at 3.16 cm^{-1} and B" was set equal to B'. The Coriolis coupling constant and the torsional barrier height were both neglected. Values for the constants used appear in the figure caption.

One can see that in spite of the fact that the calculated spectrum does not include R and P branch structure, there is reasonable agreement with the experimental results in fig. 8b for the major features. Unfortuately, the shoulders present to the blue of the Q-branch maxima are not reproduced. For the $^{R}Q_{K}$ series in a symmetric top, the R branch can be somewhat more intense than the P branch. Thus the weak feature at 3402 cm^{-1} may be attributable to an R branch of $^{R}Q_{0}$, as it peaks in the correct position for the expected rotational temperature of ≈ 20 K and a rotational constant of 0.3 cm^{-1}.

There is certainly a possibility that these features might be due to hot bands. A more likely explanation would be that this anomalous structure involves a rotation of the entire NH_3-H^+-NH_3 ion about its C_3 axis rather than just one NH_3 subunit about its local axis. As stated earlier, this structure would have half the spacing of the internal rotation structure, and could lead to peaks located roughly half way between the internal rotation Q branches. Such issues can be resolved by more detailed studies at higher spectral resolution; these are presently underway.

The simulation seems successful in that the relatively large splitting in the $\Delta K=0$ and $\Delta K=-1$ subbands are reproduced, as is the smaller splitting in the $\Delta K=+1$ subband. This splitting arises in the simulation through the introduction of a small amount of vibration-vibration coupling into the energy expression through the Δv constant. The fact that the fit obtained for this spectrum did not require recourse to the formalism for a torsional barrier suggests, as in the case of 2-butyne, that the internal rotation is nearly free. That this should be the case is not entirely obvious from the standpoint of molecular geometries. In 2-butyne the distance between the hydrogens on different methyl substituents is about 4.9 Å. This distance is about 3.4 Å for the ab initio[12] structure $NH_4^+(NH_3)$ (about 0.2 Å less for the symmetric structure). The N-N distance in this ion is comparable to the N-C distance in the T-shaped van der Waals complex NH_3-CO_2, which also has a low barrier to internal rotation of less than 14 cal/mol.[49] From the

relatively successful modeling of the spectrum in the same way as dimethylacetylene (See fig. 6.) and the strong dependence of the appearance of the internal rotation bands on the torsional barrier height, we conclude that an upper limit to the torsional barrier height can be placed at about 10 cm^{-1}. In order to apply this theory to the larger clusters, it must be adapted for the particular geometry and the complete nuclear permutation inversion (CNPI) group.

The frequency of the central $^{R}Q_0$ band for n=1 as compared to n>1 (these will be compared later) and the absence of two bands of comparable intensity (one each for "NH_4^+" and "NH_3" groups) suggest that, contrary to the ab initio results, the equilibrium structure of $N_2H_7^+$ is the symmetric one. With this configuration, the cluster would best be described by the formula $H_3N{\cdot}H^+{\cdot}NH_3$ rather than $NH_4^+{\cdot}NH_3$. It should be possible to determine the structure conclusively when a H_2 messenger study is performed as in the case of $H_5O_2^+$ and/or the spectrum is recorded at sufficiently high resolution to determine the rotational constant B=C. The rotational constant will allow an estimation of the N-N separation, which in turn should indicate whether the proton is equally shared by the nitrogens.

For the $H_5O_2^+$ system studied previously by a "messenger" technique, the small perturbation by a H_2 molecule on the $H_5O_2^+$ cluster is thought to lead to the formation of an asymmetric structure involving species similar to H_3O^+ and H_2O.[50,51] Since the isolated $H_5O_2^+$ species is best thought of

as $H_2O{\cdot}H^+{\cdot}OH_2$ rather than $H_3O^+{\cdot}OH_2$, the presence of the weakly bound "messenger" led to a dramatically different spectrum, providing qualitative confirmation that the isolated $H_5O_2^+$ has a symmetric equilibrium structure. The definitive confirmation, of course, will probably come from a determination of the much lower vibrational frequencies involving the hydrogen bonded proton, as these are very sensitive to the structure.

3.3.2.2. $NH_4^+(NH_3)_2$:

The spectrum for the $NH_4^+(NH_3)_2$ cluster ion appears in fig. 4b. With a ΔH° of solvation of 17.5 kcal/mol for the n=1 -> n=2 clustering step[7], this cluster is too strongly bound for two photons of 3000 cm^{-1} light to easily predissociate a solvent molecule unless a significant amount of internal excitation is already present. As in the case of the n=1 cluster, the two-color excitation scheme was used to study this system.

Ab initio calculations for the structure of the n=2 cluster by Hirao et al.[12] predict that the cluster should have the C_{2v} symmetry assumed by Schwarz. Alignment of the solvent ammonias along two of the four available binding sites in the first solvation shell yields an ammonium ion whose stretching vibrations can be roughly divided into two categories: hydrogen bonded and non hydrogen bonded. In the bonded category we have a symmetric and an antisymmetric mode, each involving the solvated core N-H bonds and appearing at relatively low frequency. In the nonbonded category we have a symmetric and an antisymmetric mode, each

involving the unsolvated core N-H bonds and appearing at relatively high frequency. For the NH_3 solvent molecules, a symmetric stretch (ν_1) and a doubly degenerate antisymmetric stretch (ν_3) is expected; these involve the three free N-H bonds of the NH_3 subunit (See fig. 3.). For this study, we will consider the vibrational bands of equivalent subunits in the complex to be degenerate for all ammoniated ammonium complexes.

Schwarz observed two broad peaks that he assigned to transitions involving modes of the NH_4^+ ion. A broad feature was observed in the 2400-2600 cm^{-1} region which was tentatively assigned to the low frequency N-H stretches, and a relatively narrow unidentified peak was observed at 2280 cm^{-1}. This latter peak we suspect may actually be the symmetric stretch of the two bound N-H oscillators. A higher frequency feature at 3360 cm^{-1} was assigned to the two free N-H stretches.

In this work, the low frequency peak lies below the lowest frequency accessible to the present laser system, but a series of transitions in the 3400 cm^{-1} region are observed. Shown in fig. 6b, Schwarz's peak around 3360 cm^{-1} is resolved into two main bands. The first, which seems to be split into two maxima at 3392 and 3395 cm^{-1} is assigned to the antisymmetric N-H stretches of the two free N-H oscillators of the ammonium core. Under the notational scheme discussed in Chapter I, these bands would be designated $^2 0^o N\text{-}H^f_a$.

The symmetric stretch of these N-H bonds was not observed. This is

not particularly surprising as it has been observed previously that the symmetric stretch of complexed ammonia has a particularly low infrared transition dipole moment.[52]

A series of subbands is present slightly to the blue, with similar structure as the feature in the n=1 spectrum and has been assigned to the ν_3 band of the ammonia solvent molecules. Under our new notation we would designate this band as $^{3}1^{o}N\text{-}H^{f}_{a}$. With $^{R}Q_0$ at 3413.7 cm^{-1} and an average spacing between adjacent components of 12.6 ± 0.3 cm^{-1}, this structure is again due to internal rotation of the ammonia subgroups. For this cluster, where the perturbation of the NH_3 solvent molecules is less, the subband spacing agrees very well with the 12 cm^{-1} expected for free ammonia rotation about its C_3 axis. If the assignment of the ν_3 subbands is correct with respect to K, then this band falls nicely into the progression established by n=1 and n=3-7 (we will discuss this series in more detail later). However, this assignment appears to have some intensity anomalies; $^{P}Q_1$, for example, appears much more intense than $^{R}Q_1$. While this anomaly could possibly be due to an experimental artifact, one possible explanation is that the ν_3 state of the NH_3 subunits somehow interacts with the antisymmetric stretch of the free N-H oscillators of the core. Since the upper state of $^{P}Q_1$ is about 25 cm^{-1} closer to this state than that of the upper level of $^{R}Q_1$, $^{P}Q_1$ is in a position to borrow more intensity. However, it is not clear why these levels should interact, and there is no corresponding

frequency anomaly. A more attractive explanation is that the core antisymmetric stretching band is actually quite broad, 15-20 cm^{-1}, and therefore the intensity of ${}^{P}Q_1$ appears large because it resides on the shoulder of this band. We therefore take ${}^{R}Q_0$ at 3414 cm^{-1} as the most likely assignment.

3.3.2.3. $NH_4^+(NH_3)_3$:

The spectrum for the n=3 ammoniated ammonium ion appears in figs. 4c and 7a. The expected geometry should have roughly C_{3v} symmetry with the solvent molecules associating with three of the hydrogens on the central ammonium ion. Schwarz analyzed the vibrations for the NH_4^+ core under these conditions in terms of distorted T_d symmetry. Under this framework, six fundamentals are expected for the core, all infrared active. Of these, those that might be of a high enough frequency for the present laser system to excite are the stretching motions of the core; ν_1', characterized primarily by the symmetric stretch of the hydrogen bonded core N-H's, ν_3', the antisymmetric stretch involving the free N-H bond, and ν_3", the antisymmetric stretch involving the hydrogen bonded N-H's. Of these, ν_3' should appear at a higher frequency than either ν_1' or ν_3", which should have roughly the same frequency. One would also expect to observe transitions involving the solvent NH_3's.

In fig. 7a, two strong absorptions are observed at 2660 and 2692 cm^{-1}, in agreement with Schwarz's low resolution observation of a single strong

peak at 2682 cm^{-1}. Labeled with a 'B' in fig. 7a, these could be assigned to the fundamentals of the ν_1' and ν_3" vibration discussed above. An alternative and somewhat more plausible assignment is that these two peaks, which are of equal intensity, arise from lifting the degeneracy of the ν_3" doubly degenerate mode. The small peak at 2615 cm^{-1} is then taken to be ν_1'. Of course, a high quality ab initio calculation of the intensities may be able to indicate which assignment is correct.

It is interesting to note that our spectrum of n=3 shows a very broad background absorption in the 2600-3100 cm^{-1} region which is so nearly featureless it is almost a continuum at our level of spectral resolution. When the spectrum was taken with a decreased backing pressure behind the nozzle resulting in a rotationally warmer expansion, the peaks broadened by more than 30 cm^{-1} and the "continuum" became much more prominent relative to these peaks. A glance at Schwarz's n=3 spectrum indicates that the absorption is more intense in the 400 cm^{-1} region to the blue of the intense 2680 cm^{-1} peak than 400 cm^{-1} to the red, although in each case there is measurable absorption for the entire 400 cm^{-1} expanse. It will be seen later that the spectra of all the larger clusters show some absorption in the region above the ion core hydrogen bonded N-H stretches. We believe this to result from hot bands and combination bands involving these stretches and those of the hydrogen bonds themselves. The latter might be expected to have frequencies of 50-400 cm^{-1} for n=2-10, with the

largest frequencies associated with the smallest values of n.

The free N-H stretching vibration ν_3' appears at 3374 cm^{-1}, again near the 3365 cm^{-1} measured by Schwarz. Also observed is the antisymmetric stretch of the solvent NH_3's centered at 3416.8 cm^{-1} with the internal rotation structure observed previously (see fig. 4c for an expanded view of this region.). An inspection of the intensities of the Q-branches shows some enhancement in the K=±3 stacks, consistent with the spin statistics expected for an ammonia rotating about its C_3 axis.

3.3.3.4. $NH_4^+(NH_3)_4$:

Thermodynamic measurements and theoretical structural calculations indicate that the n=4 cluster ion represents the completion of the first solvation shell of the NH_4^+ ion. With four degenerate NH_3 solvent molecules, the cluster has the same T_d symmetry as the isolated ion core species[14,15] (see fig. 8a). Therefore, only two fundamentals of the core should be infrared active: ν_3, the triply degenerate antisymmetric stretch, and ν_4, the doubly degenerate bending mode.

In the survey spectrum reported previously[18] (See fig. 7b.), four main features are observed. The most prominent feature was assigned by Schwarz to the fundamental of the ν_3 vibration. The value from the present work of 2865 cm^{-1} agrees well with Schwarz's measurement of 2867 cm^{-1} for the position of this band. This band is connected to the analogous core vibration in the n=3 spectrum with a dashed line labeled 'B' in the figure.

Although the doubly degenerate ν_4 bending mode occurs at too low a frequency for either Schwarz or the present workers to measure (1400 cm^{-1} in matrices), Schwarz was able to observe the first overtone of the bending mode, $2\nu_4$, at 3087 cm^{-1}. This assignment was supported by an isotope substitution study in which a comparison of the Teller-Redlich product ratio[53] for the anti-symmetric stretch and the bending overtones in NH_4^+, ND_4^+ and CH_4, CD_4 was made. In the present work, the $2\nu_4$ band is observed at 3095 cm^{-1}. Other bands are evident in the survey spectrum that have been assigned to modes of the solvent NH_3's.

As in the previous spectra, the antisymmetric stretching vibration of the first solvent shell ammonias is observed, centered at 3419.5 cm^{-1} with the structure due to internal rotation (See fig. 4d.) . With an average separation of 12.3 cm^{-1} between adjacent components, this band can be well fit to a model in which a single ammonia molecule is rotating freely about its C_3 axis attached to a "wall". In fact, the appearance of all the ν_3 bands for n=3-6 is very similar, so that all of them could be reasonably fit at the present resolution by the same model. Using a simple symmetric top expression for the position of the Q-branches, and the Hönl-London expressions for the transition intensities, this band has been fit to a rotational temperature of 35 K with respect to the K quantum number. The strong-weak-weak-strong intensity alternation expected for a molecule with C_{3v} symmetry is easily observed here. Intensities of subbands originating

from K=0 and K=3 ($^{R}Q_0$, $^{P}Q_3$ and $^{R}Q_3$ in the figure) have about twice the intensity expected from the calculation just mentioned if nuclear spin statistics are not considered.

A second transition of the solvent molecules appears at approximately 3230 cm-1 and has been tentatively assigned to $2\nu_4$, the first overtone of the ν_4 bending mode. It is marked by a dashed line labeled 'D' in fig. 7b. There is a small possibility that the ν_1 symmetric stretching band overlaps with $2\nu_4$, but this is unlikely because it would require a much larger shift of the symmetric stretch in NH_3 upon complexation compared to that of the antisymmetric stretch, 100 cm^{-1} vs. 30 cm^{-1}. Since the complexation of NH_3 generally results in a reduction of ν_1 intensity relative to ν_3,[54] we believe that the ν_1 absorption is very weak and was consequently unobserved for n=4.

The disappearance of the 3374 cm^{-1} band in the n=3 spectrum which was assigned to the free N-H stretching motion of the core oscillator not bound by a solvent molecule, shows that the fourth solvent NH_3 indeed occupies the last first shell site on the NH_4^+ ion.

3.3.2.5. $NH_4^+(NH_3)_5$:

All of the thermodynamic and ab initio data are in agreement that the first solvent shell is filled at n=4. The ab initio calculation of Hirao et al.[12] predicts that the fifth NH_3 hydrogen bonds to one NH oscillator of a 1° NH_3. The spectrum of n=5 shows conclusively that this is correct. There is strong

support for this picture of the binding that leads to the weakening of one core NH oscillator and strengthening of the other three.

The NH_3 attached to the first solvation shell alters both spectral features associated with the NH_4^+ ion core of the cluster and the first solvation shell (1°) ammonia that this second solvation shell (2°) NH_3 is bound to. For the n=4 cluster, the ν_1 symmetric stretching vibration is not infrared active due to the T_d symmetry of the environment around the core and the core itself. By adding another NH_3 outside the first shell, this motion should become weakly IR active. Similarly, the triply degenerate antisymmetric stretch of the core, ν_3, will split into a doubly degenerate antisymmetric stretching component of higher frequency, ν_3', similar to that for the n=4 cluster, and a lower frequency component, ν_3'', dominated by the N-H stretching motion of the core bound to both a 1° and a 2° NH_3.

In the spectrum shown in fig. 7c for the n=5 cluster, the small, sharp feature observed at 2890 cm-1 and labeled 'C' is assigned to the symmetric stretching motion of the core, ν_1'. The weak intensity of this band is consistent with the only slight breaking of the symmetry of the core by the 2° ammonia.

Another new, broad feature centered at 2650 cm^{-1}, labeled 'A' in the figure, is correlated with the addition of an NH_3 into the second solvation shell. The fact that this feature greatly increases in relative intensity as the number of solvent molecules increases beyond n=5 (see the following

section), lends support to the notion that it involves a vibration coupled to the second solvation shell ammonias. We assign it to the low frequency component of the antisymmetric stretch of the core, ν_3". The large width of the feature (50-60 cm^{-1} FWHM) even at the low rotational temperatures of this study suggests that extensive hydrogen bonding is involved. The intense 2910 cm^{-1} band, 'B', also associated with an oscillator involved in hydrogen bonding, is relatively narrow (25 cm^{-1} FWHM). This peak can be clearly assigned to ν_3'. The smaller width of this band, even when compared to ν_3 in $NH_4^+(NH_3)_4$, correlates with the strength of the hydrogen bonding interaction.

A series of weak absorptions appear in the 3000-3200 cm^{-1} region. The group of two peaks centered at 3010 cm^{-1} and an additional set of two peaks centered at 3110 cm^{-1} probably correlate to the features in the n=4 spectrum at 3010 and 3095 cm^{-1}, respectively. There, the identity of the first feature was uncertain, and there was strong evidence from Schwarz that the second was due to the first overtone, $2\nu_4$ of the triply degenerate bending mode of the core. Based on the latter identification, we tentatively assign the 3110 cm^{-1} group to a similar bending motion. Because of the loss of degeneracy produced by the second shell ammonia, the bending mode can be expected to split into a high frequency and a low frequency component, the lower of which would probably be most closely associated with the three equivalent core oscillators. A splitting of 30 cm^{-1}, as observed, does not

seem unreasonable. The 3010 cm^{-1} set of peaks is presumably an overtone or combination band. One possibility is a combination of the ν_1' and intense ν_3' modes (2890 and 2910 cm^{-1} peaks) with the intense low frequency hydrogen bond stretching modes. This would place the stretching frequency of the three equivalent hydrogen bonds at about 110 cm^{-1}, which also does not seem unreasonable. Another possibility is that these peaks are due to a bending overtone of the core oscillator with attached 1° and 2° NH_3 ligands. In this case, the 3110 cm^{-1} group would be assigned to the bending overtone of the other three oscillators.

The addition of an NH_3 into the second shell should also have an effect on the 1° ammonia to which it attaches. If the bonding occurs through the sort of hydrogen bond illustrated in figure 8b, one would expect the 12 cm^{-1} characteristic spacing of free internal rotation of 1° NH_3 to disappear when the 1° NH_3 is bound to a 2° NH_3. The antisymmetric stretching motion of the 1° solvent molecule would also be split into a low frequency hydrogen bound component and two higher frequency free N-H stretching motions: a symmetric stretching component and an antisymmetric one.

Centered at 3419.8 cm^{-1} and shown in expanded view in fig. 4e is the now familiar structure due to internal rotation of the 1° NH_3's superimposed on the antisymmetric stretching vibration of the subgroups. Band 'E' in fig. 7c, at 3364 cm^{-1}, however, is a new feature not observed for n=4, and arises

from the presence of the 2° NH_3. The frequency is appropriate for NH oscillators which are not hydrogen bonded. This band is significantly broader than the individual components of the NH_3 ν_3 band, and shows no rotational structure at this level of resolution. It is assigned to the free N-H antisymmetric stretching motion of the 1° NH_3 bound to the 2° NH_3, denoted ^{2}1°N-H^f_a in the new notation.

The band labeled 'D' in fig. 7c centered at 3230 cm^{-1}, has gained considerably in intensity from n=4 to n=5. We assign this feature to two overlapping bands, one due to the bound N-H oscillator of the 1° NH_3, ^{1}1°N-H^b_s. The other band is due to $2\nu_4$ of the three equivalent unbound 1° NH_3 subunits, although the remaining 1° NH_3 and the 2° NH_3 may also contribute intensity by N-H bending overtones. By n=6, we certainly expect the majority of intensity in the solvent region of the spectrum to come from the N-H stretch of 1° hydrogen bonded oscillators, although we cannot rule out significant contribution from bending overtones. Once again, ab initio calculation might help to clarify this. It seems, however, that the structure of n=5 is of the sort given in figure 8b. It is also clear due to the lack of the 3370 cm^{-1} feature found in the n=5 to 8 spectra, that in the n=4 spectrum there is essentially no n=4 isomer with a 1°-2° NH_3 hydrogen bond.

The contribution of the outer shell NH_3 N-H oscillators to the n=5 spectrum is minor and could not be identified. When the n=8 spectrum is discussed later, however, it will be suggested that the barrier to internal

rotation is higher for outer NH_3 subunits in n=5-8 complexes than for nonbonded 1° NH_3 in n=1-7 complexes.

3.3.2.6. $NH_4^+(NH_3)_6$:

As the number of solvent molecules around the NH_4^+ increases, the production of isoenergetic conformers becomes more likely. A consequence of this is that speculations about the detailed structure of the larger ammoniated ammonium ions becomes less certain. However, it seems reasonable to suppose that the structure of the first solvation shell is reasonably well-preserved and that the addition of subsequent ammonias tends to occur predominantly through the sort of hydrogen bonding scheme discussed in the previous section. The spectra are found to be consistent with this assumption.

Working from the premise that additional solvent molecules bind to successive first shell ammonias, we presume that by the n=6 cluster two of the four available second shell sites are occupied. Using the n=5 cluster as a model for the spectrum, we would expect the components of the core vibrational band assigned to a stretching motion where N-H bonds of the core are bound to both a 1° and a 2° NH_3 (^{2}0°N-H^{b,b}) to increase in relative intensity. Conversely, the feature associated with the antisymmetric stretch of the core bound only to 1° ammonias should decrease in relative intensity (^{2}0°N-H^b_a).

A glance at fig. 7d shows that this is the case, as peak 'A' increases

dramatically in intensity relative to peak 'B'. Recall that 'A' was first observed in the n=5 spectrum and is therefore associated with the onset of the second solvation shell. In addition to a sharp increase in intensity, it has also shifted to higher frequency, 2720 cm^{-1}. Again, this band is assigned to a stretching motion of the core where the N-H bonds involved are themselves bound to both a 1° and a 2° NH_3 (^{2}0°N-H^b_a). We call it an antisymmetric stretch because symmetric stretches, in general, seem to carry less intensity. At 2920 cm^{-1}, the symmetric stretching motion of the core oscillators bound to only 1° ligands is observed (^{2}0°N-H^b_s), and is labeled 'C' in fig. 7d. The antisymmetric stretching motion of the same core oscillators, ^{2}0°N-H^b_a, is observed at 2950 cm^{-1} and labeled 'B'. A broad band whose maximum occurs at 3020 cm^{-1} is observed and is tentatively assigned to the first overtone of the overlapping core bending modes ^{2}0°N-H$^{b,b}_b$ and ^{2}0°N-H^b_b, with a possible contribution from a combination band involving ^{2}0°N-H^b and the hydrogen bond stretch.

The effect of further occupation of the second solvation shell should also have an effect on the spectroscopy of the first solvation shell ammonias. The structure due to internal rotation of the 1° solvent molecules is still observed, but at much lower relative intensity. With $^RQ_0$ centered at 3422 cm-1, this structure lies slightly to the blue of the analogous n=4 and 5 bands (See fig. 6f.). The structure assigned to the free N-H antisymmetric stretching motion of the 1° ammonias bound by the second solvation shell

ammonias $^{2}1°N\text{-}H^{f}_{a}$, 'E' in fig. 7d, has greatly increased in relative intensity, and appears at 3368 cm^{-1}. Similarly, the $^{1}1°N\text{-}H^{b}_{s}$ mode has increased in intensity and appears at 3225 cm^{-1}. This feature is labeled 'D'.

The weak feature at about 3320 cm^{-1} is probably the symmetric stretch ν_1 of the two 2° ammonias, overlapped with the symmetric stretch of free N-H oscillators of those 1° subunits with an attached 2° NH_3. There is a slight indication that a very weak band is present here in the n=5 spectrum as well. While the ν_1 and ν_3 bands in isolated NH_3 have comparable intensity, it has been clear that in the complexes n=1-5 the ν_3 band of NH_3 subunits carries much more intensity than ν_1. The appearance of ν_1 at n=6 with comparable intensity to ν_3 could then be taken as an indication of how weakly the second shell NH_3 subunits are bound.

The 3320 cm^{-1} band, upon close inspection, seems to consist of two peaks at 3310 and 3325 cm^{-1}. A careful comparison of the n=7 spectrum in the same region reveals similar structure. By analogy with the symmetric stretch observed in the spectrum of liquid ammonia[55] at 3300 cm^{-1} and similar structure observed in clusters of neutral ammonia clusters[56], we tentatively assign the 3310 cm^{-1} peak to the symmetric stretch of primary subunits, $^{2}1°N\text{-}H^{b}_{s}$. By analogy to ν_1 in isolated NH_3, we tentatively assign the 3325 cm^{-1} peak to ν_1 of the two second shell ammonias. The two remaining first shell unbound ammonias are presumed to constitute a minor contribution.

3.3.2.7. $NH_4^+(NH_3)_7$:

It is obvious how most of the n=7 features in fig. 7e correlate with n=6 in fig. 7d. Most of the difference in appearance of the two spectra has to do with the modes of the NH_4^+ core at frequencies below 3100 cm^{-1}. It is very obvious that the intense 2770 cm^{-1} peak of n=7, 'A' in the figure, correlates with the 2720 cm^{-1} peak of n=6 (it will be shown later that the two peaks fall into a smooth frequency progression established by the other clusters), and we readily assign it as ^{3}0°N-H$^{b,b}_a$. The FWHM of the band is about 80 cm^{-1}, slightly less than for the analogous band in n=6. This reduction is consistent with the lower hydrogen bond strength in n=7. The intense 2950 cm^{-1} peak in n=6 and its companion at 2920 cm^{-1} ('B' and 'C' in fig. 7d.) have nearly disappeared in the n=7 spectrum. It is expected from our n=6 assignments that these two peaks should collapse into one peak of reduced intensity for n=7, if the cluster consists of an NH_4^+ core, four first shell NH_3 subunits and three second shell NH_3 subunits each hydrogen bonded to its own primary subunit. In fact, it appears that the peaks do collapse, and the reduction in intensity is surprisingly dramatic. In the spectra of the higher ammoniates, such a peak is not observed, suggesting that all of the N-H bonds of the ammonium core are experiencing hydrogen bonding with both 1° and 2°

The only new feature appears at 2870 cm^{-1} and is quite weak. This band is more prominent in the n=8 spectrum. Our very tentative

assignment is to a combination band involving the core stretching mode $^{3}0°N\text{-}H^{b,b}{}_{a}$, and the hydrogen bond to these three equivalent oscillators. If correct, this assignment places the frequency of this strongest of the hydrogen bonds in n=7 at about 70-90 cm^{-1}.

The band centered at 3050 cm^{-1} seems to be a bending overtone of the three equivalent N-H oscillators. The remaining features at 3020 and 2990 cm^{-1} might be produced by bending overtones of other N-H oscillators.

From the above discussion, it seems that the lowest energy structure consists of an NH_4^+ core with four 1° NH_3 ligands and three 2° NH_3 ligands, each attached to a different 1° subunit. There is no definitive indication for the symmetric structure $(NH_3)_3(N_2H_7^+)(NH_3)_3$, analogous to the species $(H_2O)_2(H_5O_2^+)(H_2O)_2$ which is proposed to be an intermediate in proton transfer[29], nor any other isomer. There is also no strong indication for a "cross-linking" of second shell ammonia to another ammonia subunit in the first or second shell, with the formation of large ring structures. It is clear from the ν_3' band of the propellering first shell NH_3 that this subunit is not involved in cross-linking. If there is cross-linking of two second shell ammonias, however, it may be difficult to discern from the spectrum due to the weak absorptions of these subunits and the possibility that the absorptions may overlap with those of primary ammonia.

3.3.2.8. $NH_4^+(NH_3)_{8\text{-}10}$:

One would expect that as the number of NH_3 molecules around the NH_4^+

increases, the spectrum of the ammoniated ammonium ion cluster should eventually converge. In the limiting case, this spectrum would be that of an ammonium ion solvated in a liquid ammonia environment. Spectral features associated with an ammonium ion bound to both 1° and 2° ammonias should further increase in relative intensity. Conversely, NH_4^+ stretches involved in bonding to 1° NH_3's only, should disappear at n=8 provided that the second shell, like the first shell, is filled by four ligands each bound to a separate primary ammonia. For the 1° NH_3 molecules, free rotation as observed in the n=1 to 6 spectra should be quenched for n>7. A similar band structure could take its place, but associated with 2° NH_3. Absorptions due to second and third shell ammonia might be very apparent by n=10. Stretching vibrations of the solvent subunits should begin to approach those observed in the condensed phases. Unfortunately, spectra for the n=9 and 10 clusters were limited by low signal to noise ratio to the 2600 to 3200 cm^{-1} region because of the weak absorbance in the higher frequency region and the low number density of larger mass clusters obtainable.

The IRVPD spectra for the n=8 ammoniated ammonium ion cluster appears in figs. 4g and 7f. For the higher ammoniates, the spectra are essentially the same as that of the n=8 species. Band maxima for the features observed in the n=8 to 10 spectra are listed in Table III.

Once again, the assignments stem from those of the smaller clusters.

The very intense peak at 2830 cm^{-1}, 'A', is an antisymmetric stretch of the core N-H oscillators, which is analogous to the triply degenerate ν_3 fundamental of NH_4^+ or $NH_4^+(NH_3)_4$. The weaker absorption centered at 2900 cm^{-1}, and first observed for n=7 at 2870 cm^{-1}, is probably a combination band of the ν_3 mode with the stretching mode of the hydrogen bonds between core and 1° ammonias. The peak at 3050 cm-1 is assigned to the bending overtone of the core, $2\nu_4$.

The major difference in the spectra of n=9 and 10 in the 2600-3200 cm^{-1} region from that of n=8, lies in the slight blue shift of the intense band at 2820 cm^{-1} for n=8. It appears at 2829 and 2841 cm^{-1} in the n=9 and 10 spectra, respectively. The frequencies of other bands have converged more quickly.

Intensities and positions of peaks in the 3200-3500 cm^{-1} region differ only slightly from the n=6 spectrum with the notable exception of the internal rotation structure, which is absent. The 3220 cm^{-1} peak ('D' in fig. 7f) is assigned primarily to ^{4}1°N-H^b_a, with perhaps contributions from $2\nu_4$ of 2° NH_3. We believe the 3320 cm^{-1} peak to be ν_1 of 2° NH_3, with the weak shoulder at 3300 cm^{-1} attributed to the symmetric stretch of the two equivalent N-H bonds of the 1° NH3 subunits. The peak at 3380 cm-1 ('E' in fig. 7f) is easily assigned to the antisymmetric stretch of the two equivalent N-H bonds of the 1° subunits bound by 2° NH3's.

The appearance of the band which peaks at 3415 cm-1 is very different

from that of the smaller clusters in the same region. The structure observed for n=7 was similarly weak and began to appear a bit broadened, but sharp structure from internal rotation of the 1° NH_3's was still apparent. The corresponding band for n=8 shown in fig. 4g is unmistakably broadened, shifted slightly to the red and no structure due to internal rotation is evident. (Due to the weak signal for this cluster, a larger wavelength increment between data points and longer averaging time at each point was used for this trace. Spectral resolution is slightly larger than 1 cm^{-1}, but is still well inside the expected 12 cm^{-1} structure for internal rotation.)

It appears that this feature is actually the ν_3 band of 2° NH_3. Evidently the 2° subunits are not able to propeller in the same manner as the 1° NH_3's. The latter suggestion is supported, as the loss of structure and a red shift of about 6 cm^{-1} would be expected for NH_3 subunits with a relatively high barrier to internal rotation. It is quite possible that the 2° NH_3's do not attach via a linear hydrogen bond thereby resulting in an orientation not along the 2° NH_3's local C_3 axis. It is known from microwave spectroscopy that the neutral ammonia dimer is not held together by a hydrogen bond.[57] If something similar is happening in these large clusters, a larger barrier to internal rotation could result. Cross-linking between 2° subunits would also explain the loss of internal rotation structure.

Another explanation for a higher internal rotation barrier of 2° NH_3 as compared to unbound 1° NH_3 is related to the low symmetry of 1° NH_3 compared to the NH_4^+ core. When a 2° NH_3 attaches to 1° NH_3 with its C_3 axis coincident with an NH bond vector of the 1° subunit, that 1° subunit has only two equivalent N-H bonds. The potential function for internal rotation of 2° subunits therefore seems likely to be more complicated, with perhaps a somewhat higher barrier. In any case, there seems to be no doubt that the dominant structure involves 4 1° NH_3 ligands and 4 2° ligands, each attached to a different 1° subunit. Our preferred structure for the $NH_4^+(NH_3)_8$ complex is that shown in fig. 8c.

3.4 SUMMARY AND CONCLUSIONS:

The infrared vibrational predissociation spectra of the ammoniated ammonium ions contain two main classes of spectral features: those that can be assigned to motions of the NH_4^+ ion core of the cluster, and those that can be attributed to the NH_3 solvent molecules. The core vibrations observed can be easily understood in terms of the ν_3 (antisymmetric stretch), ν_1 (symmetric stretch) and $2\nu_4$ (degenerate bending) modes of the NH_4^+ ion in several cases, with the application of distorted tetrahedron theory. The most prominent solvent vibrations that are observed are assigned to transitions arising from the first solvent shell (1°) ammonias; transitions of second shell (2°) subunits account for relatively weak features appearing only in the spectra of the largest clusters. For the 1° NH_3 molecules not perturbed by second solvation shell (2°) NH_3's, the strongest transitions assigned are analogous to ν_3 (the doubly degenerate antisymmetric stretch) and $2\nu_4$ (the bending mode) of NH_3. For the ν_3-type mode, rotational structure is observed on the vibrational transition that has been assigned to an internal rotation of the ammonias about their local C_3 axes. The internal rotation structure is observed as a consequence of the selection rule $\Delta K=\pm 1$ for this perpendicular band (perpendicular with respect to the C_3 axis of the NH_3 subunit whose ν_3 vibration is excited), where K is the quantum number for angular momentum about the NH_3 C_3 axis. Such a structure is also expected for the ν_4 fundamental, but not for

the ν_1 or ν_2 modes.

Trends in the measured vibrational frequencies are observed for both core and solvent vibrations in the $NH_4^+(NH_3)_n$ species which converge at large n. The ν_3 antisymmetric stretching vibration for the 1° solvent molecules was first observed in the n=1 cluster. With $^RQ_0$ centered at 3398.4 cm^{-1}, this feature shifts further to the blue and decreases in relative intensity with increasing cluster size. The frequencies of the central $^RQ_0$ (K = 0) bands measured for this transition are plotted as a function of cluster size in fig. 9a. The band origins in each case lie about 6 cm^{-1} to the red of the listed frequency. The band origin of free NH_3 in the gas phase is 3444 cm^{-1}. (See Table I. Reference e.) It can be seen that, as in the case of other cluster ions observed previously, such as the hydrogen cluster ions, H_n^+ and the hydrated hydronium ions, the converged value of this solvent transition lies significantly below the value for the free molecule due to the red-shift imposed by the solvation interaction even at large distances from the ion core.

A similar plot for the frequencies of the antisymmetric stretching vibration of the core bound to only 1° NH_3's is shown in fig. 9b. The first point in the plot for the n=2 cluster is from Schwarz's measurement which he tentatively assigned to the component of the antisymmetric stretch of the NH_4^+ ion bound by two NH_3's. We observe the analogous feature in the n=3-7 spectra shift to the blue and decrease in relative intensity, converging by

the n=7 spectrum to 2989 cm^{-1}. The frequencies for similar core stretching vibrations with an attached 2° NH_3 as well, are plotted in fig. 11c.

The spectra have clearly indicated, in agreement with previous thermochemical measurements and theoretical calculations, that a well-defined shell structure exists. The first solvent shell is completed by four ligands. The fifth ligand hydrogen bonds to a 1° NH_3, with only one N-H bond of the 1° subunit directly affected. Successive ammonia ligands hydrogen bond to other 1° subunits in the same way until the n=8 complex shown in fig. 10c is obtained. In this complex each 1° subunit is bound by one 2° subunit.

In the complexes n=1-7, any 1° NH_3 which is not bonded to a 2° subunit has a ν_3 band which exhibits the structure characteristic of nearly free internal rotation of that 1° subunit. A 1° NH_3 which **is** bonded to a 2° subunit might well undergo internal rotation, but the characteristic spacing of the Q-branches in the associated ν_3 band will be less than the 1 cm^{-1} laser linewidth employed for these studies. For the 2° NH_3, the barrier to internal rotation about the local C_3 axes evidently is higher, or the transition fails to carry sufficient oscillator strength to be observed, as the spectrum of the n=8 cluster indicates no such structure.

For the n=9 and 10 complexes, it is not yet clear what binding sites(s) the outermost ligands occupy. If they attach to 2° NH_3 subunits, one would expect a new band to appear, red-shifted by perhaps a hundred

wavenumbers from the core ν_3 stretch at ≈2830 cm^{-1}. This is not observed. It may be that the 9th and 10th ligands attach loosely to 1° NH_3 subunits. Therefore, although we believe that some sort of shell structure is completed at n=8 ($NH_4^+(NH_3)_8$), this structure is not so well defined as that filled at n=4. We could, for example, say that the 9th and 10th ligands enter the 2' shell rather than 3; the second shell might be 1/3 or 1/2 full when it contains 4 ligands. In any case, it is useful to note that the convergence plot of fig. 9c seems to show a slight kink at n=8, with such small frequency shifts for n=9,10 that the binding of their ligands is apparently quite weak.

The spectra which were obtained for n=9-10 are quite similar to that of n=8, indicating that the NH_4^+ core, at least, is affected only slightly in its infrared absorption properties by the addition of these ligands. Of course, there may be other properties of the core or of the rest of the complex, which are more significantly affected. The infrared probe is sensitive to bond length and bond strength, and we can say that these characteristics of the NH_4^+ core are no longer changing. It is probable that these properties are likely to show significant discontinuities for certain larger values of n, if special structures form.

A comparison of the spectra of ammonium salts with weakly interacting counter ions such as NO_3^- or ClO_4^- in ammonia solution with that of the n=8 ionic cluster shows unmistakable similarity, particularly at low temperatures. For the more strongly interacting counter ion Cl^- the

spectrum is still very similar, especially for a mole ratio NH_3:$ClNH_4$ of 1:6 (See fig. 2 of ref. 3.). In general, the broad, intense absorption in the 2800 cm-1 region of ammonium salts should be associated with a ν_3 type vibration of solvated NH_4^+. In the 3200-3500 cm^{-1} region, the spectrum is quite similar to that of liquid ammonia[52] or neutral ammonia clusters $(NH_3)_n$ (n=3-5)[53]. So far as the infrared spectra are concerned, the n=8 complex is already quite close to an NH_4^+ in a liquid-like environment. In other words, the very strong "chemical-like" bonding of the NH_4^+ to the solvent molecules gets diluted over the large number of subunits by n=8 so that the interaction of the ionic core with additional NH_3's is comparable to that between neutral NH_3's.

While the spectra of crystalline ammonium salts have been well understood for many years, that of the same salts in NH_3 solution has been more difficult to interpret. The liquid phase vibrational bands tend to be very broad, even when compared to those of the solid phase, and the relative intensities of the bands can vary dramatically with the chemical conditions. The spectra of cold ammoniated ammonium clusters in the gas phase can therefore contribute a great deal to our understanding of the interactions present in such solutions.

TABLE I: Molecular Constants for NH_4^+, and NH_3.
(All units are in cm^{-1} except ζ which is dimentionless.)

Molecule or Ion:	Symmetry	Molecular Constants:	Reference
NH_4^+	T_d	ν_1: 3270 ± 25	a
		ν_2: 1669	c
		ν_3: 3343.26	e
		ν_4: 1447.22	f
		A: 5.9293 ± 0.0002	e
		B: "	e
		C: "	e
		ζ: 0.0604	e
NH_3	C_{3v}	ν_1: 3336.2	b
		ν_2: 950	d
		ν_3: 3444	d
		ν_4: 1627	d
		A: 6.30	g
		B: 9.941	g
		C: "	g
		ζ: 0.06	g

[a]P. Botschwina, J. Chem. Phys. **87**, 1453 (1987), scaled ab initio value.

[b]W.S. Benedict, E.K. Plyler and E.D. Tidwell, J. Chem. Phys. **32**, 32 (1960).

[c]D.J. DeFrees and A.D. McLean, J. Chem. Phys. **82**, 333 (1985), scaled ab initio value.

[d]T. Shimanouchi, Tables of Molecular Vibrational Frequencies, U.S. Dept. of Commerce, Natl. Stand. Ref. Data Ser. Natl. Bur. Stand. **39** (U.S. GPO, Washington, D.C., 1972).

[e]M.W. Crofton, and T. Oka, J. Chem. Phys. **79**, 3157 (1983); **86**, 5983 (1987).

[f]M. Polak, M. Gruebele, B.W. DeKock and R.J. Saykally, Mol. Phys. **66**, 1193 (1989).

[g] G. Herzberg, Electronic spectra of Polyatomic Molecules (Van Nostrand, Princeton, N.J., 1967).

TABLE II. Vibrational frequencies for the ammoniated ammonium ions. Experimental frequencies from this work were found using the IRMPD technique. Units are in cm^{-1}.

This Work	Previous Work[a]	Assignment	
$NH_4^+(NH_3)$			
3376.6 3377.4	3420 (shoulder)	$^PQ_2$	NH_3 ν_3 asym. stretch
3387.0 3387.8		$^PQ_1$	
3397.4 3398.2		$^RQ_0$	
3409.2		$^RQ_1$	
3419.5		$^RQ_2$	
3392.0		$^PR_1(J)$? (see text)	
3402.1		$^RR_0(J)$? (see text)	
3412.4		$^RR_1(J)$? (see text)	
$NH_4^+(NH_3)_2$			
3392.0		$^PQ_2$ of NH_3 ν_3 overlapped with NH_4^+ free N-H asym str	
3395.4	3360	NH_4^+ free N-H asym str	
3401.9		$^PQ_1$	NH_3 ν_3 asym stretch

This Work	Previous Work[a]	Assignment	
3413.7		$^{R}Q_0$	
3425.8 3426.8		$^{R}Q_1$	
$NH_4^+(NH_3)_3$			
2615		NH_4^+ ν_1' (^{3}0°N-H^b_s)?	
2660 2692		NH_4^+ ν_1' (^{3}0°N-H^b_s) or ν_3'' (^{3}0°N-H^b_a))	
3374.1	3365	NH_4^+ free N-H Str ν_3' (^{1}0°N-H^f_a)	
3390.8 3393.1		$^{P}Q_2$	NH_3 ν_3 asym. stretch
3404.2 3404.9		$^{P}Q_1$	
3416.8		$^{R}Q_0$	
3429.0 3429.9		$^{R}Q_1$	
3439.6		$^{R}Q_2$	
3452.3		$^{R}Q_3$	
$NH_4^+(NH_3)_4$			
2865	2867	NH_4^+ asym stretch ν_3 (^{4}0°N-H^b_a)	
3095	3087	NH_4^+ Bend $2\nu_4$ (^{4}0°N-H^b_b)	
3383.0 3384.3		$^{P}Q_3$	NH_3 ν_3 asym. stretch

This Work	Previous Work[a]	Assignment	
3393.5 3394.2		$^{P}Q_2$	
3407.8 3408.4		$^{P}Q_1$	
3420.5		$^{R}Q_0$	
3432.8 3433.3		$^{R}Q_1$	
3443.3 3444.1		$^{R}Q_2$	
3454.9 3456.5		$^{R}Q_3$	
$NH_4^+(NH_3)_5$			
2650		NH_4^+ ν_3'' stretch ($^{1}0°N\text{-}H^{b,b}_{s}$)	
2880		NH_4^+ ν_3' sym stretch ($^{3}0°N\text{-}H^{b}_{s}$)	
2910		NH_4^+ ν_1' asym stretch ($^{3}0°N\text{-}H^{b}_{a}$)	
3010 (two peaks)		See text for tentative assignment	
3110 (two peaks)		NH_4^+ bend overtone (see text)	
3228		Overlap of NH_3 $2\nu_4$ and $^{1}1°N\text{-}H^{b}$	
3364.4		NH_3 free N-H asym str ($^{2}1°N\text{-}H^{f}_{a}$)	
3382.7 3383.8		$^{P}Q_3$	1° NH_3 ν_3 asym. stretch

This Work	Previous Work[a]	Assignment	
3394.1 3395.2		PQ_2	
3407.2 3408.2		$^{P}Q_1$	
3419.8		$^{R}Q_0$	
3433.0		$^{R}Q_1$	
3443.5		$^{R}Q_2$	
3455.6 3456.3		$^{R}Q_3$	
$NH_4^+(NH_3)_6$			
2720		$^{2}0°N\text{-}H^{b,b}_{a}$	
2910		$^{2}0°N\text{-}H^{b}_{s}$	
2950		$^{2}0°N\text{-}H^{b}_{a}$	
3020		NH_4^+ bend overtone	
3228		1° NH3 H-bonded str ($^{1}1°N\text{-}H^{b}$)	
3368.4		1° NH_3 free N-H str ($^{2}1°N\text{-}H^{f}_{a}$)	
3398.2		$^{P}Q_2$	1° NH_3 ν_3 asym. stretch
3410.8		PQ_1	
3423.7		$^{R}Q_0$	
3435.7		$^{R}Q_1$	

This Work	Previous Work[a]	Assignment
3448		$^{R}Q_2$
$NH_4^+(NH_3)_7$		
2770		$^{3}0°N\text{-}H^{b,b}{}_{a}$
2870		Combination of above with hydrogen bond stretch
2955		$^{1}0°N\text{-}H^{b}$
3050		NH_4^+ bending overtone
3220		$^{1}1°N\text{-}H^{b}$
3375		$^{2}1°N\text{-}H^{f}{}_{a}$
3415		Overlap of $^{3}1°N\text{-}H^{f}{}_{a}$ and $^{3}2°N\text{-}H^{f}{}_{a}$ (?), unable to assign subbands for $^{3}1°N\text{-}H^{f}{}_{a}$
$NH_4^+(NH_3)_8$		
2820		$^{4}0°N\text{-}H^{b,b}{}_{a}$ (NH_4^+ ν_3)
2910		Combination of above with hydrogen bond stretch?
3050		$^{4}0°N\text{-}H^{b,b}{}_{b}$ overtone (NH_4^+ $2\nu_4$)
3220		$^{1}1°N\text{-}H^{b}$ for each of four "identical" subunits, possible overlap from 2°NH3 2ν4
3300		$^{2}1°N\text{-}H^{f}{}_{s}$
3320		2° NH3 ν1 ($^{3}2°N\text{-}H^{f}{}_{s}$)?
3380		$^{2}1°N\text{-}H^{f}{}_{a}$

This Work	Previous Work[a]	Assignment
3415		2° NH3 ν3 ($^{3}2°$N-H^{f}_{a})
$NH_4^+(NH_3)_9$		
2829		NH_4^+ ν_3 asym stretch
$NH_4^+(NH_3)_{10}$		
2841		NH_4^+ ν_3 asym stretch

FIGURE CAPTIONS:

1. The normal vibrations of tetrahedrally symmetric NH_4^+. ν_3 and ν_4 are three fold degenerate, while ν_1 and ν_2 are one and two fold degenerate, respectively. Arrows in the figure indicate the direction of motion but are not to scale with the amplitudes. (See ref. 53)

2. Mass spectra showing the $NH_4^+(NH_3)_n$ cluster distribution as a function of ion source conditions. For 2a, the $NH_3/H_2/Ne$ mixture flowed through a liquid nitrogen trap to reduce the NH_3 concentration. The source backing pressure was raised to obtain 2b, and the trap bypassed to obtain 2c. The $NH_3/H_2/Ne$ mixture was ≈ 1:10:100.

3. Normal modes of NH_3. Only one linear combination has been shown for the doubly degenerate modes ν_3 and ν_4. Again, arrows in the figure indicate the direction of motion but are not to scale for the amplitude of the motion. (See ref. 53.)

4. Vibrational predissociation spectra of $NH_4^+(NH_3)_n$ (n=1-6 for 4a-4f, respectively) in the 3370-3470 cm^{-1} region, showing the internal rotation subbands. 4g is the same region for the n=8 cluster which does not show

the internal rotation structure. (Due to poor signal to noise, a larger wavelength increment was used in scan 4g than the scans in 4a-f, but averaging time was increased.) The notation is discussed in the text. Corresponding subbands are connected by dashed lines.

5. C_{3v} and D_{3h} equilibrium structures for $N_2H_7^+$. The energies are expected to differ by only a few kcal/mole, with the relative energy ordering uncertain.

6. Simulated and experimental spectrum of $N_2H_7^+$ for D_{3h} equilibrium structure of fig. 6b. The simulation includes only Q branch transitions, since these are expected to dominate the spectrum. While the two traces show similarities, there are substantial differences as well. Rotational constants used in the simulation: A'=3.20cm^{-1}, A"=3.16cm^{-1}, B'=B"=0.16cm^{-1}, T=30K, ΔV=-1.0, ζ=0.0.

7. Vibrational predissociation spectra of $NH_4^+(NH_3)_n$ (n=3-8 for 7a-7f, respectively) in the 2600-3500 cm^{-1} region. Bands forming clear series in n are connected by dashed lines.

8. Proposed structures for the n=4,5 and 8 complexes. The hydrogen bonds

are denoted by dashed lines. It is not certain that the hydrogen bonding between 1° and 2° NH_3 is linear.

9a. Plot of the $^RQ_0$ bands for the internal rotation structure associated with the 1° NH_3's antisymmetric stretching transition as a function of cluster size. A discontinuity is noted at the n=5 cluster attributed to the formation of the second solvation shell.

9b. Plot of the peak intensity of the antisymmetric stretching band for the ammonium ion core bound only to 1° NH_3 molecules as a function of cluster size. Filled circles represent data obtained from this work. The filled square was obtained from ref. 17. The series shows eventual convergence as n increases. See text for discussion.

9c. Plot of the peak intensity of the antisymmetric stretching band for the ammonium ion core bound to both 1° and 2° NH_3 molecules as a function of cluster size. Converged values are similar to those observed for solutions of ammonium salts dissolved in liquid ammonia. See text for discussion.

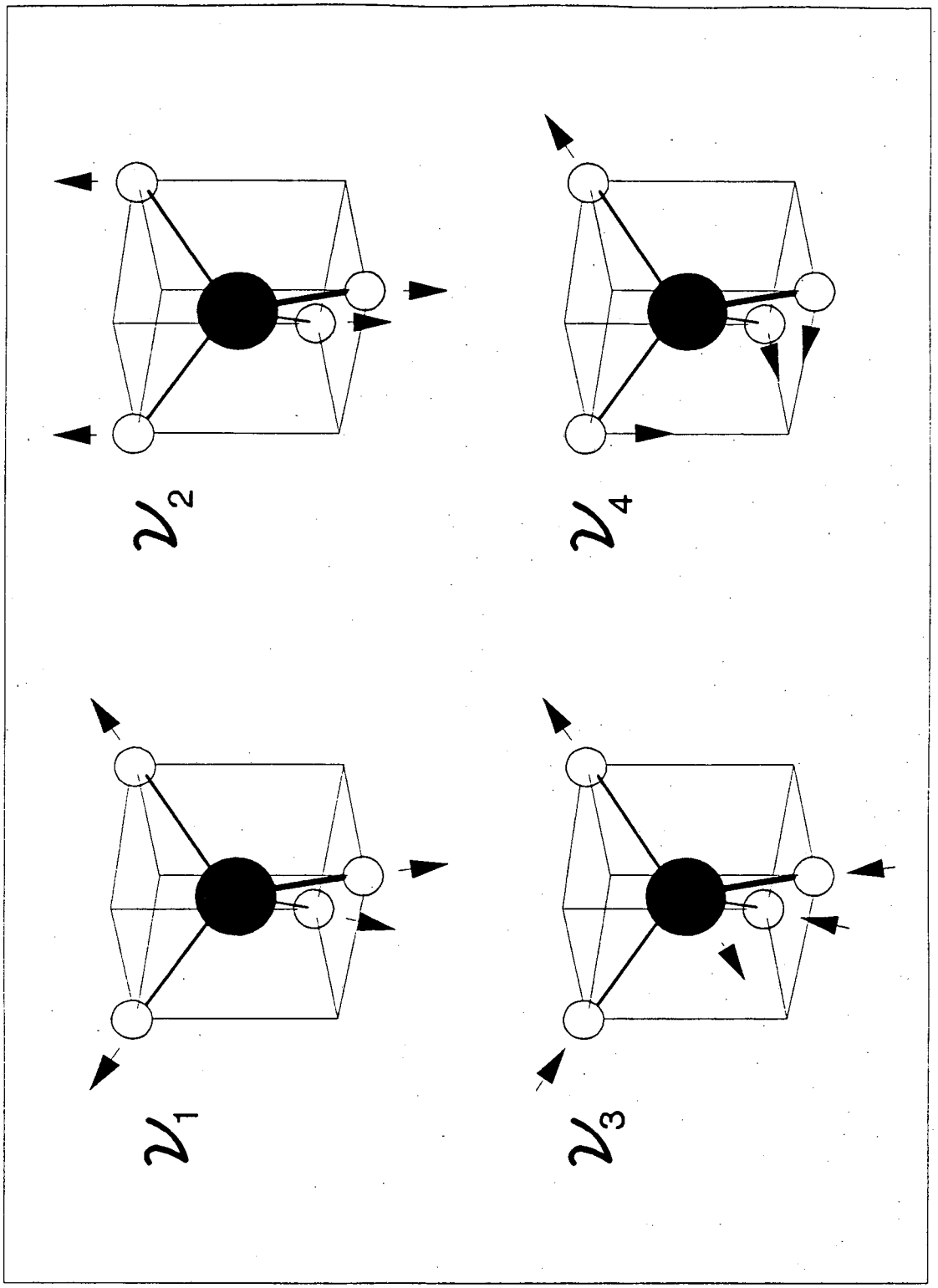

Figure 1.

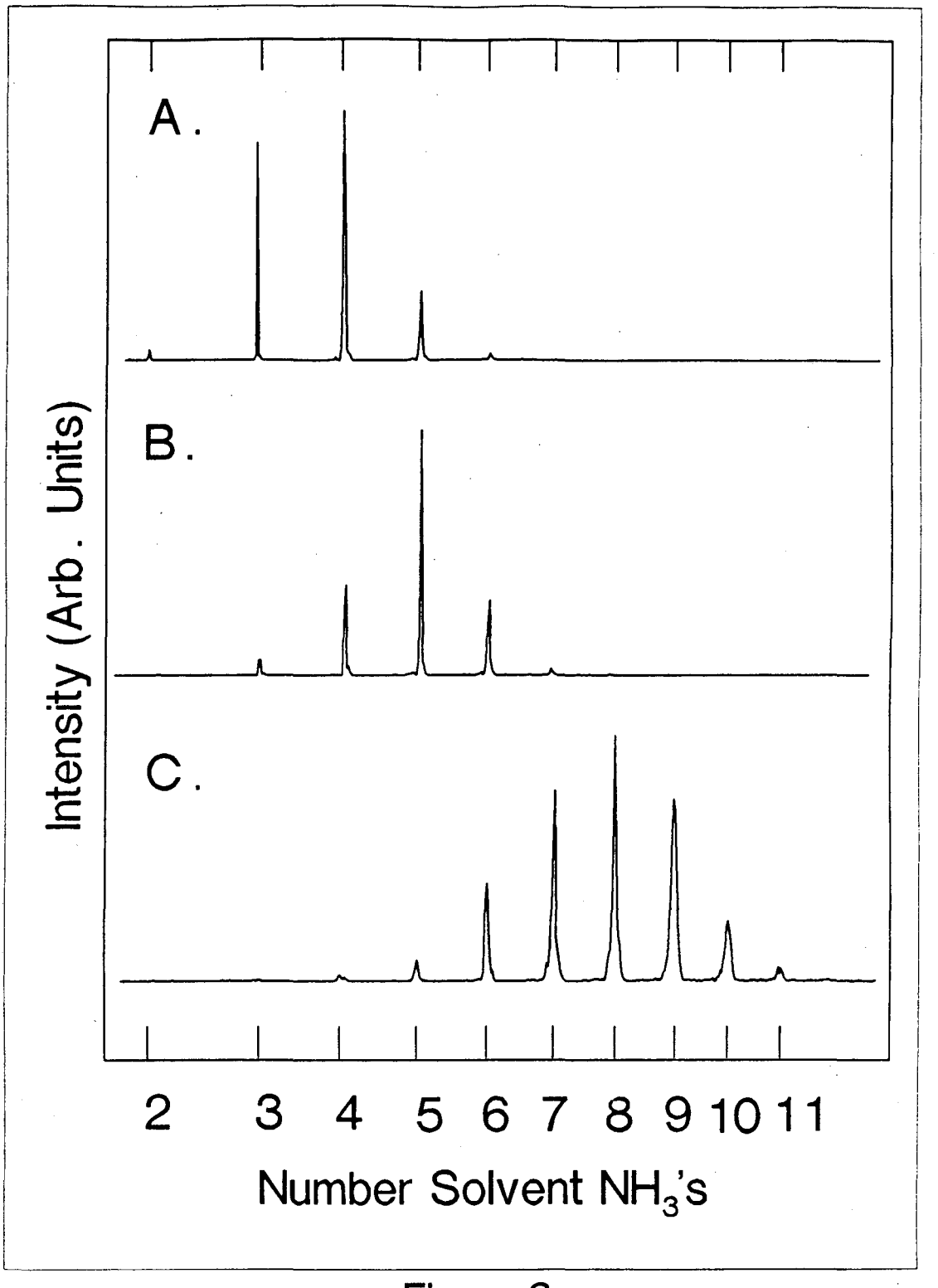

Figure 2.

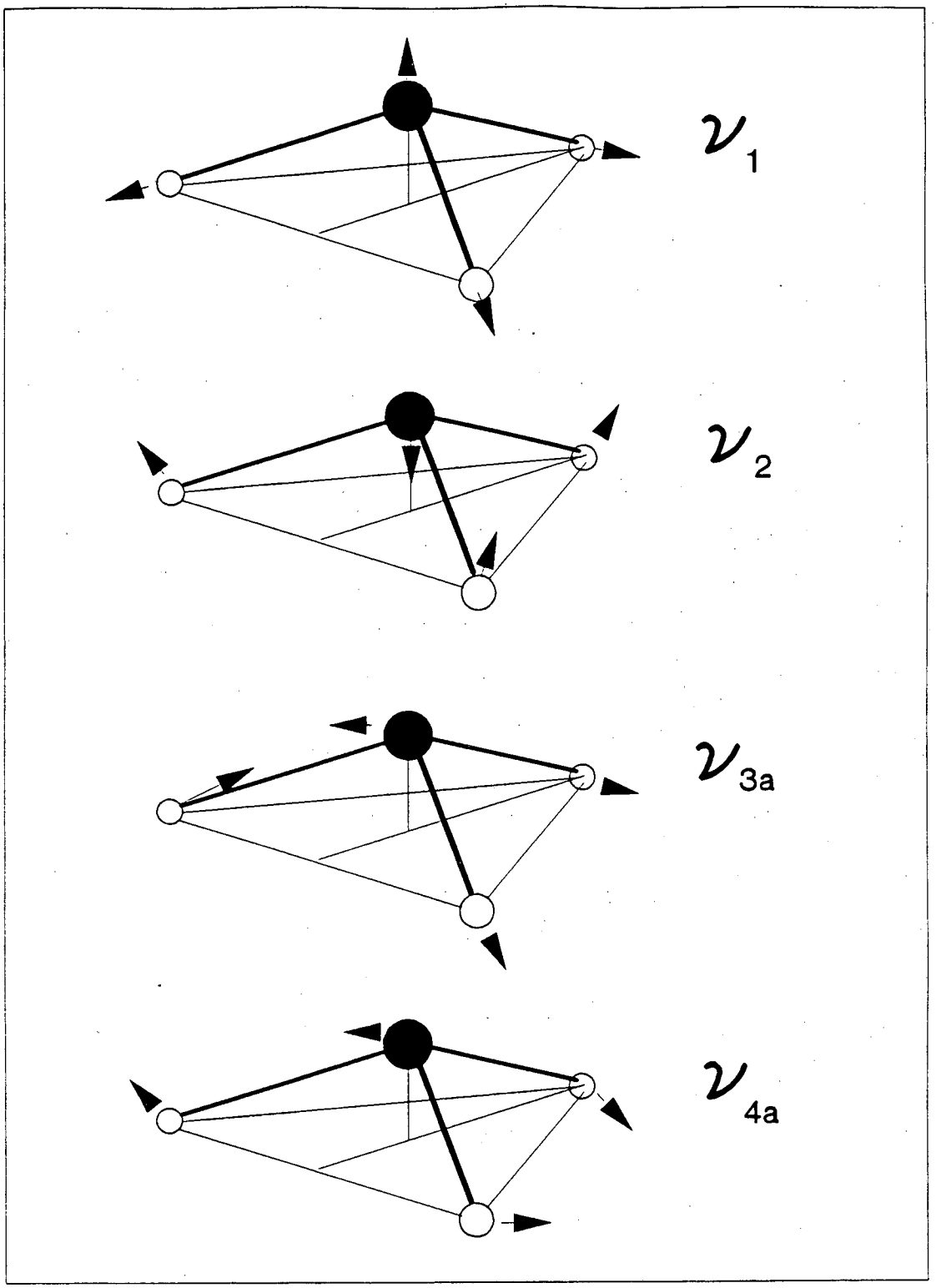

Figure 3.

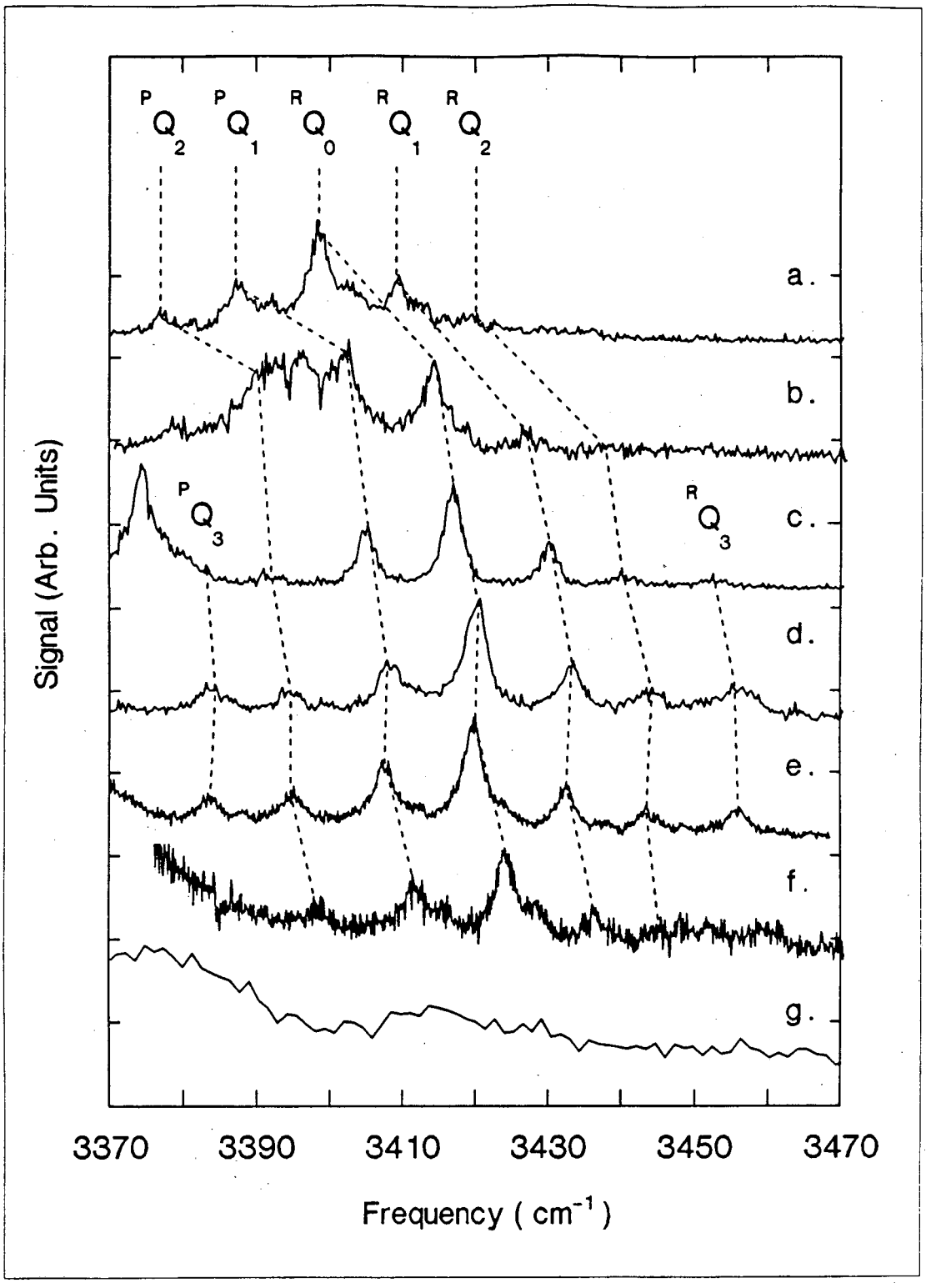
P Q2
P Q1
R Q0
R Q1
R Q2
a.
b.
P Q3
R Q3
c.
d.
e.
f.
g.
Signal (Arb. Units)
3370
3390
3410
3430
3450
3470
Frequency (cm-1)

Figure 4.

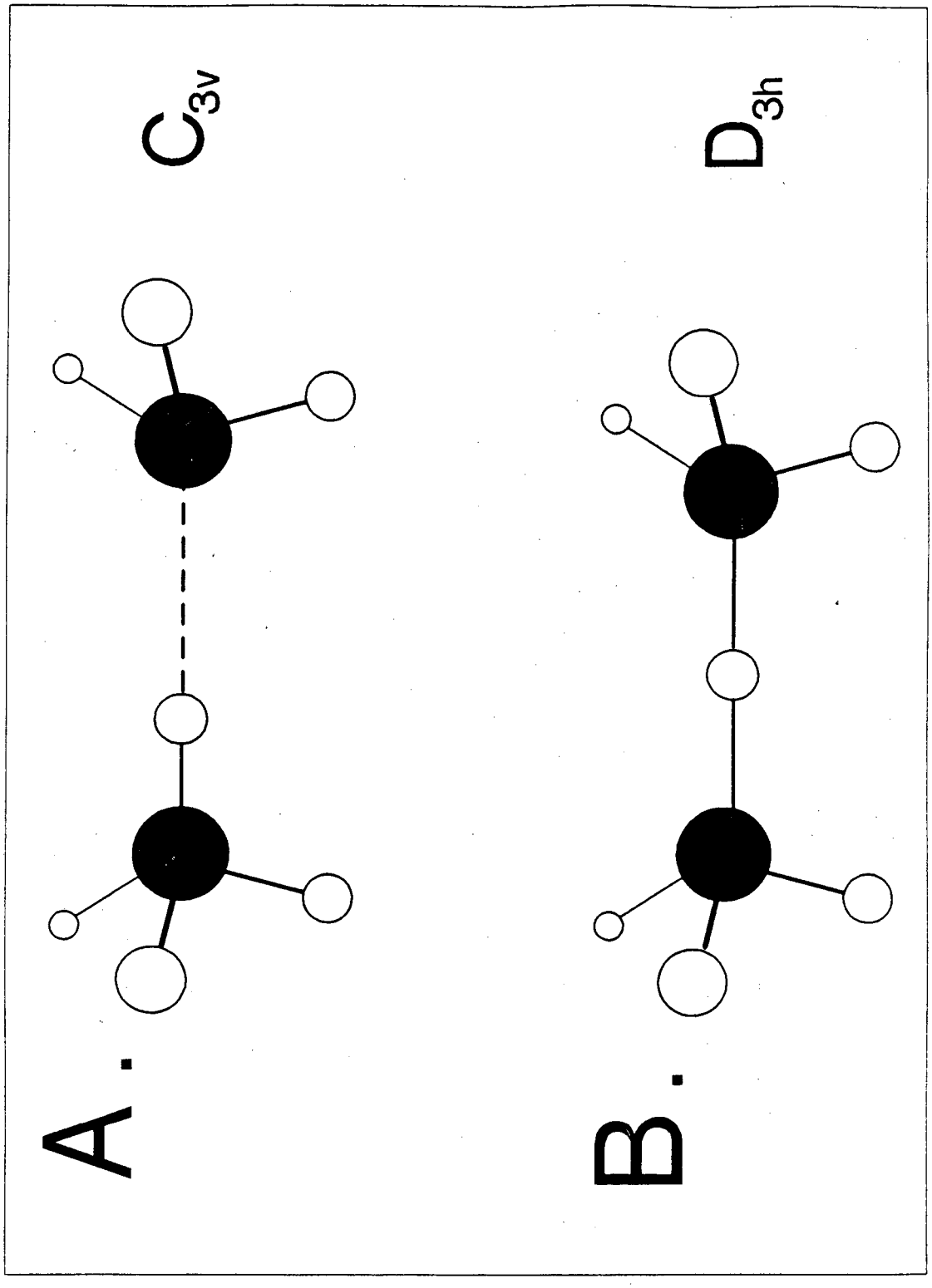

Figure 5.

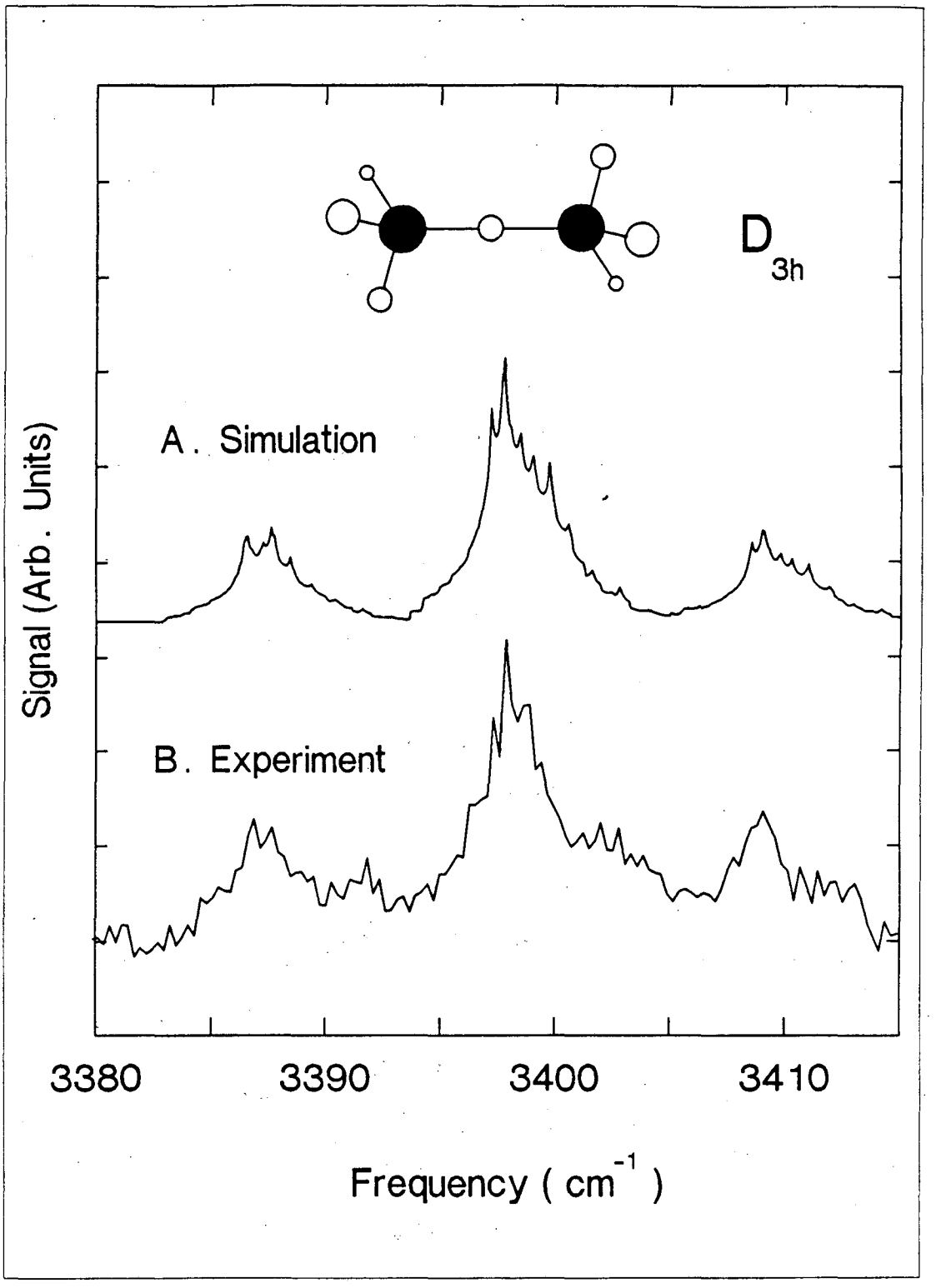
D
3h
A . Simulation
B . Experiment
Signal (Arb. Units)
3380
3390
3400
3410
Frequency (cm-1)

Figure 6 .

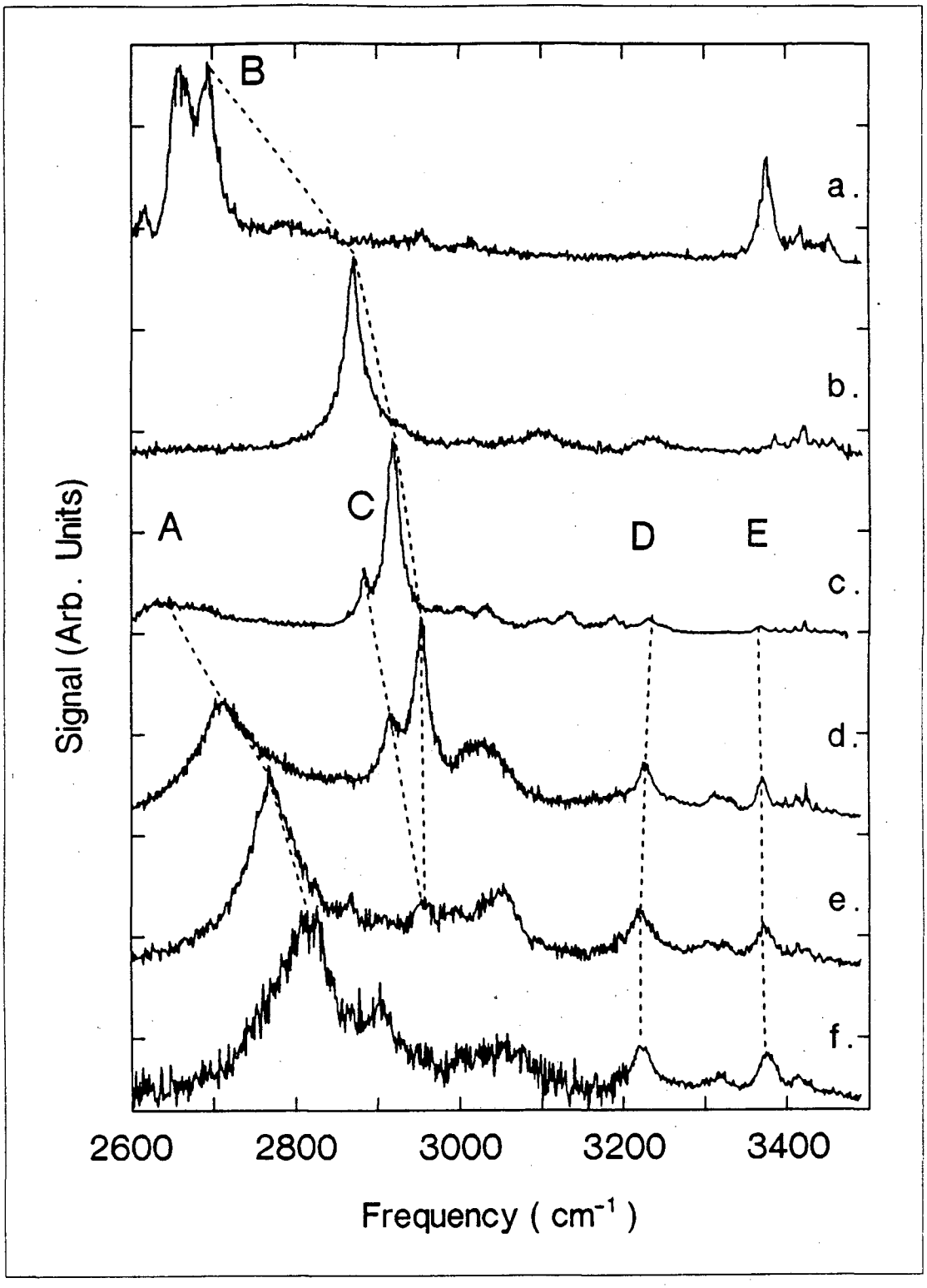
B
a.
b.
A
C
D
E
c.
d.
e.
f.
Signal (Arb. Units)
2600
2800
3000
3200
3400
Frequency (cm^{-1})

Figure 7.

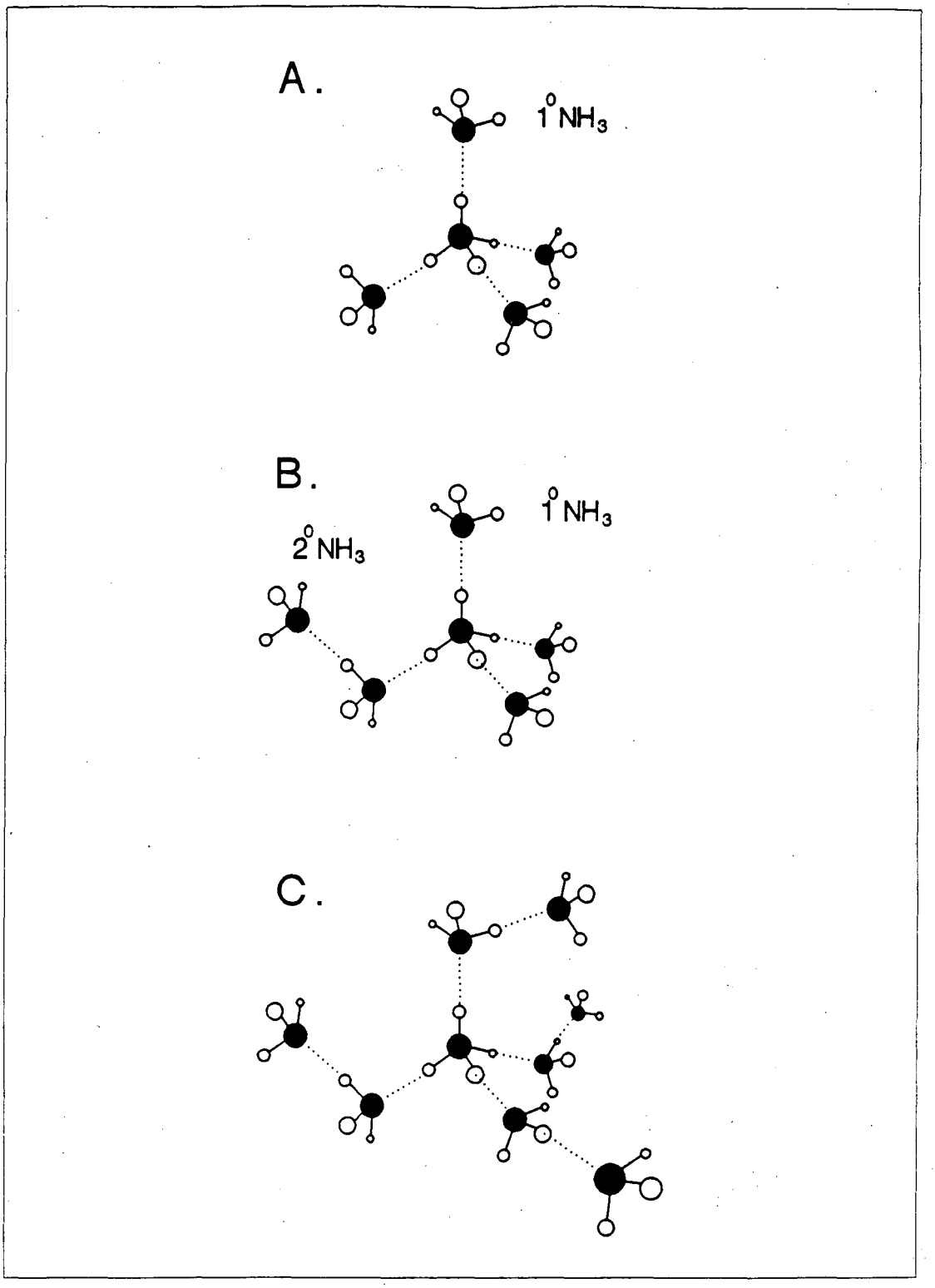

Figure 8.

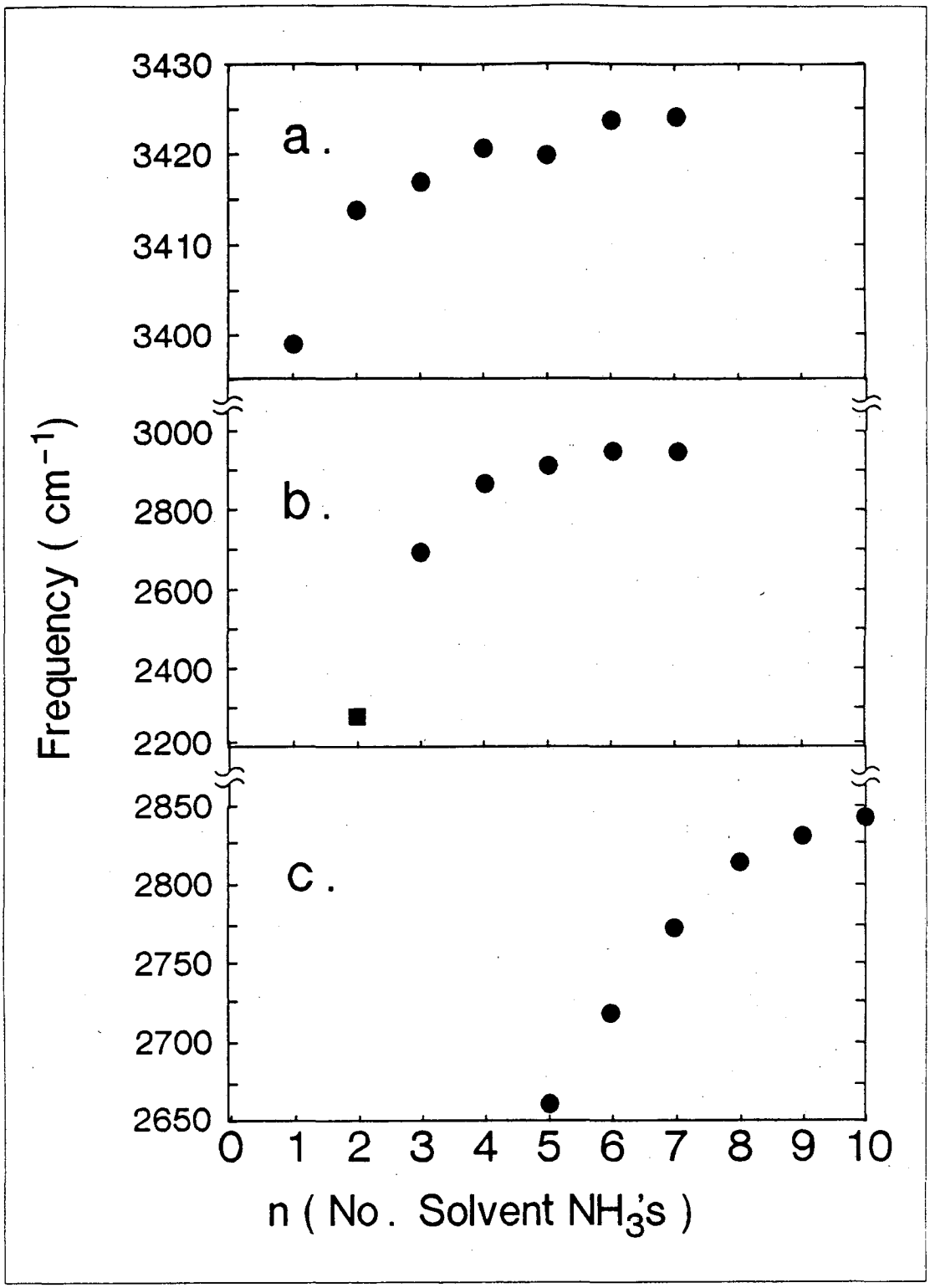
3430
3420
3410
3400
a.
3000
2800
2600
2400
2200
b.
2850
2800
2750
2700
2650
c.
Frequency (cm^{-1})
0 1 2 3 4 5 6 7 8 9 10
n (No. Solvent NH_3's)

Figure 9.

REFERENCES:

1. Epicurus, "Letter to Herodotus", Trans. C. Bailey, in The Stoic and Epicurean Philosophers, Ed. W.J. Oates (New York: Random House, 1940).

2. E.L. Wagner and D.F. Horning, J. Chem. Phys. **18**, 296 (1949).

3. J. P. Mathieu and H. Poulet, Spectrochim. Acta A **16**, 696 (1960).

4. J. Corset, P. V. Huong and J. Lascombe, Spectrochim. Acta A **24**, 2045 (1968).

5. A. M. Hogg and P. Kebarle, J. Chem. Phys. **43**, 449 (1965).

6. A. M. Hogg, R. M. Haynes, and P. Kebarle, J. Am. Chem. Soc. **88**, 28 (1966).

7. S.K. Searles and P. Kebarle, J. Phys. Chem. **72**, 742 (1968).

8. J. D. Payzant, A. J. Cunningham and P. Kebarle, Can. J. Chem. **51**, 3242 (1973).

9. I. N. Tang and A. W. Castleman Jr., J. Chem. Phys. **62**, 4576 (1975).

10. M. R. Arshadi and J. H. Futrell, J. Phys. Chem. **78**, 1482 (1974).

11. S. T. Ceyer, P. W. Tiedemann, B. H. Mahan, and Y. T. Lee, J. Chem. Phys. **70**(1), 14 (1979).

12. A. Pulman and A.M. Armbuster, Chem. Phys. Lett. **36**, 558 (1975).

13. K. Hirao, T. Fugikawa, H. Konishi, and S. Yamabe, Chem. Phys. Lett. **104**, 184 (1984).

13. C. S. Gudeman and R. J. Saykally, Ann. Rev. Phys. Chem. **35**, 387 (1984).

14. M. W. Crofton and T. Oka, J. Chem. Phys. **79**, 3157 (1983); **86**, 5983 (1987).

16. Eckhard Schafer and Richard J. Saykally, J. Chem. Phys. **80**(9), 3969 (1984).

17. H. A. Schwarz, J. Chem. Phys. **72**, 284 (1980).

18. J. M. Price, M. W. Crofton and Y. T. Lee, J. Chem. Phys. **91**, 2749 (1989).

19. S.W. Bustamente, Ph.D. Thesis, Univeristy of California at Berkeley, (1983).

20. S.W. Bustamente, M. Okumura, D. Gerlich, H. S. Kwok, L. R. Carlson, and Y. T. Lee, J. Chem. Phys. **86**, 508 (1987).

21. M. Okumura, Ph.D. Thesis, University of California at Berkeley, (1986).

22. L. I-C. Yeh, Ph.D. Thesis, University of California at Berkeley, (1988).

23. H.A. Enge, Rev. Sci. Instrum. **30**, 248 (1959); C.F. Giese **30**, 260 (1959); C-S. Lu and H.E. Carr **33**, 823 (1962).

24. S. Taya, I. Kanomatata, H. Hirose, T. Noda, and H. Matsuda, Int. J. Mass Spectr. and Ion Phys. **26**, 237 (1978).

25. W. Demtröder Laser Spectroscopy: Basic Concepts and Instrumentation. (Springer-Verlag Press, New York, 1982); and V. S. Letokhov Nonlinear Laser Chemistry: Multiple-Photon Excitation (Springer-Verlag press, New York, 1983).

26. R.N. Daly, Rev. Sci. Instrum. **31**, 264 (1960).

27. See ref. 18.

28. P.J. Robinson and K.A. Holbrook, Unimolecular Reactions, (Wiley-Interscience, New York, 1972).

29. R. Remington and H.F. Schaefer III., unpublished results.

30. M.D. Newton and S. Ehrenson, J. Am. Chem. Soc. **93**, 4971 (1971).

31. M.D. Newton, J. Chem. Phys. **67**, 5535 (1977).

32. A. Potier, J.M. Leclercq, and M. Allavena, J. Phys. Chem. **88**, 125 (1984).

33. G.V. Yukhnevich, E.G. Kokganova, A.I. Pavlyuchko, and V.V. Volkov, J. Mol. Struct. **122**, 1 (1985).

34. M. Okumura, L.I-C. Yeh, J.D. Meyers, and Y.T. Lee, J. Chem. Phys. **85**, 2328 (1986).

35. L.I-C. Yeh, M. Okumura, J.D. Myers, J.M. Price and Y.T. Lee, J. Chem. Phys. **91**(12), 7319 (1989).

36. C.I. Ratcliffe and D.E. Irish, Water Science Reviews 2, F. Franks, ed. (Cambridge University Press, Cambridge, 1986); Water Science Reviews 3, 1988.

37. S. Scheiner and L.B. Harding, J. Am. Chem. Soc. **103**, 2169 (1981).

38. K. Hirao, T. Fujikawa, H. Konishi, and S. Yamabe, Chem. Phys. Lett. **104**, 184 (1984).

39. S. Scheiner, Acc. Chem. Res. **18**, 174 (1985).

40. W. S. Benedict, E. K. Phyler, and E. D. Tidwell, J. Chem. Phys. **32**, 32 (1960).

41. G. Herzberg, Infrared and Raman Spectroscopy (Van Nostrand, Princeton, 1945).

42. W.F. Bennett and C.F. Meyer, Phys. Rev. **32**, 888 (1928).

43. N.L. Owen, "Studies of Internal Rotation by Microwave Spectroscopy" in Internal Rotation In Molecules W.J. Orville-Thomas, ed. (Wiley Interscience, New York, 1974).

44. P.R. Bunker and H.C. Longuet-Higgins, Proc. Roy. Soc. (London), Ser. A **280**, 340 (1964).

45. D. Papousek, J. Mol. Spectr. **28**, 161 (1968).

46. W.B. Olson and D. Papousek, J. Mol. Spectr. **37**, 527 (1971).

47. I. M. Mills and H.W. Thompson, Proc. Roy. Soc. (London), Ser. A **226**, 306 (1954).

48. J. Nakagawa, M. Hayashi, Y. Endo, S. Saito and E. Hirota, J. Chem. Phys. **80**, 5922 (1984).

49. G.T. Fraser, K.R. Leopold, and W. Klemperer, J. Chem. Phys. **81**, 2577 (1984).

50. M. Okumura, L. I-C Yeh, and Y.T. Lee, J. Chem. Phys. **83**, 3705, (1985).

51. M. Okumura L.I-C Yeh, J.D. Meyers, and Y.T. Lee, J. Chem. Phys. **85**, 2328, (1986).

52. G.C. Pimentel, M.O. Bulanin, and M. Van Theil, J. Chem. Phys. **36**, 500 (1962).

53. G. Herzberg, Infrared and Raman Spectra of Polyatomic Molecules (D. Van Nostrand, New York, 1945) p. 231, 307.

54. G.C. Pimentel, M.O. Bulanin and M. Van Thiel, J. Chem. Phys. **36**, (1962).

55. J.F. Bertran, J. Mol. Str. **95**, 9 (1982); J. Corset and J. Lascombe, J. Chem. Phys. **64**, 665 (1967).

56. M. Vernon, Ph.D. Thesis, University of California, Berkeley, 1982.

57. D.D. Nelson, Jr., G.T. Fraser, and W. Klemperer, J. Chem. Phys. **83**, 6201 (1985).

CHAPTER IV.

The Hydrated Ammoniated Ammonium Ion Clusters:

$NH_4^+(NH_3)_n(H_2O)_m$ (n+m = 4)

"Moreover, the atoms must move with equal speed, when they are borne onwards through the void, nothing colliding with them. For neither will the heavy move more quickly than the small and light, when, that is, nothing meets them: nor again the small more quickly than the great, having their whole course uniform when nothing collides with them either..."

- Epicurus, "Letter to Herodotus", c.a. 200 B.C.[1]

4.1 INTRODUCTION:

Previously, the observation of the infrared spectra of the mass selected ionic clusters $NH_4^+(NH_3)_n$, and $H_3O^+(H_2O)_m$ (n=1 to 10 and m=1 to 8) has been reported (See Chapters II and III).[2] In these studies, the differences between two given neutral solvent molecules in a cluster come only from their positions within the solvation shell structure about the ion. It was found in these experiments, that for the smaller ammoniated ammonium ions (n=1 to 6), the spectra revealed structures that could be assigned to the nearly free internal rotation of the solvent molecules within the clusters. In contrast, the hydrated hydronium ions showed no such structure. In the case of the ammoniated ammonium ions, this free rotation manifested itself only in the first solvation shell. The present work extends these studies of the solvated proton to the chemically heterogeneous environments found in the "mixed" clusters, where the NH_4^+ ion core of the cluster is surrounded by both water and ammonia molecules. Presented here are the spectra for the ammonium ion, NH_4^+, solvated by four solvent molecules (either water or ammonia in any combination) over the frequency range of 2600 to 4000 cm^{-1}.

4.1.1 Previous Experimental Studies

Previous experimental studies of the mixed clusters have been limited to kinetic and thermodynamic measurements of the reactions:

$$NH_4^+(NH_3)_n(H_2O)_{m-1} + H_2O \rightleftharpoons NH_4^+(NH_3)_n(H_2O)_m \quad (1)$$

and,

$$NH_4^+(NH_3)_{n-1}(H_2O)_m + NH_3 \rightleftharpoons NH_4^+(NH_3)_n(H_2O)_m \quad (2)$$

Summarized in Table I of Chapter I are measurements of the ΔH°, of formation for the reactions shown above, for the n+m=4 cluster ion systems in the gas phase and for several other values of n+m. The table also shows the analogous data for the pure $NH_4^+(NH_3)_n$, $H_3O^+(H_2O)_m$ and $NH_4^+(H_2O)_m$ systems over a range of cluster sizes.

Measurements of this sort may be used to obtain structural information about a complex by mapping the ΔH° of formation for individual clustering steps as a function of cluster size. Discontinuities in this curve at a particular value of n or m, suggest the completion of a solvation shell about the ion. Meot-Ner and others have developed a quantitative method for evaluating these data to determine whether an ion has distinct solvation shells for a particular ligand type.[3] The pure hydrated hydronium, $H_3O^+(H_2O)_m$ and the ammoniated ammonium $NH_4^+(NH_3)_n$ systems both show discontinuities which have been correlated with the completion of the first solvation shell. For hydronium solvated by water the first shell fills at the m=3 cluster, and for ammonium solvated by ammonia the n=4 cluster represents the completion of the first shell.

Previous spectroscopic measurements from this laboratory have supported these conclusions. Features were observed in both the hydrated hydronium ions and the ammonium ions that could be correlated with the first solvation shell ligands (1°) being perturbed by the presence of ligands in the second solvation shell (2°) at m=4, and n=5, respectively (See Chapters II and III). These features were not observed in the smaller clusters.

Thermodynamic measurements on the mixed cluster system where the ammonium ion is solvated by only water, $NH_4^+(H_2O)_m$, have not revealed the strong discontinuity at the m=4 to m=5 clustering step one might expect. Recent results my Meot-Ner et. al. do show a small discontinuity, but it can be removed by adjusting the ΔH° of formation for the m=3 to m=4 clustering step by only 1 kcal/mol. Within the experimental accuracy, there is no solvation shell effect for this ion. This suggests that there are a number of structural isomers of nearly equal energy associated with this system. The binding energy of a H_2O to the NH_4^+ ion core is apparently close to that of a H_2O to a 1° water molecule.

An examination of the ΔH° of formations for the three systems discussed so far, hydronium solvated by water, ammonium solvated by ammonia, and ammonium solvated by water shows that the ammonia molecule is more strongly bound in the smaller clusters than is the water molecule. In the largest clusters studied, the situation reverses, and water

becomes more strongly bound than ammonia. The "crossing point" is the n or m=4 clustering step. One sufficient, but not necessary interpretation of this data is that the ammonia molecule is more strongly bound in 1° solvation sites than is the water molecule and that the water is more strongly bound in 2° sites than the ammonia.

The above interpretation has some fairly strong support. Recent results from Shinohara et. al. wherein neutral clusters of ammonia and water in various proportions are ionized by VUV radiation have shown strongly enhanced stability of the $NH_4^+(NH_3)_n(H_2O)_{m=1}$ species starting at n+m=5.[4] For the clusters containing a total of five solvent molecules, it seems that the H_2O binds more strongly to the 1° NH_3's than does an ammonia. This comes from the fact that the relative intensity of the $NH_4^+(NH_3)_4(H_2O)_{m=1}$ ion is much larger than $NH_4^+(NH_3)_5$ even at substantially elevated partial NH_3 concentrations in the supersonic expansion from which the neutral clusters were formed.

4.1.2 Previous Theoretical Studies

Theoreticians have investigated both the thermodynamics and the structures of the mixed cluster systems as well. In a recent series of calculations, Deakyne has predicted the structures and stabilities for $NH_4^+(NH_3)_n$ n=3,4 and $NH_4^+(H_2O)_m$ for m=2-4.[5] These results are in general, consistent with the recent experimental results by Meot-Ner et. al. (See Ref. 5.), in that they show that at equilibrium, a number of structural isomers

can exist for the ammonium ion solvated by water at the m=4 level of solvation, and perhaps even at m=3.

Ab Initio calculations for the smallest hydrated ammonium ion have also been performed. The $NH_4^+(H_2O)_m$ system has been investigated by several workers for m=1,n=0[6]. These data suggest that the binding of the water to the cluster in this system occurs via simple hydrogen bonding, with the H_2O aligned along one of the N-H bonds of the ammonium ion along its C_2 axis.

Unfortunately, there has been to our knowledge no ab initio investigation of the higher hydrates of the n+m=4 cluster ion system. In fact, experimental data in this area are also rather sparse, with the measurements of Pyzant et. al. in 1975 (See ref. 24, Chapter I.) constituting the only systematic thermodynamic measurements on the substituted ions with m>1. Part of the motivation for the present work is to obtain information which may inspire a detailed theoretical investigation of these interesting systems where solvent-solvent interactions are of comparable strength to the solvent-ion core interactions. Previous results on the hydrated hydronium and ammoniated ammonium ions have shown that the technique of vibrational predissocation spectroscopy can reveal the location of a ligand within the solvation shell structure about an ion when the ligands are all the same. It will be shown for present case of the mixed

cluster ions, similar information can be obtained, even though the spectra increase in complexity.

4.2 EXPERIMENTAL DETAILS:

The experimental apparatus used in this work has been described previously (see Refs. and Chapter I).[7,8,9,10] Briefly, the hydrated ammoniated ammonium cluster ions were produced from a high pressure corona discharge source and subsequent supersonic expansion. Schematic diagrams of the source and the experimental apparatus are shown in figs. 1 and 2 of Chapter I. The corona discharge was maintained in 100-200 torr of gas (Matheson ultra high purity (UHP) He typically seeded with 10% UHP H_2 and trace amounts of H_2O and NH_3) flowing past a 1.2 KV potential from the discharge tip of the needle to the source body maintained at approximately 350 V above ground. The discharge current under these conditions ranged from 40-200 μamps. The source could be cooled from outside the machine by contact with a liquefied gas reservoir and was usually maintained at approximately -30° C. After passing through the discharge region, the ionized gas undergoes collisionally induced vibrational relaxation in the 1.0 mm long by 3.0 mm diameter drift region before expanding through the 70 μm expansion nozzle. It is estimated that an ion undergoes some 10^5 collisions in this region before leaving the source, resulting in the ion relaxing to a vibrational temperature near that of the source body by the time it reaches the nozzle.

Most of the clustering of the neutral gas around the ionic species and rotational cooling takes place during the supersonic expansion between the

nozzle and the skimmer. Typical pressures in the source chamber are 4 x 10^{-5} to 2 x 10^{-4} torr while running the experiment. To prevent internal excitation and dissociation of the ionic clusters through collisions with the background gas in the expansion and to maintain a narrow kinetic energy distribution for the clusters, the potential of the skimmer was maintained within 1 volt of that of the source body. A shielding grid surrounding the expansion region maintained at 350 V prevented stray fields from affecting the ion trajectories in this region.

After the skimmer, the ion beam enters a second differential pumping region containing collimating and focusing optics. The pressure in this second region is typically an order of magnitude lower than that of the source region. The beam is then directed into a third differentially pumped region maintained at 10^{-8} torr and through the entrance slits of a 60° sector magnet mass analyzer (Resolution = $M/\Delta M$ = 200). To aid in transmission of the ion beam and to enhance mass resolution, a set of quadrupole lens pairs is placed before and after the magnet.[11,12]

The mass selected beam passes into the final differentially pumped region maintained at 10^{-9} torr. Here, the beam is bent 90° in a DC quadrupole field, decelerated to less than 0.5 eV, and focused into a radio frequency (RF) octopole ion trap through an entrance aperture lens. Ions are typically allowed into the trap for 1 ms before the potential of the entrance lens is raised, and the ions confined inside the octopole.

The confined, mass selected clusters are then vibrationally excited by a pulsed, tunable infrared laser. (Quanta Ray, IR WEX 8 ns pulse, 0.3 - 1.2 cm^{-1} resolution, 0.7cm^{-1} absolute frequency accuracy, 0.2 - 1.0 mj/pulse in the 2600-4000 cm^{-1} region) The density of ionic clusters in the ion trap is not high enough to allow the measurement of photon absorptions directly. In order to detect the absorption of an IR photon by an ionic cluster, IR multiphoton dissociation processes were used to exclusively dissociate the vibrationally excited ionic clusters. In previous publications, we have described a number of excitation schemes for the study of ionic clusters using this technique. Depending on the density of states and the dissociation energy of the species under study, one of two excitation schemes described below was employed.

For clusters studied here, the energy required to predissociate one solvent molecule is exceeded by absorbing two photons in the usual tuning range of 2.5-3.8 μm. At an energy in the 2600-4000 cm^{-1} region, all of the ionic clusters (n=1-10) are literally in the "quasi-continuum" region[13] after the absorption of one photon and an additional IR photon from the tunable laser may be absorbed to induce vibrational predissociation. For very small cluster ions, however, fragments are not usually detectable with the tunable laser only, presumably because the fluence was not sufficient for the absorption of more than two photons. For these ions, use of the CO_2 laser with an irradiation time of at least 10 msec at >10 watts/cm^2 is usually

required to achieve a measurable degree of dissociation of vibrationally excited clusters. In those instances where spectra of a given ion were obtained by both one and two color schemes, they were found to be the same within experimental error, indicating that spectral features in the multiphoton dissociation spectra normally reflect the cross section for absorption of the first photon rather well.[21]

If the clusters absorb sufficient energy through one of the schemes described above, the loss of one or more solvent molecules from the parent cluster may occur. The potential on the exit aperture is lowered 1 msec after the laser pulse, extracting cluster ions of all masses from the trap. These ions are filtered by a second mass analyzer, a quadrupole mass spectrometer tuned to pass only the daughter ions smaller than the parent cluster by one solvent molecule.

Daughter ions are counted using a Daly ion detector[14] for each laser shot. Background daughter ion counts resulting from the decay of metastable parent ions in the RF ion trap are monitored in a separate data cycle with the laser off at each wavelength, and subtracted from the laser on signal. Typical background count rates usually amount to no more than 1% of the signal at the stronger absorption maxima.

Laser power is monitored at each data point and spectra are normalized for the tunable infrared power using a simple linear power

dependence. For a typical experiment, signals were averaged for about 600 laser shots at each wavelength in the 2600 to 4000 cm^{-1} region.

4.3 RESULTS AND ANALYSIS:

4.3.1. Mass Spectra

The distribution of ionic clusters produced by the corona discharge source could be shifted by altering the temperature of the source body, the backing pressure of the supersonic expansion, or the ratio of NH_3 to H_2O in the He carrier gas. Little dependence was observed between the peak of the cluster ion distribution and the magnitude of the current used in the discharge for a given value of the above parameters, indicating that the ions were at a reasonable equilibrium with the temperature of the source body before expansion through the nozzle.

Maintaining a high level of mass resolution for the first mass spectrometer is of critical importance, as NH_3 and H_2O differ by only one mass unit. The quality of the mass resolution and the distribution of cluster sizes produced by the source could be easily monitored by sweeping the field of the 60° sector magnet and counting the ions that arrive at the Daly detector with the second mass filter set to transmit all ions. One such mass spectrum with the assigned mass peaks is shown in fig. 1. This spectrum was taken using a low concentration of ammonia and only trace ammounts of water in the He carrier gas (<1%) , a backing pressure of 200 torr behind the nozzle and with the source body cooled to -30°C through contact with liquid freon 12. One can see that under these conditions, nearly complete separation of the different n,m pairs could be obtained. A

very low difference between the applied voltages on the source nozzle and the skimmer in the expansion region was required (≤1 Volt) to maintain this level of resolution. Fringing field effects degrade the resolution at higher voltage differences.

One will note that the mass of $H_3O^+(H_2O)_m(NH_3)_n$ is the same as $NH_4^+(NH_3)_{n-1}(H_2O)_{m+1}$. This could conceivably lead to contamination of a spectrum by cluster ions with a different ion core. However, when a hydronium species H_3O^+ encounters NH_3, a proton transfer reaction is very likely to take place resulting in the formation of the species NH_4^+ and H_2O. Since the proton affinity of H_2O is 6.5 eV vs. 8.9 eV for NH_3,[15] the energy released by the process is in the neighborhood of 2 eV, or about 40 kcal/mole. The strong favoring of the proton transfer reaction to the ammonium side is what leads us to assign the mixed cluster peaks in our mass spectra to the isomers containing an ammonium rather than a hydronium core.

4.3.2 IR Vibrational Predissociation Spectra:

4.3.2.1 $NH_4^+(NH_3)_4$: (n=4,m=0)

The spectrum of the pure ammoniated ammonium ion $NH_4^+(NH_3)_4$ appears in figs. 5a and 6a. Presented in previous publications, (See ref. 2.) these data are shown for completeness. Theoretical calculations and IR spectra support a structure for this cluster where the ammonium ion is solvated by four equivalent 1° NH_3 molecules. Spectroscopic measurements, theoretical calculations and thermodynamic measurements all suggest that this structure represents the completion of the first shell of the ammonium ion. No evidence has been found either spectroscopically or from theoretical calculations for a significant equilibrium contribution from other structural isomers. In this case the binding energy of an NH_3 to the NH_4^+ ion is significantly greater than to a 1° NH_3 molecule. A schematic representation for the structure of this cluster appears in fig. 9a.

Three main transitions are assigned for this ion in the 2600 to 4000 cm^{-1} region. The first and most intense, at 2865cm^{-1} is due to the triply degenerate antisymmetric stretching mode, ν_3 of the NH_4^+ ion core of the cluster (See fig. 2 and table I.). This band was first observed in the early direct absorption measurements of ammonia in a glow discharge performed by Schwarz in 1980.[16] Our measured position for the cold cluster ion agrees well with the 2867cm^{-1} value he obtained at significantly higher temperatures.

The second, much weaker feature at 3095cm^{-1} was also observed by Schwarz at 3087cm^{-1}. This has been assigned to the first overtone of the doubly degenerate bending mode $2\nu_4$ of the ion core (See fig. 2 and table I). Schwarz was able to perform measurements of the totally deuterated cluster, and used this bend in conjunction with the antisymmetric stretching motion to obtain the Teller-Redlich product ratio for this ion.[17] By a comparison of the ratio obtained from methane and deuterated methane spectra, he was able to demonstrate that in the n=4 cluster, the central ion had T_d symmetry.

The third major band system had not been observed in any direct absorption experiment. Centered at 3420.5cm^{-1} this vibrational transition arises from the triply degenerate antisymmetric stretch ν_3 of the solvent ammonia molecules (See fig. 3 and table I.). Superimposed on the band are a series of subbands spaced by approximately 12 cm^{-1}, or roughly twice the rotational constant of ammonia about its C_3 axis. We have assigned this structure to the nearly free internal rotation of the solvent ammonias about their N-H-N hydrogen bonds to the ion core. The notation used in the assignment tables to describe this structure is that reserved for vibration-rotation transitions of strongly prolate symmetric top molecule. While this notation is not strictly correct for an internal rotation transition of a subgroup within a spherical top molecule, we find it convenient, as it follows from the intuitive picture of an ammonia molecule attached to a "wall"

along its C_3 axis that is free to rotate. At the present level of spectroscopic resolution, the experimental data can be fit to the limit of experimental error by such a model. No absorptions were observed at higher frequencies. Further discussion of this system may be found in ref. 2.

4.3.2.2 $NH_4^+(NH_3)_3(H_2O)$: (n=3,m=1)

The n=3, m=1 cluster is a particularly interesting case. On one hand it should be one of the simpler clusters in the n+m=4 series to assign as the differences between its spectrum and that of the pure n=4 ammoniated ammonium ion are due only to the exchange of a single ligand. On the other hand, of the mixed clusters, none has a lower energy difference for the exchange reaction:

$$NH_4^+(NH_3)_{n+1}(H_2O)_{m-1} + H_2O \rightleftharpoons NH_4^+(NH_3)_n(H_2O)_m + NH_3 \qquad (3)$$

According to Payzant, (See ref. 24, Chapter I.) a ΔH° of only 0.8 Kcal/mole separates these two species for the n=3, m=1 system. A consequence of this, discussed earlier is that since the water appears to bind quite strongly to the 2° ligands, a number of structural isomers could conceivably contribute to the spectrum at equilibrium. The spectrum for this ion appears in figs 5b and 6b. Some possible structural isomers appear in fig. 7b(I-III).

Starting at low frequency, we observe a strong transition at 2808cm^{-1} that seems to correlate with the 2865cm^{-1} peak of the pure n=4 ammoniated ammonium ion. If we assume for the moment, a cluster geometry of the sort shown in fig. 7b(I), where the water is attached to one of the N-H bonds

of the ion core, we see that the environment around the ion has assumed a symmetry distorted from its original T_d configuration. If we look at the vibrations of the ammonium ion under this distorted T_d framework, we find that the original triply degenerate asymmetric stretch, ν_3 would evolve into a pair of doubly degenerate stretches, $\tilde{\nu}_3$' where two of the N-H bonds are still in contact with 1° NH_3's only, and a singly degenerate asymmetric stretch, ν_3" where the N-H oscillation involves contact with the 1° H_2O.

The ν_3' stretch is expected to be of a **lower** frequency than the original ν_3 vibration, as the electron donating capacity of the water molecule is less than that of an ammonia. Consequently, the ammonium ion bonds involved only with 1° NH_3's in this cluster will be proportionally weaker than they would in the pure ammoniated ammonium ion case. The ν_3" band however, is of different type than previously measured. Here the N-H bond is coupled to a 1° water molecule. The frequency of this stretch is expected to be of **higher** frequency than the corresponding N-H stretch with a 1° NH_3 involved, as the binding energy of the ammonia to the core is so much larger than that of the water. -- We assign the ν_3" band to the feature appearing at 3174cm^{-1}.

This breaking of the T_d symmetry about the NH_4^+ ion would allow the ν_1 symmetric stretch of the ion to become weakly IR active. This vibration has been observed previously in the spectra of the $NH_4^+(NH_3)_3$ and $NH_4^+(NH_3)_5$ systems. In each case, the band was of lower frequency than the

antisymmetric stretch and of reduced intensity. (32 cm^{-1} to the red for the n=3 cluster of the antisymmetric stretching band, and 30 cm^{-1} to the red in the n=5 system.) The weak feature observed at 2697cm^{-1} for the n=3, m=1 system we tentatively assign to the analogous ν_1 type stretch.

If the cluster assumed either isomer 7b(II) or 7b(III), a similar breaking of the ν_3 band of the core into higher and lower frequency components should be observed, but with the high frequency component being shifted to much higher frequency than for isomer 7b(I) as a result of it being unbound. A similar free N-H stretch is observed in the $NH_4^+(NH_3)_3$ system. Occurring at 3374.1cm^{-1}, this feature was extremely sharp compared to the hydrogen bonded stretches at lower frequency. We have assigned the analogous stretch to the feature appearing at 3378cm^{-1} in the n=3, m=1 spectrum. This shift to higher frequency of +4cm^{-1} can be attributed to the slight electron donating contribution from the water, not available in the pure n=3 ammoniated ammonium ion case. Which of the two isomers, 7b(II) or 7b(III) gives rise to this structure will be discussed below.

At higher frequencies, contributions to the spectrum from the solvent molecules are observed. Centered at 3418cm^{-1} is the same ν_3 antisymmetric stretch of the solvent NH_3's with the internal rotation structure observed in $NH_4^+(NH_3)_4$. Above 3600cm^{-1} new features appear, obviously correlated with the addition of a water to the cluster. Shown in fig. 6f is the spectrum of

the pure hydrated hydronium ion $H_3O^+(H_2O)_4$. This spectrum shows three main features, the symmetric and antisymmetric H_2O stretches ν_1 and ν_3 and a free O-H stretch of a 1° H_2O bound by a H_2O in the second solvation shell (Recall that for the hydronium ion, the first shell fills at m=3.). These peaks appear at 3647, 3708, and 3733 cm^{-1}, respectively. There is an obvious correlation between the symmetric stretch peak and the 3642 cm^{-1} feature in the n=3,m=1 spectrum. We assign it to the symmetric stretch of the water.

Unlike the pure hydrated hydronium ions, the spectrum of the mixed clusters show features which can be assigned to the internal rotation of the water molecules in the first solvation shell. Assuming the observed structures come from those clusters assuming the structure of isomer 7b(I), the internal rotation the water may undergo is limited to motion about its local C_2 axis. Separation of the $\Delta K=\pm 1$ Q-branch stacks should be about twice the rotational constant of the H_2O molecule about this axis since the rotational constant for the rest of the complex is so small. Indeed, the observed separation between the three features assigned to this motion is about 29 cm^{-1}, or 2 x B_{H20} = 14.5 cm^{-1}. We have assigned the features at 3716, 3744 and 3774 to the $^PQ_1$, $^RQ_0$, and $^RQ_1$ bands superimposed on the ν_3 vibration of the water. Without taking in account the statistical weights for these transitions, at our present estimated kT of 25cm^{-1}, one would expect

the K=1 structure ($^{P}Q_1$ and $^{R}Q_1$) to be less intense than the K=0 ($^{R}Q_0$) band from the Boltzman factor:

$$\frac{I(K-1)}{I(K-0)} = e^{-(14.5/25)} = 0.56 \qquad (4)$$

However, for water, the statistical weight with respect to K quantum number is 1 for K=even and 3 for K=odd. Taking this into account, the calculated 1.68 : 1 : 1.68 ratio is much more in keeping with the observed intensities. This sort of structure is limited to a perpendicular transition, which explains why the parallel symmetric stretching transition shows no such structure.

This internal rotation structure should not be observable for the alternate isomer in fig 7b(II), as the influence of the NH_3 in the 2° site wold quench the free rotation. Such structure might be observed for the isomer in fig. 7b(III), where the H_2O is in the 2° site, but no such structure is observed for the larger hydrated hydronium ions from 2° H_2O's. While this by no means precludes such structure in the case of the mixed cluster, we have been able to make consistent assignments of all the observed rotational structure with reference only to isomer 7b(I), where the water assumes a 1° site attached to the N-H bond of the NH_4^+ along its C_2 axis.

One feature in this region which is not explained by isomer 7b(I) is the band at 3700 cm^{-1}. This feature is significantly broader than the nearby internal rotation structure, suggesting that hydrogen bonding is involved.

We have assigned this to the free O-H stretch of a 1° H_2O bound by a 2° NH_3 **vis** isomer 7b(II). This structure is consistent with the observed free N-H stretch transition of the core, but is rather surprising, given H_2O's propensity to bind to 2° sites over ammonia. One would expect that isomer 7b(III), with the water in the 2° site to be more likely.

Temperature dependent studies have been performed, where the backing pressure used in the supersonic expansion has been doubled, and the source body has been maintained at a lower temperature while the spectrum for this ion has been measured. A significant decrease in intensity of the free O-H stretching band relative to the free N-H stretch of the core was observed. This suggests the presence of a mixture of isomer 9b(II) and 9b(III) at equilibrium, with isomer 7b(III) being more stable.

A variation on isomer 7b(I). merits some discussion. It might be possible that the water molecule would bind to the ammonium ion oriented along the p orbital containing the lone pair electrons of the oxygen. In this case the water molecule would be substantially tilted from the orientation shown in the figure. This tilted orientation of H_2O is observed in the hydrogen bonding of ice, HX-H_2O (X=Cl, Br, etc.) and other complexes[18]. There is no definite evidence in the spectrum for the tilted variation of the isomer, however.

4.3.2.3 $NH_4^+(NH_3)_2(H_2O)_2$: (n=2,m=2)

As the mixed cluster becomes more hydrated, contributions to the spectrum resulting from the presence of the ammonia solvent molecules drastically diminish. For both the NH_4^+ core stretches bound to NH_3's and those of the 1° NH_3's themselves, there is a general reduction in intensity relative to core vibrations involved with bonds to the 1° H_2O's, and H_2O solvent transitions.

Assume for a moment the cluster geometry shown in fig. 7c(I), where the two water molecules assume 1° solvation sites around the ion. Under this configuration, the environment around the NH_4^+ has something like C_{2v} symmetry. Consequently, the original triply degenerate ν_3 antisymmetric stretch, and the singly degenerate ν_1 symmetric stretch of the ion core would evolve into two symmetric and antisymmetric pairs. One pair would be dominated by the N-H stretches of the NH_4^+ bound only to waters, and an analogous symmetric/antisymmetric pair for the N-H's bound only to ammonias.

At 2749 cm^{-1} is the peak we assign to the antisymmetric stretch of the ammonium ion bound only to 1° NH_3's. Slightly to the red of this feature at 2700 cm^{-1} is a shoulder we assign to the weaker symmetric stretch. At higher frequencies the analogous symmetric/antisymmetric stretching pair are observed at 3121 and 3154 cm^{-1} of the N-H stretches bound to 1° H_2O's. As in the case of the pure ammoniated ammonium ions, and the n=3, m=1

system, the symmetric stretches are of lower relative intensity than the antisymmetric stretches.

The transitions due to the absorptions of the solvent molecules are essentially the same as those observed for the n=3, m=1 cluster. The ν_3 band of the ammonias appears at the same frequency and with the same internal rotation structure observed before. This feature is significantly reduced in relative intensity as one might expect. The water stretches, both symmetric and antisymmetric show the same general structure: the symmetric band appearing at 3642 cm^{-1} is at the same frequency with greatly increased relative intensity. the antisymmetric stretch still shows the internal rotation structure observed for n=3, m=1, but the peaks are significantly broader. Assignments and peak positions appear in table II.

There is evidence for the existence of isomers other than where all the waters and ammonias assume 1° solvation sites. The free N-H stretching mode is again observed at 3381 cm^{-1} as is a peak which corresponds to the free O-H stretch of the a water at 3701 cm^{-1} bound by a ligand in a 2° site. Several isomers could again produce these structures. Further discussion of the possible binding sites for the ligands in the mixed clusters will be limited to the conclusions section.

4.3.2.4 $NH_4^+(NH_3)(H_2O)_3$ (n=1,m=3) and $NH_4^+(H_2O)_4$ (n=0,m=4):

The final two spectra in the series continue the previously observed pattern. The NH_4^+ core stretches involved in H-bonds with the NH_3's further decrease in relative intensity, and shift farther to the red with increasing hydration. The core vibrations of N-H bonds involved with H_2O increase in relative intensity. For the n=1, m=3 cluster we observe the symmetric and antisymmetric stretches of the core bound to only 1° H_2O's at 3091 as a shoulder and at 3136 cm^{-1}. Assuming that the $NH_4^+(H_2O)_4$ ion maintains the structure shown in fig 7e(I) where the 1° sites are all filled by waters, the symmetric stretch would no longer be IR active for this ion as the environment around the core has the same T_d symmetry as the ion. Indeed, only one core transition is observed for the n=0, m=4 system with any appreciable intensity. It appears at 3116 cm^{-1} and is completely analogous to the ν_3 antisymmetric stretch band in the $NH_4^+(NH_3)_4$ system.

The ν_3 transition for the solvent ammonia is, of course, absent in the n=0, m=4 spectrum, but look substantially different in the n=1, m=3 system than for previously measured spectra. --No evidence of internal rotation structure is seen, and only a broad, weak absorption is measured with a maximum at 3415 cm^{-1}.

The symmetric and antisymmetric stretches of the waters are still seen in both spectra, and the antisymmetric stretching band broadens considerably by m=4. The internal rotation structure is still observed for

the water, although by m=4, the central $^{R}Q_0$ band is present only as a partially resolved shoulder on the $^{P}Q_1$ band.

Structures from alternate isomers are observed for the n=1, m=3 system, but cannot be assigned with any certainty to the n=0, m=4 cluster. For the former, the free N-H stretch of the core is still observed at 3381 cm^{-1} and a shoulder is present to the red of the $^{P}Q_1$ band of the H_2O antisymmetric stretch at 3700 cm^{-1} that can be assigned to the free O-H stretch of a water perturbed by a ligand in a 2° site.

4.4 SUMMARY AND CONCLUSIONS:

As in the case of the hydrated hydronium and ammoniated ammonium ions, the spectra of the mixed cluster ions contain features that can be assigned to transitions arising from both the motions of the solvent molecules and the ion core of the clusters. Analysis of the solvent transitions shows that for the molecules in 1° sites, (Sites where hydrogen bonding takes place along one of the N-H bonds to the core) internal rotation about the hydrogen bond is virtually unhindered. For ammonia solvent molecules, this bond coincides with the NH_3 C_3 molecular axis. Similarly, for H_2O solvent molecules, the rotation takes place about the C_2 molecular axis.

These results are in agreement with previous measurements for the ammoniated ammonium ions, where free rotation for the NH_3 subgroups was first reported for $NH_4^+(NH_3)_4$ (See ref. 2 and Chapter III), but constitute a new phenomenon for water molecules within an ionic cluster. The only observed rotational structures measured for a hydrated hydronium ion, were found in the $H_3O^+(H_2O)$ (m=1) system.[19] Here, rotational structures were observed, but there has been little evidence that these originated from anything other than simple rotation of the whole cluster.

Internal rotation has been observed in several of the Van der Waals molecules investigated to date. H_2O-CO_2, NH_3-CO_2 among others, have been probed by both microwave and infrared spectroscopies showing internal

rotation structures.[20] As one might expect, these species were found to have low barriers to the internal rotation motion (< 15 cm^{-1}). For the more strongly bound ionic clusters, the results presented here represent the only spectra other than the ammoniated ammonium clusters in which internal rotation has been observed. This situation will doubtlessly change in the near future as more species are investigated.

The discussion of hydrated hydronium spectra in Chapter II is conspicuous for the absence of any mention of internal rotation. Indeed, the internal rotation barrier for H_2O in hydrated hydronium is clearly much higher than it is in $NH_4^+(NH_3)_3H_2O$ or for ammonia in the $NH_4^+(NH_3)_n$ complexes ($n \leq 7$). The presence of a nonbonding electron pair in the p_x and p_y orbitals of water would be a reasonable suggestion for why the solvents in the ammoniated ammonium species rotate freely ($n \leq 7$) but the waters in hydrated hydronium do not. The studies of $NH_4^+(NH_3)_3H_2O$ and similar species such as $NH_4^+(NH_3)_2(H_2O)_2$ however, where internal rotation of the waters **is** observed, show that the reluctance of H_2O to freely rotate in hydrated hydronium complexes is perhaps dictated by more complicated factors than just the electronic structure of the solvent molecules taken alone. Detailed analyses are currently under way of the mixed cluster species in hopes of better understanding the water-water and water-core interactions that give rise to these effects.

The features assigned to the motions of the ion core of the clusters also show novel effects due to the influence of the complex heterogeneous environment. Transitions have been observed arising from the motions of the N-H bonds in three types of environments: free N-H stretches, where no hydrogen bonding of the 0° N-H bond takes place; N-H stretches involved in bonds with both 1° NH_3's and N-H stretches involved in bonds with 1° H_2O's. As the ratio of water to ammonia in the cluster changes, the positions of the hydrogen bound core features changes quite systematically while for the free N-H stretches, the frequencies of the transistion changes little ($< 2\ cm^{-1}$ difference between a given n,m pair when the free N-H band can be observed.).

With increasing hydration (increasing m), the bound N-H stretches shift to the red, both those involving ammonia and those involving water, indicating that the core bonds are weakening. This red shift is essentially linear in m, and is due to the fact that ammonia is a supperior electron donating species compared to water.

After an initial red shift of the ammonium ion stretching frequency from its gas phase value of 3343.26 cm^{-1} due to the influence of the ligands, it was found for the ammoniated ammonium ions, that the core vibrational frequencies increased with increasing n as the ammonia molecules could donate more and more electron density to the core, strengthening the core N-H oscillators. For a value of n+m=4, the maximum electron donating

capacity of the ligands will be found in the case where the core is surrounded by the most basic environment possible, pure ammonia, or n=4, m=0. As the environment becomes less and less basic as m increases, the core bonds weaken, and not surprisingly, a redshift occurs. The frequencies of the N-H core stretching vibrations bound to both water and ammonia in the n+m=4 cluster ion series are plotted in fig. 8 as a function of m. One can see that there is a strong shift of the frequencies of the core vibrations with increasing m even though the two ligands (water and ammonia) are bound with nearly the same energy and only differ by one mass unit.

Our understanding of the way atoms and molecules are held "by the entanglement of their own interlocking shapes" (See Chapter I, ref. 1.) has been greatly enhanced in recent years by the study of cluster systems. Studying the infrared spectroscopy of ionic clusters has been shown to be a valuable way of learning about the organization of molecules around an ion, and the onset of solution phase properties. Future studies employing this technique will undoubtedly lead to further insight into the nature of these complex interactions.

TABLE Ia: Molecular Constants for NH_4^+, NH_3 and H_2O.
(All units are in cm^{-1} except ζ which is dimentionless.)

Molecule or Ion:	Symmetry	Molecular Constants:	Reference
NH_4^+	T_d	ν_1: 3270 ± 25	a
		ν_2: 1669	c
		ν_3: 3343.26	e
		ν_4: 1447.22	f
		A: 5.9293 ± 0.0002	e
		B: "	e
		C: "	e
		ζ: 0.0604	e
NH_3	C_{3v}	ν_1: 3336.2	b
		ν_2: 950	d
		ν_3: 3444	d
		ν_4: 1627	d
		A: 6.30	g
		B: 9.941	g
		C: "	g
		ζ: 0.06	g

[a]P. Botschwina, J. Chem. Phys. **87**, 1453 (1987), scaled ab initio value.

[b]W.S. Benedict, E.K. Plyler and E.D. Tidwell, J. Chem. Phys. **32**, 32 (1960).

[c]D.J. DeFrees and A.D. McLean, J. Chem. Phys. **82**, 333 (1985), scaled ab initio value.

[d]T. Shimanouchi, Tables of Molecular Vibrational Frequencies, U.S. Dept. of Commerce, Natl. Stand. Ref. Data Ser. Natl. Bur. Stand. **39** (U.S. GPO, Washington, D.C., 1972).

[e]M.W. Crofton, and T. Oka, J. Chem. Phys. **79**, 3157 (1983); **86**, 5983 (1987).

[f]M. Polak, M. Gruebele, B.W. DeKock and R.J. Saykally, Mol. Phys. **66**, 1193 (1989).

[g] G. Herzberg, Electronic spectra of Polyatomic Molecules (Van Nostrand, Princeton, N.J., 1967).

TABLE Ib: Molecular Constants for H_3O^+ and H_2O.
(All units are in cm^{-1} except ζ which is dimentionless. Rotational constants are for the ground vibrational state.)

Molecule	Symmetry	Molecular Constants:	Reference
H_2O	C_{2v}	ν_1: 3832.2	d
		ν_2: 1648.5	d
		ν_3: 3942.5	e
		A: 27.877	f
		B: 14.512	f
		C: 9.285	f

[a] P.R. Bunker, W.P. Kraemer and V. Špirko, J.Molec. Spec. **101**, 180 (1983). -- Scaled ab initio value.

[b] D-J. Liu and T. Oka, J. Chem. Phys. **84**(3), 1312 (1986); and references therein.

[c] M.H. Begemann, G.S Gudeman, J. Pfaff, and R.J. Saykally, Phys. Rev. Lett. Vol. 51, No. 7. 554 (1983). -- Constants listed are for the symmetric states.

[d] M. Wolfsberg, A.A. Massa and J.W. Pyper, J. Chem. Phys., **53**, 3138 (1970).

[e] W.S. Benedict, N. Gailar, and E.D. Plyler, J. Chem. Phys., **24**, 1139 (1956).

[f] G. Herzberg, Electronic spectra of Polyatomic Molecules (Van Nostrand, Princeton, N.J., 1967).

Table II. Observed Vibration-Internal Rotation Transitions and Assignments for the $NH_4^+(NH_3)_n(H_2O)_m$ (n+m=4) Ionic Clusters.

Observed Transition Frequency (cm^{-1})	Assignment	
$NH_4^+(NH_3)_4$ n=4, m=0:[a]		
2865	ν_3 NH_4^+ Asym. Str. (^{4}0°N-H^b_a)	
3095	$2\nu_4$ NH_4^+ Bend (^{4}0°N-H^b_b)	
3383.0 3384.3	$^PQ_3$	ν_3 Asym. Str. of the (1°) NH_3's (^{3}1°N-H^f_a)
3393.5 3394.2	$^PQ_2$	
3407.8 3408.4	$^PQ_1$	
3420.5	$^RQ_0$	
3432.8 3433.3	$^RQ_1$	
3443.3 3444.1	$^RQ_2$	
3454.9 3456.5	$^RQ_3$	
$NH_4^+(NH_3)_3(H_2O)$ n=3, m=1:		
2697	ν_1 NH_4^+ Sym. Str.? (^{3}0°N-H^b_s)	
2808	ν_3' NH_4^+ Asym. Str. involving H-Bonds only to NH_3's. (^{3}0°N-H^b_a)	
3007	$2\nu_4$ NH_4^+ Bend. (^{3}0°N-H^b_b)	

Observed Transition Frequency (cm^{-1})	Assignment	
3174	ν_3" NH_4^+ Asym. Str. involving H-Bond to a (1°) H_2O. (^{1}0°N-H^b_a)	
3378.2	Free N-H Str. of NH_4^+ (^{1}0°N-H^f)	
3393.9	$^PQ_2$	ν_3 Asym. Str. of the (1°) NH_3's (^{3}1°N-H^f_a)
3404.4	$^PQ_1$	
3417.5	$^RQ_0$	
3428.1	$^RQ_1$	
3441.2	$^RQ_2$	
3454.5	$^RQ_3$	
3462.4	$^RQ_4$	
3475.6	$^RQ_5$	
3483.6	$^RQ_6$	
3642.2	ν_1 Sym. Str. of (1°) H_2O (^{2}1°O-H^f_s)	
3699.6	Free O-H Str. (1°) H_2O bound by (2°) NH_3 (^{1}1°O-H^f)	
3716.1	$^PQ_1$	ν_3 Asym. Str. of the (1°) H_2O (^{2}1°O-H^f_a)
3743.7	$^RQ_0$	
3774.1	$^RQ_1$	
3827.1	$^RQ_2$?	
$NH_4^+(NH_3)_2(H_2O)_2$ n=2, m=2:		

Observed Transition Frequency (cm^{-1})	Assignment	
2749	ν_3 NH_4^+ Asym. Str. involving H-Bonds only to (1°) NH_3's. (^{2}0°N-H^b_a)	
2970	$2\nu_4$ NH_4^+ bend ?. (^{2}0°N-H^b_b)	
3121	ν_1 NH_4^+ Sym. Str. involving H-Bonds only to (1°) H_2O's. (^{2}0°N-H^b_s)	
3154	ν_3 NH_4^+ Asym. Str. involving H-Bonds only to (1°) H_2O's. (^{2}0°N-H^b_a)	
3380.9	Free N-H Str. of NH_4^+ (^{1}0°N-H^f)	
3404.4	$^PQ_1$	ν_3 Asym. Str. of the (1°) NH_3's (^{3}1°N-H^f_a)
3417.5	$^RQ_0$	
3428.1	$^RQ_1$	
3438.6	$^RQ_2$	
3451.8	$^RQ_3$	
3642.2	ν_1 Sym. Str. of free (1°) H_2O's (^{2}0°O-H^f_s)	
3701.1	Free O-H Str of (1°) H_2O's bound by (2°) NH_3's (^{1}1°O-H^f)	
3718.8	$^PQ_1$	ν_3 Asym. Str. of the (1°) H_2O (^{2}1°O-H^f_a)
3740.9	$^RQ_0$	
3774.1	$^RQ_1$	
$NH_4^+(NH_3)(H_2O)_3$ n=1, m=3:		
3091	ν_1 NH_4^+ Sym. Str. involving H-Bonds only to (1°) H_2O's. (?) (^{3}0°N-H^b_s)	

Observed Transition Frequency (cm^{-1})	Assignment	
3136	ν_3 NH_4^+ Asym. Str. involving H-Bonds only to (1°) H_2O's. (^{3}0°N-H^b_a)	
3381.0	Free N-H Str. of NH_4^+ (^{1}0°N-H^f)	
3414.9	"ν_3" Weak N-H Str. of NH_3 (No internal rotation structure observed.). (^{2}1°N-H^b_a)	
3642.2	ν_1 Sym. Str. of free (1°) H_2O's (^{1}1°O-H^f_s)	
3699.6	Free O-H Str. of (1°) H_2O's bound by (2°) NH_3? (Weak) (^{1}1°O-H^f)	
3718.8	$^PQ_1$	ν_3 Asym. Str. of the (1°) H_2O (^{2}1°O-H^f_a)
3739.5	$^RQ_0$	
3768.6	$^RQ_1$	
$NH_4^+(H_2O)_4$ n=0, m=4:		
3116	ν_3 NH_4^+ Asym. Str. involving H-Bonds only to (1°) H_2O's. (^{4}0°N-H^b_a)	
3642.2	ν_1 Sym. Str. of free (1°) H_2O's (^{2}0°O-H^f_s)	
3719.0	$^PQ_1$	ν_3 Asym. Str. of the (1°) H_2O (^{2}1°O-H^f_a)
3738.2	$^RQ_0$?	
3749.2	$^RQ_0$?	
3763.0 3771.4	$^RQ_1$	

[a] Data for the n=4, m=0 system has been reported previously. (See ref. 2.)

FIGURE CAPTIONS:

1. Mass spectrum of the ions produced from the corona discharge source in the n+m=4 region. Mass resolution is sufficiently good to discriminate between individual n,m pairs.

2. The normal vibrations of tetrahedrally symmetric NH_4^+. υ_3 and υ_4 are three fold degenerate, while υ_1 and υ_2 are one and two fold degenerate, respectively. Arrows in the figure indicate the direction of motion but are not to scale with the amplitudes. (See ref. 17.)

3. Normal modes of NH_3. Only one linear combination has been shown for the doubly degenerate modes υ_3 and υ_4. Again, arrows in the figure indicate the direction of motion but are not to scale for the amplitude of the motion. (See ref. 17.)

4. Normal modes of H_2O. Again, arrows in the figure indicate the direction of motion but are not to scale with the amplitudes.

5. Vibrational predissociation spectra of $NH_4^+(NH_3)_n(H_2O)_m$ (n+m=4) in the 2600-3100 cm^{-1} region. Bands forming clear series are connected by dashed lines.

6. Vibrational predissociation spectra of $NH_4^+(NH_3)_n(H_2O)_m$ (n+m=4) in the 3100-4000 cm^{-1} region, containing the vibrational bands for both H_2O and NH_3 solvent molecules. Internal rotation structures are observed for both water and ammonia molecules in contrast to the pure hydrated hydronium ions where no internal rotation was observed. Corresponding bands are connected by dashed lines. See text for discussion.

7. Proposed structures for the n+m=4 complexes. The hydrogen bonds are denoted by dashed lines. Several isomers are required in some cases to explain the spectrum for the clusters of a particular n,m pair.

8. Plot of the peak of the antisymmetric stretching bands for the ammonium ion core bound to 1° NH_3 molecules (triangles) and bound to 1° H_2O molecules (circles) as a function of hydration number (m) in the n+m=4 clusters. The series shows a linear dependence upon the degree of hydration, decreasing with increasing m. This is consistent with ammonia's

supperior electron donating capability compared to water's. See text for discussion.

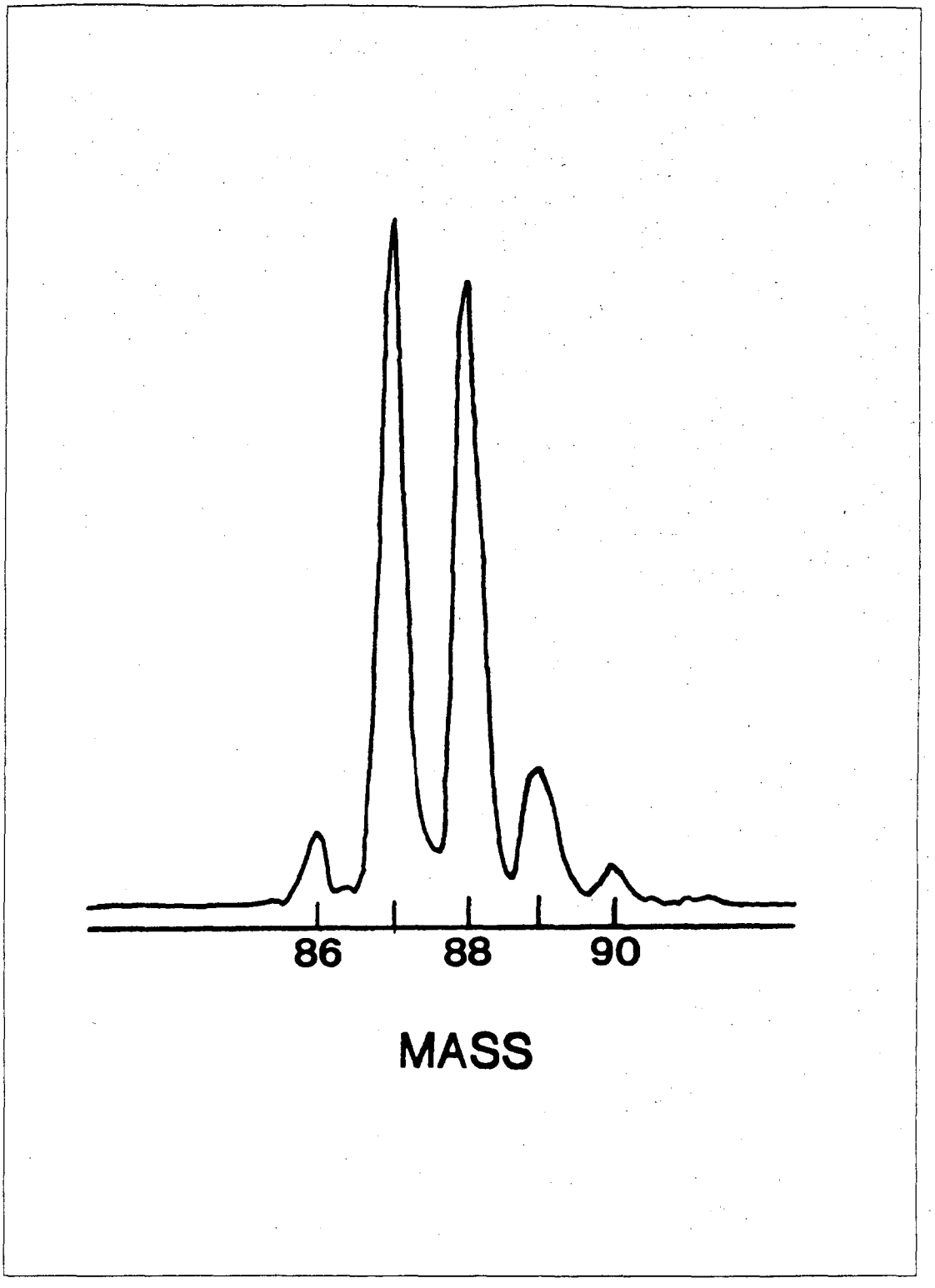

Figure 1.

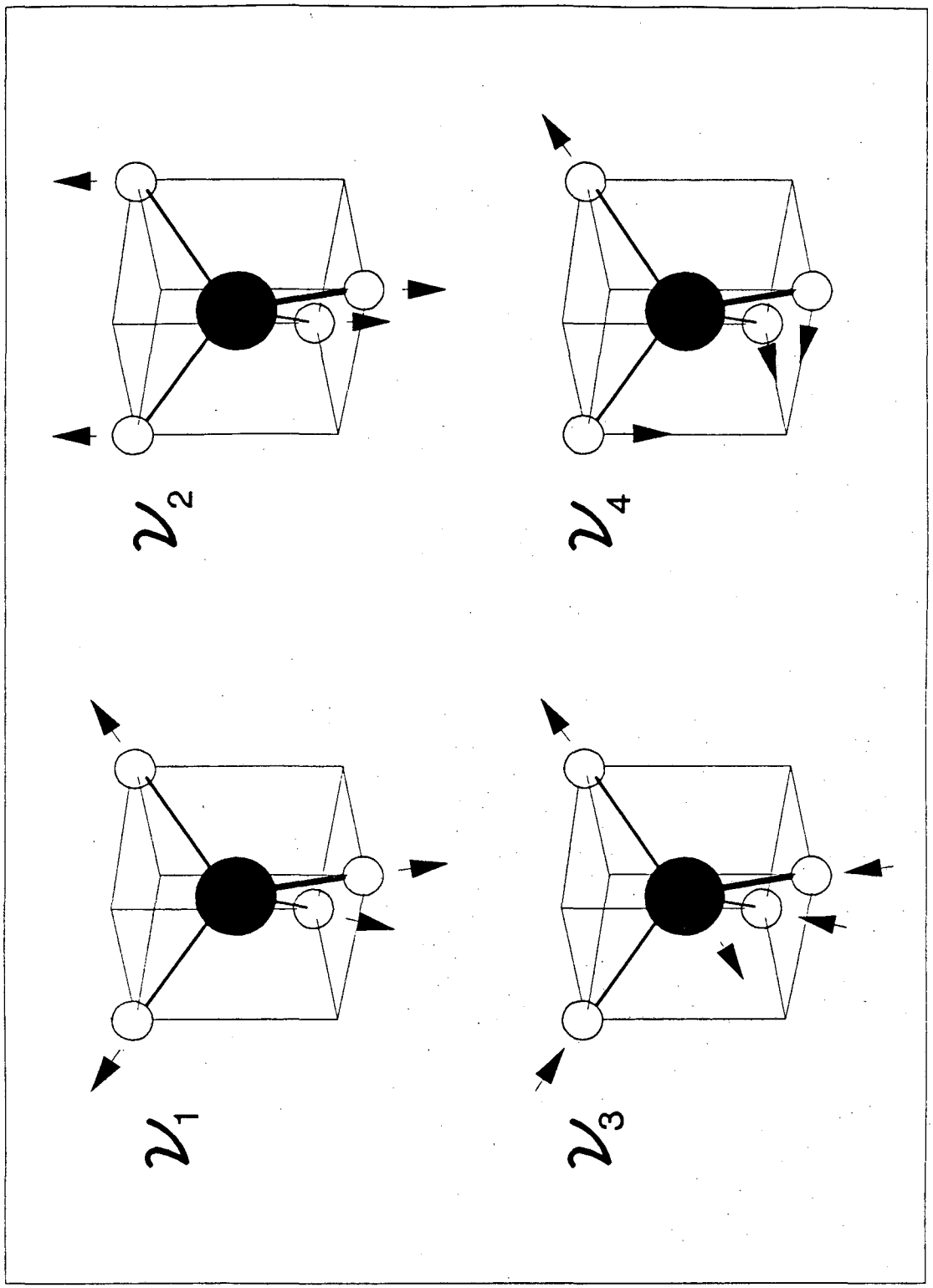

Figure 2.

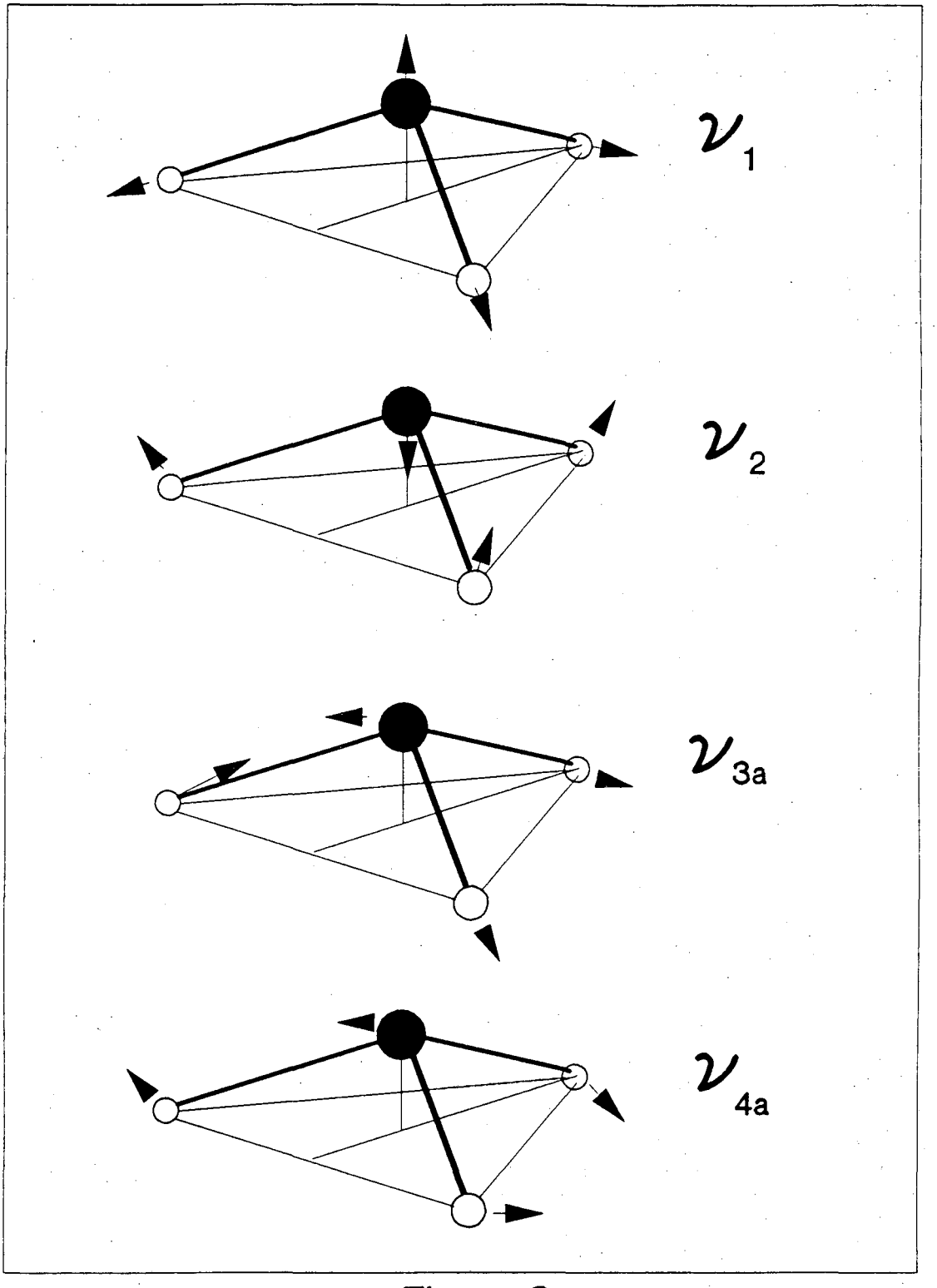

Figure 3.

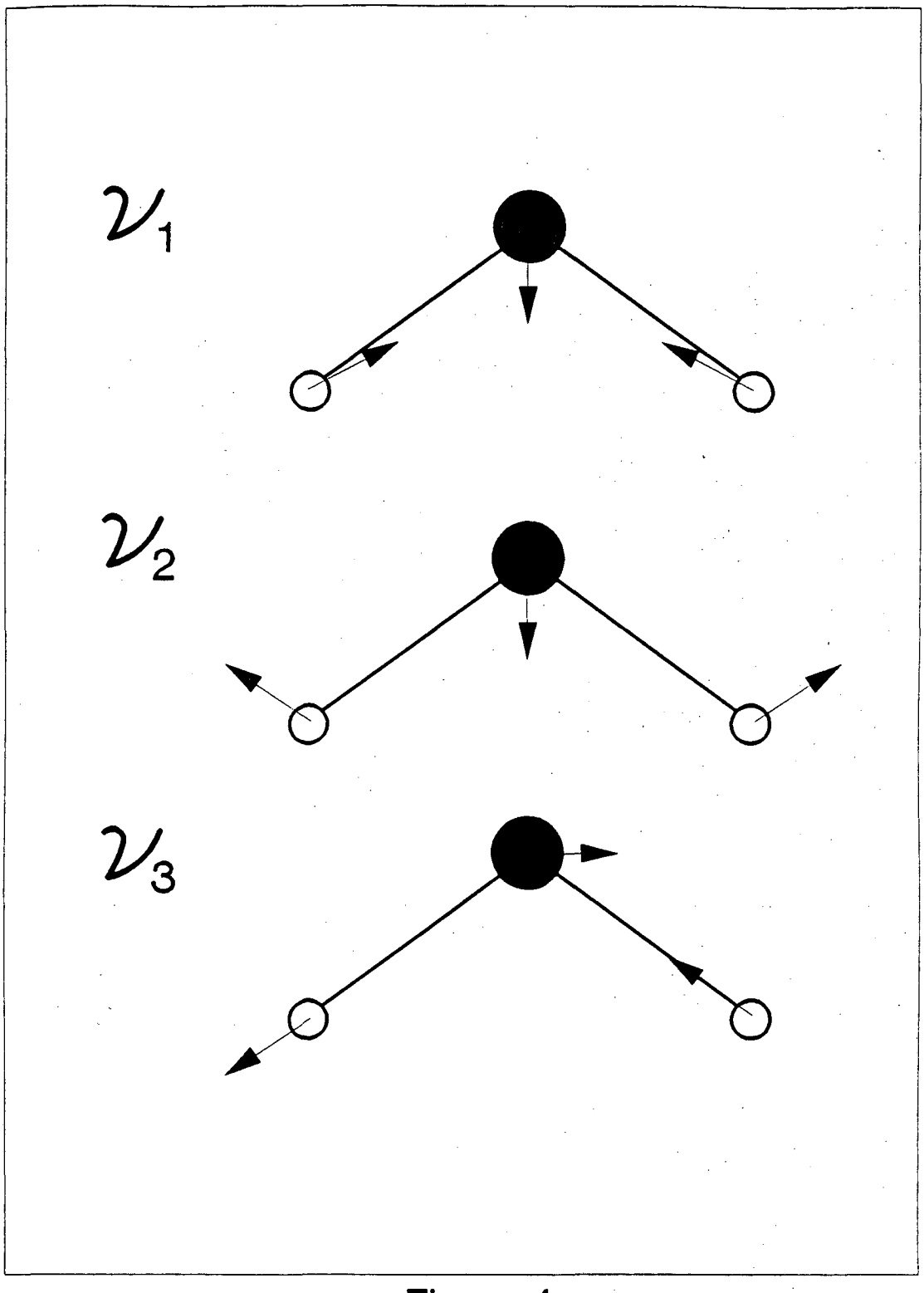

Figure 4.

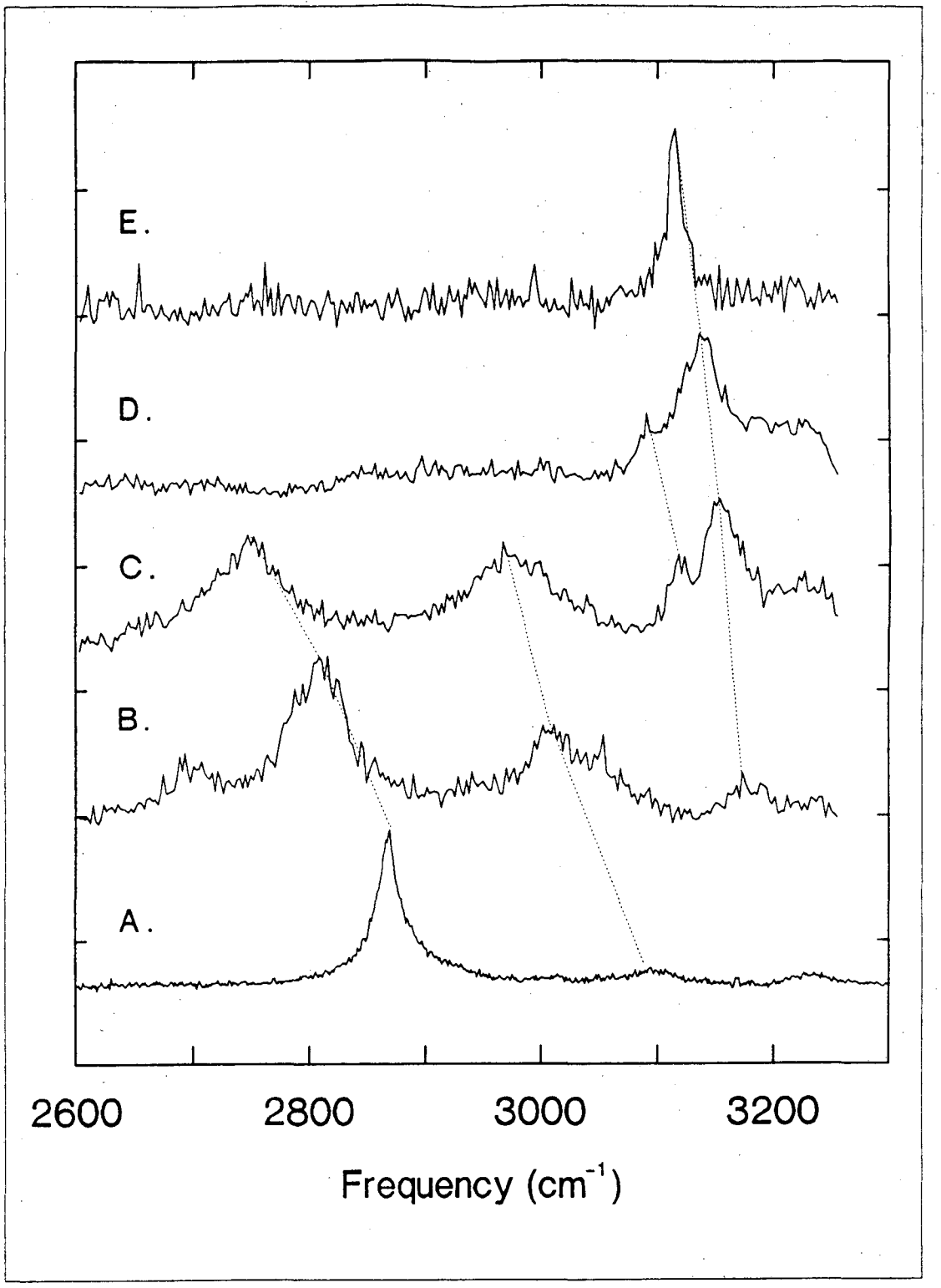

Figure 5.

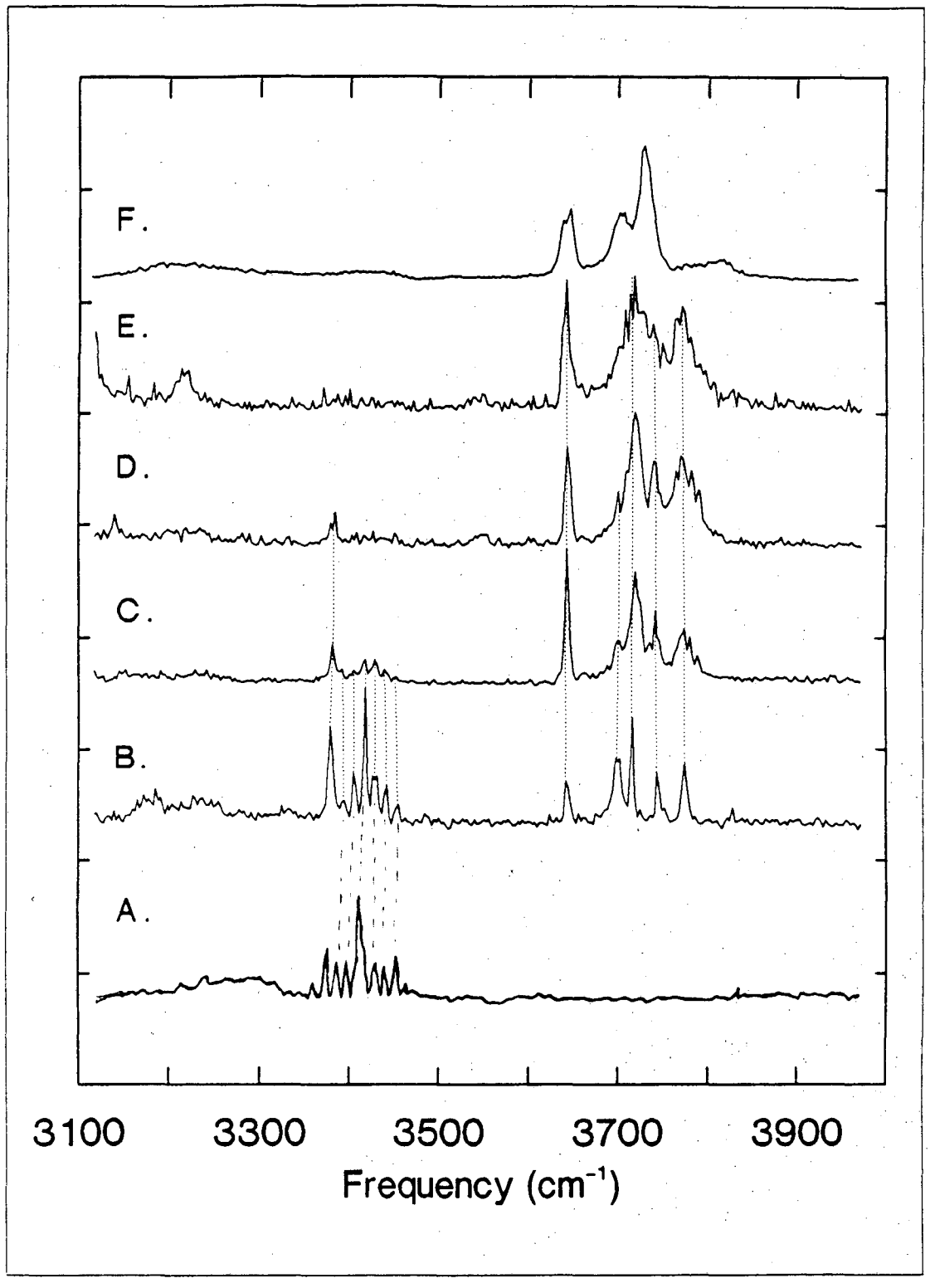

Figure 6.

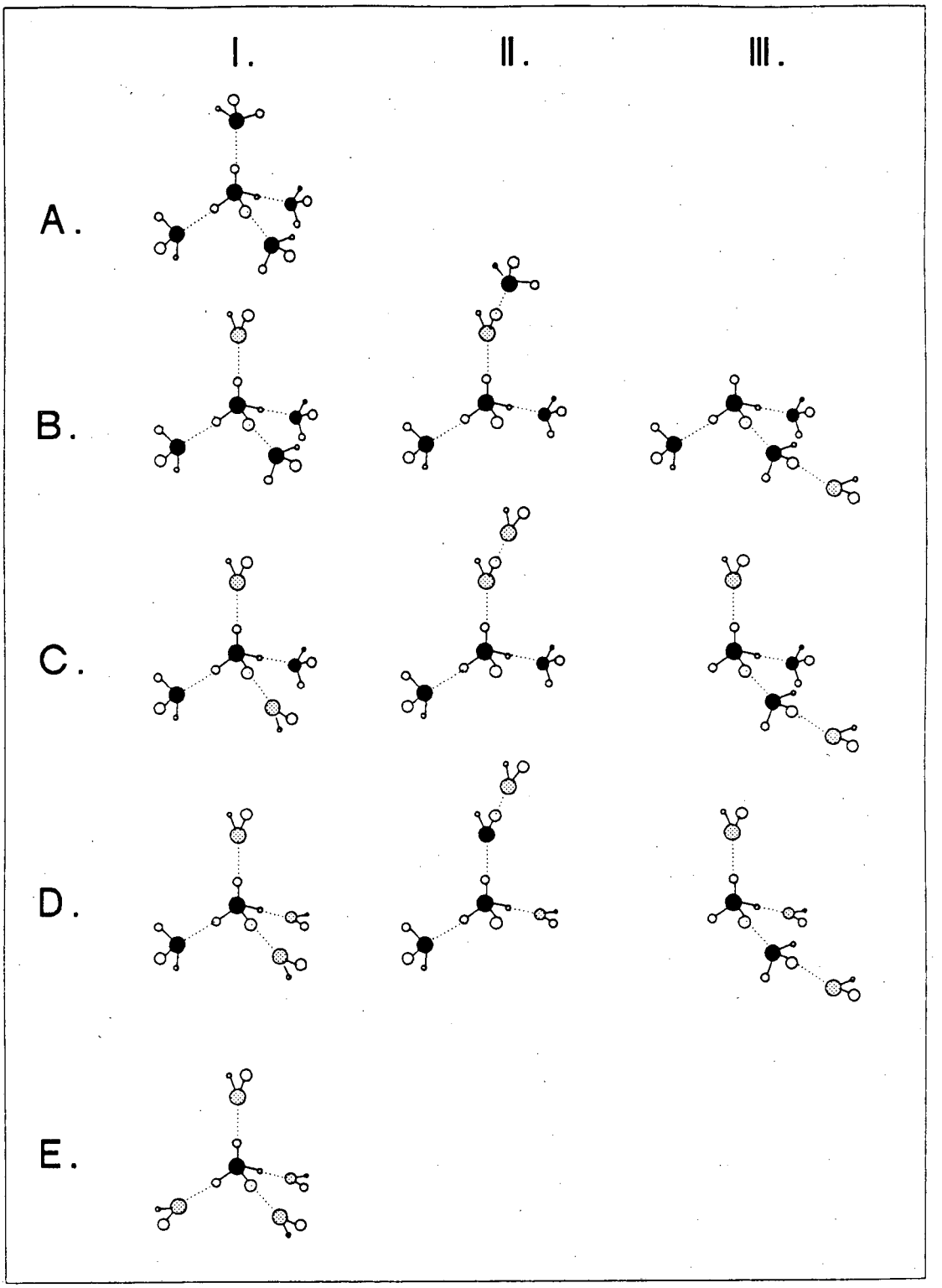

Figure 7.

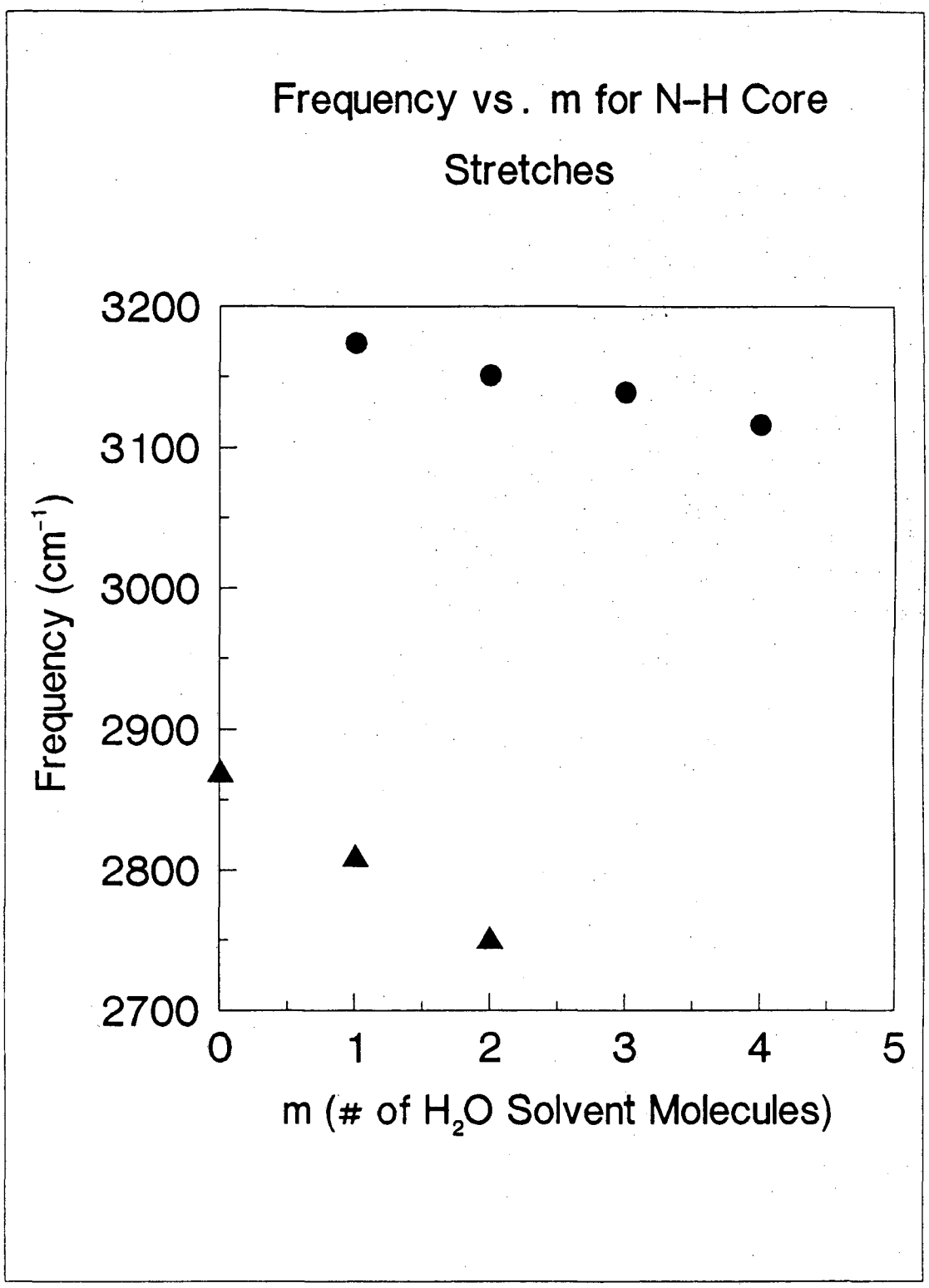
Frequency vs. m for N-H Core Stretches
3200
3100
3000
2900
2800
2700
Frequency (cm-1)
0
1
2
3
4
5
m (# of H2O Solvent Molecules)

Figure 8.

REFERENCES:

1. Epicurus, "Letter to Herodotus", Trans. C. Bailey, in The Stoic and Epicurean Philosophers, Ed. W.J. Oates (New York: Random House, 1940).

2. J.M. Price, M.W. Crofton and Y.T. Lee, J. Chem. Phys. **91**, 2749 (1989); J.M. Price, M.W. Crofton and Y.T. Lee, J. Phys. Chem., Accepted (1990); M.W. Crofton, J.M. Price and Y.T. Lee, to be submitted, J. Chem. Phys. (1990).

3. M. Meot-Ner, C.V. Speller, J. Phys. Chem. **90**, 6616 (1986).

4. U.N. Nagashima, H.S. Shinohara, N. Nishi, and H. Tanaka, J. Chem. Phys. **84**, 209, (1985).

5. C.A. Deakyne, J. Phys. Chem. **90**, 6625 (1986).

6. H-J Bohm aand I.R. McDonald, J. Chem. Soc., Faraday Trans. 2, **80**, 887 (1984); A. Pullman, P. Claverie, and M-C Cluzan, Chem. Phys. Lett. **117**, No. 5, 419 (1985); M. Welti, T-K Ha, E. Pretsch, J. Chem. Phys. **83**, 1959 (1985).

7. S.W. Bustamente, Ph.D. Thesis, University of California at Berkeley, (1983).

8. S.W. Bustamente, M. Okumura, D. Gerlich, H. S. Kwok, L. R. Carlson, and Y. T. Lee, J. Chem. Phys. **86**, 508 (1987).

9. M. Okumura, Ph.D. Thesis, University of California at Berkeley, (1986).

10. L. I-C. Yeh, Ph.D. Thesis, University of California at Berkeley, (1988).

11. H.A. Enge, Rev. Sci. Instrum. **30**, 248 (1959); C.F. Giese **30**, 260 (1959); C-S. Lu and H.E. Carr **33**, 823 (1962).

12. S. Taya, I. Kanomatata, H. Hirose, T. Noda, and H. Matsuda, Int. J. Mass Spectr. and Ion Phys. **26**, 237 (1978).

13. W. Demtröder Laser Spectroscopy: Basic Concepts and Instrumentation. (Springer-Verlag Press, New York, 1982); V. S. Letokhov Nonlinear Laser Chemistry: Multiple-Photon Excitation (Springer-Verlag press, New York, 1983).

14. R.N. Daly, Rev. Sci. Instrum. **31**, 264 (1960).

15. S.G. Lias, J.F. Liebman and R.D. Levin, J. Phys. Chem. Ref. Data **13**, 695 (1984).

16. H.A. Schwarz, J. Chem. Phys., **72**, 284 (1980).

17. G. Herzberg, Infrared and Raman Spectra of Polyatomic Molecules (D. Van Nostrand, New York, 1945) p. 231, 307.

18. In: The Hydrogen Bond: Recent Developments in Theory and Experiments, Ed., P. Schuster, G. Zundel, and C. Sandorfy (North-Holland Publishing Company, New York 1976).

19. M. Okumura, L. I-C. Yeh, and Y.T. Lee, J. Chem Phys., **83**, 3705 (1985); **88**, 79 (1988).

20. NH_3-CO_2: G.T. Fraser, K.R. Leopold, and W. Klemperer, J. Chem. Phys. **81**, 2577 (1984); H_2O-CO_2: K.I. Peterson, and W. Klemperer, J. Chem. Phys. **80**, 2439 (1983); C_2H_4-H_2O: K.I. Peterson, and W. Klemperer, J. Chem. Phys. **85**, 725 (1986).

Appendix 1.

Data Aquisition Program

The ion spectroscopy machine has undergone several changes in the last four years: new sources have been built, a new computer system has been installed, and new lasers have been integrated into the experiment. The details of the modifications to the machine during my time on the experimental apparatus may be found in lab notebooks 18 through 21. Two of the programs I have written for the control of the experiment and the analysis of data may be found in this and the following appendix. While more code than these two programs are required for the actual operation of the apparatus, these programs form the core of the software drivers and are presented here for reference.

```
{$M 10000,20000,20000}
PROGRAM Machine10;

{ Object oriented version of program }

{ This is the new IBM AT compatible program designed to replace the
assembly language monument, 'S' written by Sanford Bustamente (See S.W.
Bustamente, Ph.D. Thesis, University of California, Berkeley, 1983) to
drive the machine from the old LSI 11 computer system.  His excellent
program, with later additions by Mitchio Okumura, provided control over
the molecular ion spectroscopy machine for nearly a decade.  My
contribution, produced with help from Gereon Neidner-Schatteburg is
presented below.  It is hoped that this code may also provide a reliable
and hopefully friendly companion in the late evening hours of data
aquisition. }

{ The code below is written in Turbo Pascal Ver. 5.5 }

USES
  Crt,
  Codes,
  Graph,
  Grafmax,
  Camtunit,
  Flcontr3,
  Forms,
  JPTools,
  MenuMax,
  Dos;


TYPE
  DeviceType = (Magnet,Q_Pole,Laser,Trap,Nothing);

  DataType = (SignalandBackground,Background,Signal,Power,Null);

  Param = record
   Filename   : String[10];
   Directory  : String[20];
   Num_Chan   : LongInt;
   Num_Cycles: Longint;
   Num_Scans  : LongInt;
   Start_V    : Real;
   End_V      : Real;
   Start_T    : Real;
   End_T      : Real;
   Start_M    : Real;
   End_M      : Real;
   Start_W    : Real;
   End_W      : Real;
   Etalon_In  : Boolean;
  End;

CONST
  AtoD_Converter : Integer = 14;
  DtoA_Converter : Integer = 12;
  Pulse_Generator: Integer = 1;
  Quad_Scaler    : Integer = 16;
  Timing_Gen     : Integer = 22;

  P1: Param = (
```

```
    Filename:' ';
    Directory:'A:\';
    Num_Chan:500;
    Num_Cycles:3;
    Num_Scans:1;
    Start_V:2.500;
    End_V:3.000;
    Start_T:1;
    End_T:10;
    Start_M:20;
    End_M:60;
    Start_W:765.0;
    End_W:760.0;
    Etalon_In:False );


VAR
  P                                    : Param;
  MainChoice, ScanChoice, I            : Integer;
  Crate_Number, n, f, a, q, x          : Integer;
  d,E                                  : Integer;
  Trap_Delay                           : Integer;
  d1,d2                                : longint;
  CH                                   : Char;
  DeviceString                         : String[30];
  DisplayString                        : String[30];
  Out_String                           : String[20];
  Dummy_string                         : String[10];
  status_string                        : string;
  string1,string2                      : string;
  Device                               : DeviceType;
  Data                                 : DataType;
  StringVar                            : String[30];
  StringVar2                           : String[30];
  SigandBack                           : Array[1..1000] of longint;
  Back                                 : Array[1..1000] of longint;
  LaserPower                           : Array[1..1000] of longint;
  Sig                                  : Array[1..1000] of longint;
  dye_w_length                         : Array[1..1000] of real;
  ir_w_number                          : Array[1..1000] of real;
  Ymax                                 : Real;
  XMax,Xmin                            : Real;
  Direction                            : Char;
  Cross                                : Pointer;
  b_c, d_c                             : array [1..8] of integer;
  lam_mask                             : array [1..8] of integer;
  inhibit_data,allow_data              : integer;
  Scanning                             : boolean;
  help_page                            : boolean;
  halt_scan                            : boolean;
  laser_narrow                         : boolean;
  bidirectional_laser_scan             : boolean;
  up_scan                              : boolean;
  key_mode_flag                        : boolean;
  new_data_flag                        : boolean;
  i_choice                             : integer;
  clock_rate                           : integer;
  b_scan,l_scan,k_scan,j_scan,i_scan   : Integer;
                                              { indices in scan loops }
  n_scan                               : integer;
  ch_scan                              : Char;
  i_cross                              : integer;
```

```
  n_repeat                              : integer;
  Actual_Channel                        : integer;
  save_channel                          : integer;
  Device_Menu                           : MenuArray;
  Hi_Lo_Res_Menu                        : MenuArray;
  Save_Menu                             : MenuArray;


PROCEDURE Init_Device_Menu;
  Begin
     Storemenu (Device_menu[1],' A. Magnet ',2,10);
     Storemenu (Device_menu[2],' B. Quadrupole ',3,10);
     Storemenu (Device_menu[3],' C. Laser ',4,10);
     Storemenu (Device_menu[4],' D. Trap ',5,10);
     Storemenu (Device_menu[5],' E. Nothing ',6,10);
  End;

PROCEDURE Init_Hi_Lo_Res_Menu;
  Begin
   Storemenu (Hi_Lo_Res_menu[1],' A. Without Etalon (Low Resolution)
',4,30);
   Storemenu (Hi_Lo_Res_menu[2],' B. With Etalon    (High Resolution)
',5,30);
  End;


PROCEDURE Make_Device_Menu;
  Begin
     Closegraph;
     Menuchoice:=0;
     ClrScr;
     TextBackground(Blue);
     ClrScr;
     TextColor(Cyan);
     Box(1,1,79,25,2);
     TextColor(Yellow);
     gotoxy(1,1);
     Write(' Scanning Options:');
     MakeMenu(Device_menu,5);
     Case menuchoice of
       1:Begin Device:=Magnet;  DeviceString:='Magnet '; End;
       2:Begin Device:=Q_Pole;  DeviceString:='Quadrupole '; End;
       3:Begin
          Device:=Laser;
          DeviceString:='Laser ';
          Repeat
           MakeMenu(Hi_Lo_Res_Menu,2);
           Case Menuchoice of
            1: p.etalon_in:=false;
            2: p.etalon_in:=true;
           End; {Case}
          Until (Menuchoice=1) or (Menuchoice=2);
         End;
       4:Begin Device:=Trap; DeviceString:='Trap '; End;
       5:Begin Device:=Nothing; DeviceString:='Nothing '; End;
     end;
  Init_Graphics;
 End;


PROCEDURE Parameters_form;
```

```
Var
 F: Form;

Begin
 Closegraph;
 Color(backcolor);
 clrscr;
 TextBackground(Blue);
 ClrScr;
 TextColor(Cyan);
 Box(1,1,79,25,2);
 TextColor(Yellow);
 Gotoxy(1,1);
 Write('Machine Parameters: ');

 gotoXY(1,25);
 write('<Esc> to quit');

 F.Init(2,3,78,23);

 F.Add(NEW(fStrPtr,Init(3,2,'File Name:          ',10)));
 F.Add(NEW(fstrPtr,Init(3,3,'Directory:          ',20)));

 F.Add(NEW(fIntPtr,Init(3,5,'Number of Channels: ',1,1000)));
 F.Add(New(FintPtr,Init(3,6,'Number of Cycles:   ',1,1000)));
 F.Add(New(FIntPtr,Init(3,7,'Number of Scans:    ',1,10)));

 F.Add(New(FrealPtr,Init(3,10,'Starting Voltage:   ',6,3)));
 F.Add(New(FrealPtr,Init(3,11,'Ending Voltage:     ',6,3)));

 F.Add(New(FrealPtr,Init(3,14,'Starting Delay:     ',5,2)));
 F.Add(New(FrealPtr,Init(3,15,'Ending Delay:       ',5,2)));



 F.Add(New(FrealPtr,Init(3,18,'Starting Mass:      ',7,3)));
 F.Add(New(FrealPtr,Init(3,19,'Ending Mass:        ',7,3)));

 F.Add(New(FrealPtr,Init(35,5,'Starting Wavelength: ',7,3)));
 F.Add(New(FrealPtr,Init(35,6,'Ending Wavelength:   ',7,3)));
 F.Add(New(JPButtonPtr,Init(35,7,'Etalon in:           ')));

 f.Put(P);
 F.show(true);

 If F.edit =cesc then f.get(p);

 If P.Etalon_In then Laser_Narrow:=true;

 F.done;

 Init_Graphics;

End; { Parameters Form }


PROCEDURE Init_Save_Menu;
  Begin
     Storemenu (Save_menu[1],' A. Filename: ',2,10);
     Storemenu (Save_menu[2],' B. Save Directory: ',3,10);
     Storemenu (Save_menu[3],' C. Save Data ',4,10);
     Storemenu (Save_menu[4],' D. Retrieve Data ',5,10);
```

```
    Storemenu (Save_menu[5],' E. Directory ',6,10);
    Storemenu (Save_menu[6],' F. Format Disk A: (High Dens.) ',7,10);
    Storemenu (Save_Menu[7],' G. Format Disk B: (Low  Dens.) ',8,10);
    Storemenu (Save_menu[8],' H. Dos Shell ',9,10);
    Storemenu (Save_menu[9],' I. VECTOR analysis program',10,10);
    Storemenu (Save_menu[10],' J. Return.',11,10);

  End;

PROCEDURE Make_Save_Menu;
 Var D: Text;
    St:String[19];
 Begin
    CloseGraph;
    Menuchoice:=0;
   Repeat;
     TextBackground(Blue);
     ClrScr;
     TextColor(Cyan);
     Box(1,1,79,25,2);
     TextColor(Yellow);
     gotoxy(1,1);
     Write(' Options:');
     GotoXy(30,2);
     Write(P.Filename);
     GotoXY(30,3);
     Write(P.Directory);
     MakeMenu(Save_menu,10);
     Case menuchoice of
      1:Begin
         GotoXY(1,15);
         Writeln('Old Filename: ',P.Filename);
         Write('New Filename: ');
         Readln(P.Filename);
        End;
      2:Begin
         GotoXY(1,15);
         Writeln('Old Directory: ',P.Directory);
         Write('New Directory: ');
         Readln(P.Directory);
        End;
      3:Begin
         GotoXY(1,15);
         Writeln('Saving Data... ');
         Assign(D,P.Directory+P.Filename);
         ReWrite(D);
         Writeln(D, 'Filename: ',P.Filename);
         Writeln(D, 'Scanning: ',DeviceString);
         Writeln(D);
         Writeln(D,'Number Of Channels ',' ',P.Num_Chan);
         Writeln(D,'Number Of Cycles   ',' ',P.Num_Cycles);
         Writeln(D,'Number Of Scans    ',' ',P.Num_Scans);
         Writeln(D,'Starting Voltage   ',' ',P.start_V);
         Writeln(D,'Ending Voltage     ',' ',P.End_V);
         Writeln(D,'Starting Mass      ',' ',P.start_M);
         Writeln(D,'Ending Mass        ',' ',P.End_M);
         Writeln(D,'Starting Delay     ',' ',P.start_T);
         Writeln(D,'Ending Delay       ',' ',P.end_T);
         Writeln(D,'Starting Wavelength',' ',P.Start_W);
         Writeln(D,'Ending Wavelength  ',' ',P.End_W);

         Writeln(D);
```

```
    Writeln(D,'Si+Ba      BackGroundPower      Dye        IR');
    Writeln(D);
    For I:=1 to P.Num_chan do
     Writeln(D,SigandBack[i]:10,Back[i]:10,LaserPower[I]:10,
             '    ',dye_w_length[i]:15, '    ', ir_w_number[i]:13);
    Close(d);
   End;
 4:Begin
    GotoXY(1,15);
    Writeln('Retrieving Data... ');
    Assign(D, P.Directory+P.Filename);
    ReSet(D);
    Readln(D,Dummy_String,P.Filename);
    Readln(D,Dummy_String,DeviceString);
    Readln(D);
    Readln(D,st,P.Num_Chan);
    Readln(D,st,P.Num_Cycles);
    Readln(D,st,P.Num_Scans);
    Readln(D,st,P.start_V);
    Readln(D,st,P.End_V);
    Readln(D,st,P.start_M);
    Readln(D,st,P.End_M);
    Readln(D,st,P.start_T);
    Readln(D,st,P.end_T);
    Readln(D,st,P.Start_W);
    Readln(D,st,P.End_W);
    Readln(D);
    Readln(D);
    Readln(D);
    For I:=1 to P.Num_chan do
       Readln(D,SigandBack[i],Back[i],LaserPower[I],
                dye_w_length[i], ir_w_number[i]);
    Close(D);

    If devicestring = 'Magnet' then
       Device := Magnet
    else if devicestring = 'Quadrupole' then
       Device := Q_Pole
    else if devicestring = 'Laser ' then
       Device := Laser
    else if devicestring = 'Trap' then
       Device := Trap
    else if devicestring = 'Nothing' then
       Device := Nothing;

  End;

5:Begin
   Gotoxy(1,15);
   Writeln;
   Exec('c:\command.com','/C Dir/P '+P.Directory+'*.*');
   Writeln;
   Writeln('Press Return when done');
   Readln;
  End; {E}

6:Begin
   Gotoxy(1,15);
   Writeln;
   Exec('c:\command.com','/C Format A:');
  End; {F}
```

```
      7:Begin
         Gotoxy(1,15);
         Writeln;
         Exec('c:\command.com','/C Format B:');
        End; {G}

      8:Begin
         Exec('c:\command.com','');
        End; {H}

      9:Begin
         Exec('c:\tp5\exe\Analysi4.exe','');
        End; {I}

    end;
    until menuchoice = 10;
    Init_Graphics;
 End;


PROCEDURE Clear_Arrays;
 Begin
   begin
     For n:=1 to 1000 do
     Begin
     Sigandback[n]:=0;  { Initialize the Array Elements }
     Back[n]:=0;
     LaserPower[n]:=0;
     dye_w_length[n]:=0;
     ir_w_number[n]:=0;
   end;
  End;
 End;



PROCEDURE Initialize;
 Begin

 P:=P1;

 Device:=Magnet;
 Ymax:=100;
 DeviceString:='Magnet';
 DisplayString:='Sig and Back';
 Data:=SignalandBackground;

 Init_Device_Menu;
 Init_Hi_Lo_Res_Menu;
 Init_Save_Menu;


 Scanning                  := false;
 Help_page                 := false;
 halt_scan                 := false;
 laser_narrow              := false;
 bidirectional_laser_scan  := false;
 key_mode_flag             := false;
 new_data_flag             := false;
 up_scan                   := true;

 k_scan                    := 1;
```

```
j_scan                    := 1;
l_scan                    := 1;
i_scan                    := j_scan;
Actual_Channel            := j_scan;
i_cross                   := i_scan;
save_channel              := 1;


n_scan                    := P.Num_Scans;
n_repeat                  := 2;

start_w_length            := P.Start_W;
stop_w_length             := P.End_W;

clear_arrays;
Initialize_Cross;

                      { Timing Parameters to be used in  procedures
                        Set_Timing and Set_Clock_Rate }

d_c[7] := 1;              { stop (0)   /  recycle (1) }

d_c[6] := 1;  { *4 }
d_c[5] := 1;  { *2 }      { p+1 = number of channels pulsing }
d_c[4] := 1;  { *1 }

d_c[3] := 1;  { *4 }
d_c[2] := 0;  { *2 }      { 10**N hertz clock rate, N=7 external }
d_c[1] := 1;  { *1 }


b_c[1] := 100;
b_c[2] := 300;
b_c[3] := 350;
b_c[4] := 500;          { Delay-times of individual channels }
b_c[5] := 501;
b_c[6] := 850;
b_c[7] := 2000;
b_c[8] := 2500;


End;


PROCEDURE Set_Clock_Rate;         Forward;

PROCEDURE Reset_Quad_Scaler;      Forward;

PROCEDURE Screen_LAM_Requests;    Forward;


PROCEDURE Initialize_CAMAC;
 Var   i,i1 : integer;
 Begin
   Crate_Number:=1;  Crate_set(Crate_Number);
   f:= 64;           Camcl(f);
   Set_Clock_Rate;

   inhibit_data:=4;
```

```
    allow_data:=0;

    camcl(inhibit_data);
    Reset_Quad_Scaler;
    Screen_LAM_Requests;
    i1:=1;
    for i:= 1 to 8 do
     begin
       LAM_mask[i]:=i1;
       i1:=i1*2;
     end;
  End;


PROCEDURE Init_Help_Page;
 Begin
  SetActivePage(1);
  SetViewport(0,0,getMaxx,GetMaxY,Clipon);
  SetColor(White);
  ClearViewport;
  Box_Viewport(0);
  SetTexTJustify(0,1);
  SetColor(Yellow);
  OutTextXY(10,10,'HELP PAGE: ');
  OutTextXY(10,30,'Function Keys');
  SetColor(White);
  OutTextXY(10,50,'  F1   : Toggle: data screen/ Help page');
  OutTextXY(10,60,'  F2   : Quick Plot');
  OutTextXY(10,70,'  F3   : Reset device');
  OutTextXY(10,80,'  F4   : Clear data arrays');
  OutTextXY(10,90,'  F5   : Display: Signal + Background ');
  OutTextXY(10,100,'  F6   : Display: Background ');
  OutTextXY(10,110,'  F7   : Display: Signal (sb-ba)');
  OutTextXY(10,120,'  F8   : Display Power ');
  OutTextXY(10,130,'  F9   : Key Mode');
  OutTextXY(10,140,'  F10  : Toggle: Scanning/ Abort Scan');

  OutTextXY(GetMaxX div 2,50,'  Shift + F1   : Save / Retrieve Data ');
  OutTextXY(GetMaxX div 2,60,'  Shift + F2   : Nice Plot ');
  OutTextXY(GetMaxX div 2,70,'  Shift + F3   : Set Timing-Generator');
  OutTextXY(GetMaxX div 2,80,'  Shift + F4   : Dye Laser Controling');
  OutTextXY(GetMaxX div 2,90,'  Shift + F5   : Rescale Viewport to Max
');
  OutTextXY(GetMaxX div 2,100,'  Shift + F6   : Y Zoom * 10');
  OutTextXY(GetMaxX div 2,110,'  Shift + F7   : Y Zoom * 100');
  OutTextXY(GetMaxX div 2,120,'  Shift + F8   : Y Zoom * 1000');
  OutTextXY(GetMaxX div 2,130,'  Shift + F9   : Change Device');
  OutTextXY(GetMaxX div 2,140,'  Shift + F10  : Toggle:Start/Halt Scan');

  OutTextXY(10,160,'  Alt + F1   :');
  OutTextXY(10,170,'  Alt + F2   :');
  OutTextXY(10,180,'  Alt + F3   :');
  OutTextXY(10,190,'  Alt + F4   :');
  OutTextXY(10,200,'  Alt + F5   :');
  OutTextXY(10,210,'  Alt + F6   :');
  OutTextXY(10,220,'  Alt + F7   :');
  OutTextXY(10,230,'  Alt + F8   :');
  OutTextXY(10,240,'  Alt + F9   : Change Scanning Parameters');
  OutTextXY(10,250,'  Alt + F10  : ');

  OutTextXY(GetMaxX div 2,160,'  Ctrl + F1   :');
```

```
  OutTextXY(GetMaxX div 2,170,'  Ctrl + F2  :');
  OutTextXY(GetMaxX div 2,180,'  Ctrl + F3  :');
  OutTextXY(GetMaxX div 2,190,'  Ctrl + F4  :');
  OutTextXY(GetMaxX div 2,200,'  Ctrl + F5  :');
  OutTextXY(GetMaxX div 2,210,'  Ctrl + F6  :');
  OutTextXY(GetMaxX div 2,220,'  Ctrl + F7  :');
  OutTextXY(GetMaxX div 2,230,'  Ctrl + F8  :');
  OutTextXY(GetMaxX div 2,240,'  Ctrl + F9  :');
  OutTextXY(GetMaxX div 2,250,'  Ctrl + F10 : Exit the Program');
  SetActivePage(0);
 End;


FUNCTION Voltage(I:Integer):Real;
 Begin
  Case Device of
   Magnet:
    Voltage:= I*((P.End_V-p.Start_V)/p.Num_Chan)
              + P.Start_V;
   Q_Pole:
    Voltage:= I*((P.End_M-P.Start_M)/P.Num_Chan)
              + P.Start_M;
   Trap:
    Voltage:= I*((P.End_T-P.Start_T)/P.Num_Chan)
              + P.Start_T;
  End;{Case}
 End; {Voltage}


PROCEDURE Init_Pulse_Generator;
 Begin
 End;


PROCEDURE TTL_OUT; {TO STEP THE DYELASER IN BURST MODE}
 BEGIN
  a:=0;

  F:=16; d1:=1;

  {'B': D1:=32768  Change the Sign Bit
          + D1;}
  Camo24(Pulse_Generator,f,a,d1,q,x); { Send out Numstep Pulses }
  Delay(1000);
 END;


PROCEDURE Set_Timing;
 VAR  i_x,i_choice,clock_rate : integer;
      uot                     : longint;
 BEGIN
  Closegraph;
  Repeat
    ClrScr;
    writeln;
    writeln('   SET TIMING PARAMETERS!');
    writeln;
    i_x := d_c[3]*4+d_c[2]*2+d_c[1];
    uot := 1000000 div round(exp(ln(10)*i_x));
    writeln('A. Toggle: Recycle intern(1) / extern(0): ',d_c[7]);
    writeln('B. Change clock rate (old value: ',uot,' microseconds)');
    writeln('C. Change time delays ');
```

```
    writeln('Q. Quit ');
    ch := readkey;
    Case Upcase(ch) of
     'A': Begin
           if d_c[7]  = 1 then
            d_c[7] := 0
           else
            d_c[7] := 1;
            set_clock_rate;
          End;

     'B': Begin
           clrscr;
           writeln;
           writeln('Enter new clock rate');
           writeln(' 1 microsecond (6)');
           writeln('10 microseconds(5), 100 microseconds(4), 1
millisecond(3),');
           writeln('10 milliseconds(2), 100 milliseconds(1), 1
second(0),');
           write  (' external(7)      :  ');
           readln(clock_rate);
           case clock_rate of
            0 : begin  d_c[1]:=0; d_c[2]:=0; d_c[3]:=0; end;
            1 : begin  d_c[1]:=1; d_c[2]:=0; d_c[3]:=0; end;
            2 : begin  d_c[1]:=0; d_c[2]:=1; d_c[3]:=0; end;
            3 : begin  d_c[1]:=1; d_c[2]:=1; d_c[3]:=0; end;
            4 : begin  d_c[1]:=0; d_c[2]:=0; d_c[3]:=1; end;
            5 : begin  d_c[1]:=1; d_c[2]:=0; d_c[3]:=1; end;
            6 : begin  d_c[1]:=0; d_c[2]:=1; d_c[3]:=1; end;
            7 : begin  d_c[1]:=1; d_c[2]:=1; d_c[3]:=1; end;
           end; {case}
           set_clock_rate;
          End; {B}

     'C': Begin
           i_x := d_c[3]*4+d_c[2]*2+d_c[1];
           uot := 1000000 div round(exp(ln(10)*i_x));
           Repeat
            clrscr;
            writeln;

            for i:=1 to 8 do
            begin
             write  ('Channel number ',i:1,' pulses after ');
             writeln(b_c[i]:4,' * ',uot,' microseconds.');
            end;

            writeln;
            write  ('Enter number of channel to be changed or 0 to quit!
');
            readln(i_choice);
            if i_choice <> 0 then
            begin
             writeln;
             write  ('Enter new delay time for channel ',i_choice,' :
');
             readln(b_c[i_choice]);
             set_clock_rate;
            end;
          Until i_choice=0;
         End; {C}
```

```
   End; {case ch}
  Until Upcase(ch)='Q';
  ch := ' ';
  init_graphics;
 End; {Set_Timing}


PROCEDURE Set_Clock_Rate;
 Var  dt : integer;
 Begin

  Q:=0;
  X:=0;

  F:=16; A:=0; dt:=b_c[1];
  Camo(Timing_Gen,f,a,dt,q,x);    { writes set point 1 }

         A:=1; dt:=b_c[2];
  Camo(Timing_Gen,f,a,dt,q,x);    { writes set point 2 }

         A:=2; dt:=b_c[3];
  Camo(Timing_Gen,f,a,dt,q,x);    { writes set point 3 }

         A:=3; dt:=b_c[4];
  Camo(Timing_Gen,f,a,dt,q,x);    { writes set point 4 }

         A:=4; dt:=b_c[5];
  Camo(Timing_Gen,f,a,dt,q,x);    { writes set point 5 }

         A:=5; dt:=b_c[6];
  Camo(Timing_Gen,f,a,dt,q,x);    { writes set point 6 }

         A:=6; dt:=b_c[7];
  Camo(Timing_Gen,f,a,dt,q,x);    { writes set point 7 }

         A:=7; dt:=b_c[8];
  Camo(Timing_Gen,f,a,dt,q,x);    { writes set point 8 }


  d:=d_c[7]*64+d_c[6]*32+d_c[5]*16+d_c[4]*8+d_c[3]*4+d_c[2]*2+d_c[1]*1;


  F:=17; A:=0;
  Camo(Timing_Gen,f,a,d,q,x);     { writes cycle control register }

  F:=9;  A:=8; x:=0;q:=0;
  Camo(Timing_Gen,F,A,D,Q,X);     { starts the counter and the cycling }

  D:=0; F:=17; A:=13; x:=0;q:=0;
  Camo(Timing_Gen,F,A,D,Q,X);     { disables LAM by rewriting the
LAM-mask }

  D:=0; F:=11; A:=12; x:=0; q:=0;
  Camo(Timing_Gen,F,A,D,Q,X);     { clears the LAM-status bits }

 End; {Set_Clock_Rate}


PROCEDURE Check_Timer(var mask:integer);

 Var   L  :  Integer;
```

```
 Begin

  F:=17; A:=13;
  Camo(Timing_Gen,F,A,mask,Q,X);    { writes the LAM-mask }

  D:=0; F:=11; A:=12;
  Camo(Timing_Gen,F,A,D,Q,X);       { clears the LAM-status bits }

  L:=0;
  Repeat
   caml(L);                         { checks for LAM-request }
  Until L=Timing_Gen;

  D:=0; F:=17; A:=13;
  Camo(Timing_Gen,F,A,D,Q,X);       { disables LAM by rewriting the
LAM-mask }

  D:=0; F:=11; A:=12;
  Camo(Timing_Gen,F,A,D,Q,X);       { clears the LAM-status bits }

End;


PROCEDURE Reset_Quad_Scaler;

 Begin

  D1:=0; F:=9; a:=2;
  Camo24(Quad_Scaler,f,a,d1,q,x);    { Reset Counter line 2 }

  D1:=0; F:=9; a:=0;
  Camo24(Quad_Scaler,f,a,d1,q,x);    { Reset Counter line 0 }

  D1:=0; F:=10; a:=2;
  Camo24(Quad_Scaler,f,a,d1,q,x);    { Reset OverFlow line 2 }

  D1:=0; F:=10; a:=0;
  Camo24(Quad_Scaler,f,a,d1,q,x);    { Reset OverFlow line 0 }

 End;


PROCEDURE Read_Scaler(i_scan:integer);

 Begin

   D1:=0; F:=0; A:=0;
   Cami24(Quad_Scaler,F,A,D1,Q,X);  { read and reset quad scaler channel
0 }
   D1:=0; F:=2; A:=0;
   Cami24(Quad_Scaler,F,A,D1,Q,X);  { read and reset quad scaler channel
0 }

   D2:=0; F:=0; A:=2;
   Cami24(Quad_Scaler,F,A,D2,Q,X);  { read and reset quad scaler channel
2 }
   D2:=0; F:=2; A:=2;
   Cami24(Quad_Scaler,F,A,D2,Q,X);  { read and reset quad scaler channel
2 }
```

```
   SigandBack[i_scan]:=SigandBack[i_scan] + D1;

   Back[i_scan]      :=Back[i_scan]       + D2;   { store data }

 End;


Function Read_Power_Meter:Integer;

 Begin
   d:=0; f:=25; A:=2;                { Set Gain on a/d converter to HI }
   Camo(AtoD_Converter,f,a,d,q,x);

   d:=0; f:=2; A:=0;
   cami(AtoD_Converter,f,a,d,q,x);  { Read A/D Converter Value }

   Read_Power_Meter:=Abs(d);

 End;


PROCEDURE Take_Data(i:integer);
 Var: Cycle1,Cycle2:Integer;

 Begin
   for b_scan := 1 to p.num_cycles do
   begin
      Check_Timer(LAM_mask[8]);
      camcl(allow_data);
      Check_Timer(LAM_mask[6]);
      Cycle1:=Read_Power_Meter;
      Check_Timer(LAM_mask[6]);
      Cycle2:=Read_Power_Meter;
      camcl(inhibit_data);
      Read_Scaler(i);
      LaserPower[i] := LaserPower[i] + Abs(Cycle1-Cycle2);
   end;
 End; { Take_Data }


PROCEDURE Screen_LAM_Requests;

 Begin

   D:=0; F:=24; A:=0;
   camo(pulse_generator,F,A,D,Q,X); { Disables LAM-request channel 1 }

         F:=24; A:=1;
   camo(pulse_generator,F,A,D,Q,X); { Disables LAM-request channel 2 }

         F:=24; A:=0;
   camo(AtoD_Converter,f,a,d,q,x);  { Disables LAM-request of AtoD
converter }

 End;


PROCEDURE Step_Nothing(I:Integer);
  Begin
  End;

PROCEDURE Step_Quadrupole(I:Integer);
```

```
  Begin

   d:=Round(Voltage(I)*409.5/20);

   f:=16; a:=2;                    { Address of D/A converter 0 to 10 Volts
}
   Camo(DtoA_Converter,f,a,d,Q,x);

  End;{Step_Quadrupole}

PROCEDURE Step_Magnet(I:Integer);
  Begin

   d:= Round(Voltage(I)*409.5)  ;

   f:=16; a:=1;                    { Adress of D/A converter 0 to 10 Volts
}
   Camo(DtoA_Converter,f,a,d,Q,x);

  End;{Step_Magnet}


PROCEDURE Step_Trap(I:Integer);

 Begin
   Trap_Delay:=Round(100*Voltage(I));
   If Trap_Delay<=b_c[3] then
     begin
        b_c[4]:=b_c[3]+1;
        Trap_Delay:=b_c[4];
     end;
   If Trap_Delay>=b_c[5] then
     begin
        b_c[4]:=b_c[5]-1;
        Trap_Delay:=b_c[4];
     end;
   F:=16; A:=3;
   Camo(Timing_Gen,f,a,Trap_Delay,q,x);

 End; {Step_Trap}



PROCEDURE Reset_Device;
 Begin
  Case device of

    Magnet:

       begin
       d:=Round(Voltage(1)*409.5);
       f:=16; a:=1; {Reset Magnet}
       Camo(DtoA_Converter,f,a,d,q,x);
       End;

    Q_Pole:

       Begin
       d:=Round(Voltage(1)*409.5/20);
       F:=16; a:=2; {Reset Qpole}
       Camo(DtoA_Converter,f,a,d,q,x);
       end;
```

```
    Trap:
       Begin
       d:=Round(4*Voltage(1));
       F:=16; A:=3;
       Camo(Timing_Gen,f,a,d,q,x);
       End;

    Laser:
       begin
          case p.etalon_in of
             false: begin

init_laser_scan(P.Start_W,P.End_W,P.num_chan,p.etalon_in);
                    end;
             true : begin
                    {}
                    end;
          end; {case p.etalon_in}
       end; {laser}

  End; { Case }

 End;  { Reset_Device }


PROCEDURE Step_Device(I:Integer);
 Begin
  Case Device of
    Magnet:  Step_Magnet(I);
    Q_pole:  Step_quadrupole(I);
    Laser:   Begin
               Case p.Etalon_in of
                 False: dye_laser_go_to(I,p.etalon_in,up_scan);
                 True:  TTL_Out;
               End; {Case}
             End;
    Nothing: Step_Nothing(I);

    Trap:    Step_Trap(I)
  End; {Case}

 End; { Step_device}




{*******************************************************}
{**    Display windows at the bottom of the screen    **}
{*******************************************************}


PROCEDURE Display_Display;
 Begin
  SetViewport(GetMaxx-186,GetMaxY-18,GetMaxx-6,GetmaxY-3,clipoff);
  ClearViewPort;
  SetUserCharSize(5,4,5,4);
  SetTextStyle(2,horizdir,usercharsize);
  SetTextJustify(0,0);
  SetColor(White);
```

```
  Box_Viewport(0);
  SetColor(Cyan);
  OutTextXY(10,10,' Display:');
  OuttextXY(80,10,DisplayString);
 End;

PROCEDURE Display_Help;
 Begin
  SetViewport(6,GetMaxY-18,86,GetmaxY-3,clipoff);
  ClearViewPort;
  SetColor(White);
  Box_Viewport(0);
  SetColor(Cyan);
  SetTextJustify(0,0);
  OutTextXY(10,10,'Help: F1');
 End;

PROCEDURE Display_Status;
VAR i_blinck : integer;
 Begin
  SetViewport(92,GetMaxY-18,212,GetmaxY-3,clipon);
  ClearViewPort;
  SetColor(White);
  Box_Viewport(0);
  SetColor(Cyan);
  SetTextJustify(0,0);
  case scanning of
     false: if key_mode_flag then
               status_string := ' KEY MODE'
            else
               begin
                  if ch_scan = f10 then
                     begin
                        status_string := 'SCAN ABORTED';
                        setColor(yellow);
                        for i_blinck := 1 to 4 do
                           begin
                              ClearViewPort;
                              Box_Viewport(0);
                              Delay(100);
                              OutTextXY(10,10,Status_String);
                              Delay(200);
                           end;
                        Status_String := '  IDLE';
                        Delay(400);
                        SetColor(white);
                        ClearViewPort;
                        Box_Viewport(0);
                        ch_scan := ' ';

                     end
                  else
                     status_string := '  IDLE';
               end;
     true : case halt_scan of
               false: begin
                         SetColor(lightred);
                         status_string := 'SCANNING';
                      end;
               true : begin
                         SetColor(white);
                         status_string := 'HALT SCAN';
```

```
                    end;
            end; {case halt_scan}
  end; {case scanning}
  OutTextXY(10,10,status_string);
  SetViewport(0,0,GetMaxX,GetMaxY,clipon);
  SetColor(White);
 End;


PROCEDURE Display_Up_Down;
 Begin
  SetViewport(218,GetMaxY-18,338,GetMaxy-3,clipon);
  ClearViewPort;
  if scanning then
     begin
        setcolor(white);
        box_viewport(0);
        setcolor(cyan);
        SetTextJustify(0,0);
        if up_scan then
           if device <> laser then
              outtextxy(10,10,'UP-scans only')
           else
              outtextxy(10,10,'UP-scan')
        else
           outtextxy(10,10,'DOWN-scan');
     end;
  SetViewport(0,0,GetMaxX,GetMaxY,clipon);
 End;


PROCEDURE Display_Channel(j_scan:integer);
 Begin
  SetViewport(92,GetMaxY-37,212,GetMaxy-21,clipon);
  ClearViewPort;
  if scanning or key_mode_flag then
     begin
        setcolor(white);
        box_viewport(0);
        setcolor(cyan);
        SetTextJustify(0,0);
        str(j_scan,string1);
        str(p.num_chan,string2);
        out_string := string1+' of '+string2+' chan';
        outtextxy(10,10,out_string);
     end;
  SetViewport(0,0,GetMaxX,GetMaxY,clipon);
 End;


PROCEDURE Display_Scan;
 Begin
  SetViewport(218,GetMaxY-37,338,GetMaxy-21,clipoff);
  ClearViewPort;
  if scanning then
     begin
        setcolor(white);
        box_viewport(0);
        setcolor(cyan);
        SetTextJustify(0,0);
```

```
        str(k_scan,string1);
        str(n_scan,string2);
        out_string := string1+' of '+string2+' scans';
        outtextxy(10,10,out_string);
     end;
  SetViewport(0,0,GetMaxX,GetMaxY,clipon);
End;


PROCEDURE Display_Lambda;
 Begin
  SetViewport(344,GetMaxY-37,444,GetMaxy-21,clipoff);
  ClearViewPort;
  if scanning and (device = laser) then
     begin
        setcolor(white);
        box_viewport(0);
        setcolor(cyan);
        SetTextJustify(0,0);
        str((dye_w_number - YAG_w_number):8:2,string1);
        out_string := string1 + '  cm-1';
        outtextxy(3,10,out_string);
     end;
  SetViewport(344,GetMaxY-18,444,GetMaxy-3,clipoff);
  ClearViewPort;
  if scanning and (device = laser) then
     begin
        setcolor(white);
        box_viewport(0);
        setcolor(cyan);
        SetTextJustify(0,0);
        str(lambda:9:3,string1);
        out_string := string1 + ' nm';
        outtextxy(8,10,out_string);
     end;
  SetViewport(0,0,GetMaxX,GetMaxY,clipon);
End;

PROCEDURE Display_Etalon;
 Begin
  SetViewport(6,GetMaxY-37,86,GetmaxY-21,clipoff);
  ClearViewPort;
  if (device = laser) and p.etalon_in then
  begin
     SetColor(White);
     Box_Viewport(0);
     SetColor(Yellow);
     SetTextJustify(0,0);
     OutTextXY(10,10,'Etalon in');
  end;
 End;

PROCEDURE Display_Integral(Integral:LongInt);
 Begin
  SetViewport(344,GetMaxY-37,444,GetMaxy-21,clipoff);
  ClearViewPort;
  setcolor(white);
  box_viewport(0);
  setcolor(cyan);
  SetTextJustify(0,0);
  str((Integral):8,string1);
  out_string := string1;
```

```
  outtextxy(3,10,'Sum: '+out_string);
 End;

PROCEDURE Display_Plotting(Show:Boolean);
 Begin
  Case Show of
  True:
       Begin
        Out_String:=' Plotting ';
        SetViewport(344,GetMaxY-37,444,GetMaxy-21,clipoff);
        ClearViewPort;
        setcolor(white);
        box_viewport(0);
        setcolor(cyan);
        SetTextJustify(0,0);
        outtextxy(3,10,out_string);
       End;
  False:
       Begin
        SetViewport(344,GetMaxY-37,444,GetMaxy-21,clipoff);
        ClearViewPort;
       End;
  End; {Case}
 End;

PROCEDURE Display_Bottom_Info(j_channel:integer);
 Begin
  Display_Display;
  Display_Help;
  Display_Status;
  Display_Up_Down;
  Display_Channel(j_channel);
  Display_Scan;
  Display_Lambda;
  Display_Etalon;
 End;


{*********************************************************}
{*********************************************************}

PROCEDURE Plotting_Window;
 Begin
  SetViewPort(0,0,getMaxx,Getmaxy,clipon);
  Box_ViewPort(0);
  SetViewport(10,10,GetMaxx-5,GetmaxY-40,clipoff);
  ClearViewPort;
  SetColor(Cyan);
  Draw_Axis;
  Set_Title(DeviceString);

  Case Device of
  Magnet:
     begin
     Set_X_Lable('Magnet Voltage');
     XMin:=P.Start_V;
     Set_X_Min(Xmin);
     Xmax:=P.End_V;
     Set_x_Max(Xmax);
     End;
  Q_Pole:
     begin
```

```
      Set_X_Lable('Mass ');
      XMin:=P.Start_M;
      Set_X_Min(Xmin);
      Xmax:=P.End_M;
      Set_x_Max(Xmax);
      end;

   Laser:
      begin
      Set_X_Lable('Channel Number ');
      Xmin:=0;
      Set_X_Min(0);
      XMax:=P.Num_chan;
      Set_X_Max(Xmax);
       start_w_length          := P.Start_W;
       stop_w_length           := P.End_W;
      end;

   Trap:
      begin
      Set_X_Lable('Trap Time (msec) ');
      Xmin:=P.Start_T;
      Set_X_Min(Xmin);
      XMax:=P.End_T;
      Set_X_Max(Xmax);
      end;

   Nothing:
      begin
      Set_X_Lable('Channel Number ');
      Xmin:=0;
      Set_X_Min(0);
      XMax:=P.Num_chan;
      Set_X_Max(Xmax);
      end;

   end;

   Set_Y_Lable('Counts');
   Set_Y_Min(0);
   Set_Y_max(Ymax);

   SetColor(Red);
   Lable_Titles;
   SetColor(Yellow);
   Lable_Axis;

 End;


Function DisplayArray(i:Integer):Longint;
  Begin
   Case Data of

    SignalandBackground: DisplayArray:=SigandBack[i];

    BackGround: DisplayArray:=Back[i];

    Signal: DisplayArray:=SigandBack[i]-Back[i];

    Power: DisplayArray:=LaserPower[i];
```

```
   End; {Case};
  End; {Function}


PROCEDURE Plot_Data(i:Integer;c:Word);
 Begin
  Case Device of
    Magnet: Begin
       Plot_point( Voltage(i), DisplayArray(i), I,c);
       End;
    Q_Pole: begin
       Plot_point( Voltage(i), DisplayArray(i), I,c);
       End;
    Trap:   begin
       Plot_point( Voltage(i), DisplayArray(i), I,c);
       End;
    Laser:  Begin
       Plot_point( I, DisplayArray(i), I,c);
       End;
    Nothing: Begin
       Plot_point( I, DisplayArray(i), I,c);
       End
  End; {Case}
 End;


PROCEDURE Redraw(m:Integer);
VAR n : integer;
 Begin
  Plotting_Window;
  For n:=1 to m do
  Plot_Data(n,yellow);
 End;


PROCEDURE Rescale;
 Begin
  YMax:=DisplayArray(i_scan)*1.3+10;
 End;


PROCEDURE Find_Array_Max;
 Var i: Integer;
 Begin
  Ymax:=100;
  For I:=1 to P.Num_chan do
    If DisplayArray(i)>=YMax then
    YMax:=DisplayArray(i)*1.3+10;
 End;

PROCEDURE Integrate_Display;
 Var I:Integer;
     Integral:LongInt;
 Begin
  Integral:=0;
  For I:=1 to p.Num_Chan do
   Integral:=Integral+DisplayArray(I);

  Display_Integral(Integral);
 End;

PROCEDURE Key_Mode;
```

```
Var M : Integer;
Begin
   initialize_cross;
   key_mode_flag := true;
   Display_Status;
   Display_Channel(save_channel);
   display_lambda;
   SetViewPort(datarange.x1,datarange.y1,
               datarange.x2,datarange.y2,Clipoff);
   M:=save_channel;
   actual_channel := m;
   Put_Cross(M);
   Repeat
    Ch:=Readkey;
    Case Ch of
     LEFTARROW: Begin
                 SetViewPort(datarange.x1,datarange.y1,
                             datarange.x2,datarange.y2,Clipoff);
                 Put_Cross(m);
                 m:=m-1;
                 If m<1 then M:=1;
                 Direction:='B';
                 actual_channel := m;
                 Step_Device(actual_channel);
                 Put_Cross(actual_channel);
                 Display_Channel(actual_channel);

                 if device = laser then
                    display_lambda;
                 End;

    RIGHTARROW: Begin
                 SetViewPort(datarange.x1,datarange.y1,
                             datarange.x2,datarange.y2,Clipoff);
                 Put_Cross(m);
                 m:=m+1;
                 If M>P.Num_chan then
                 M:=P.num_chan;
                 Direction:='F';
                 actual_channel := m;
                 Step_Device(actual_channel);
                 Put_Cross(actual_channel);
                 Display_Channel(actual_channel);
                 if device = laser then
                    display_lambda;
                End;
    End;{case}
   Until (CH=Esc) or (ch=f9);


   save_channel := actual_channel;
   SetViewPort(datarange.x1,datarange.y1,
               datarange.x2,datarange.y2,Clipoff);
   put_cross(Save_Channel);
   SetViewport(0,0,getMaxX,GetMaxY,Clipoff);
   MainChoice :=0;
   key_mode_flag := false;
   Display_Status;
   Display_Channel(actual_channel);
   display_lambda;
End;
```

```
PROCEDURE W_Length_Mismatch;

begin
   closegraph;
   clrscr;
   writeln;
   writeln('   Wavelength mismatch! ');
   writeln('   k_scan      : ',k_scan);
   writeln('   l_scan      : ',l_scan);
   writeln('   j_scan      : ',j_scan);
   writeln('   i_scan      : ',i_scan);
   writeln('   lambda new  : ',lambda);
   writeln('   lambda old  : ',dye_w_length[i_scan]);
   writeln('   lambda incr : ',w_length_incr);
   writeln;
   readln;
   halt;
end;


PROCEDURE Rescale_Diagram;

begin
   SetViewPort(datarange.x1,datarange.y1,
               datarange.x2,datarange.y2,Clipoff);

   if (k_scan=1) and (l_scan=1) then
      redraw(i_scan)
   else
      redraw(p.num_chan);
      SetViewPort(datarange.x1,datarange.y1,
                  datarange.x2,datarange.y2,Clipoff);
end;



PROCEDURE Scan_Menue(var Ch:char); Forward;


PROCEDURE Scan;

 Begin

  initialize_cross;
  i_cross        := 0;
  i_scan         := 1;
  Ymax           := 20;
  Scanning       := true;
  halt_scan      := true;
  up_scan        := true;
  ch_scan        := ' ';
  n_repeat       := 1;
  actual_channel := i_scan;
  redraw(0);
  step_device(i_scan);

  Display_Bottom_Info(Actual_Channel);

  k_scan         := 0;

  repeat
```

```
      inc(k_scan);
      Display_Scan;

      case device of
       laser : if bidirectional_laser_scan then n_repeat := 2;
      end;

      up_scan     := true;
      l_scan      := 0;
      i_scan      := 1;
      repeat
         inc(l_scan);
         if l_scan = 2 then
            up_scan := false
         else
            up_scan := true;
         Display_Up_Down;
         j_scan := 1;
         repeat
            If Keypressed then
               Begin
                  Ch_scan:=Readkey;
                  If Ch_scan = #0 then
                  Begin
                    Ch_scan:=Readkey;
                    Scan_Menue(Ch_scan);
                  End;

               End;
            if not halt_scan then
               begin
                  Display_Channel(i_scan);
                  if device = laser then
                     begin
                        if (k_scan=1) and (l_scan=1) then
                           begin
                              dye_w_length[i_scan] := lambda;
                              ir_w_number [i_scan] := dye_w_number -
YAG_w_number;
                           end
                        else
                           begin
                               if abs(dye_w_length[i_scan]-lambda) >=
{
w_length_incr then
                                  w_length_mismatch;
 }                             end;
                           display_lambda;
                     end;
                  Reset_Quad_Scaler;

                  TAKE_DATA(i_scan);

                  if displayarray(i_scan) >= ymax then
                     rescale_diagram;

                  plot_data(i_scan,yellow);

                  {SetViewPort(datarange.x1,datarange.y1,
                               datarange.x2,datarange.y2,Clipoff);
                  if i_cross > 0 then
                     put_cross(i_cross);
                  put_cross(i_scan);
```

```
                i_cross := i_scan;}
            end;
         if not halt_scan then
            begin
               if up_scan then
                  inc(i_scan)
               else
                  dec(i_scan);
               inc(j_scan);
               if j_scan < (p.num_chan+1) then
                  begin
                     actual_channel := i_scan;

                     STEP_DEVICE(i_scan);

                  end;
            end;
      until (j_scan = p.num_chan+1) or not scanning;
      if up_scan and scanning then
         dec(i_scan)
      else
         inc(i_scan);
   until (l_scan = n_repeat) or not scanning;
 until (k_scan = n_scan) or not scanning;

 if (k_scan=n_scan) and (device=laser) then
    new_data_flag := true;

 if scanning then
    begin
       {SetViewPort(datarange.x1,datarange.y1,
                    datarange.x2,datarange.y2,Clipoff);
       put_cross(i_cross);}
    end;
 scanning := false;
 display_bottom_info(p.num_chan);

END; {procedure}



PROCEDURE HP_Plotter(Mode:Integer);
 Var D: text;
     Min_X, Max_X: Real;
     Too_Large: Integer;
     PlotMax: Real;

 Procedure Tics;
  Var i: Integer;
  Begin
   {Draw X Axis Tics}
   Delay(100);
   Write(D,'PA',Round(Min_X),',0;');
   delay(100);
   wRITE(D,'PD;');
   delay(100);
   For I:=1 to 10 do
    Begin
     Write(D,'XT;');
     delay(100);
     Write(D,'PR',round((Max_X-Min_X)/10),',0;');
     delay(100);
```

```
    End;
   Write(D,'XT;');
   Write(D,'PU;');
   I:=1;

   {Draw Y Axis Tics}
   Delay(100);
   Write(D, 'PA',Round(Min_X),',0;');
   delay(100);
   Write(D, 'PD');
   Delay(100);
   For I:=1 to 5 do
    Begin
     Write(D,'YT;');
     delay(100);
     Write(D,'PR',0,',',Round(PlotMax/5),';');
     Delay(100);
    End;
   Write(d,'YT;');
   Write(D,'PU;');
  End;

 Procedure PlotDat;
  Var X: Real;
  Begin
   Write(D,'PA',Round(100*Xmin),',0;');
   Write(D,'PD;');
   Write(D,'SP2;');
   Delay(200);
   X:=1;
   For I:=1 to P.Num_chan do
    Begin
     Delay(50);
     Case Too_Large Of

0:Write(D,'PA',(Min_X)+(X*((Max_X-Min_X))/P.Num_chan):5:2,',',DisplayArr
ay(i),';');

1:Write(D,'PA',(Min_X)+(X*((Max_X-Min_X))/P.Num_chan):5:2,',',DisplayArr
ay(i) div 10,';');
     End;
     Delay(40);
     X:=X+1;
    End;
   Write(D,'PU;');
  End;

 Procedure Lables;
  Var I: Integer;
      X: Real;
      Y: LongInt;
  Begin
  Write(D,'DT',RETURN,';');
  Write(D,'PA',Round(Min_X),',',-Round(PlotMax/20),';');
  Write(D,'SP3;');
  X:=xMin;
   For I:=1 to 6 do
   Begin
    Write(D,'LB',X:2:3,RETURN);
    Delay(100);
    Write(D,'PR',Round((MAX_X-MIN_X)/5),',',0,';');
    Delay(100);
```

```
   X:=X+((Xmax-Xmin)/5);
  End;
 Write(D,'PA',Round(Min_X)-round((Max_X-Min_X)/15),',',0,';');
 Y:=0;
  For I:=1 to 6 do
  Begin
   Write(D,'LB',Y,RETURN);
   Delay(100);
   Write(D,'PR',0,',',round(Plotmax/5),';');
   Delay(100);
   Y:=Y+Round(YMax/5);
  End;
End;

Procedure Messages;
 Begin
  Write(d,'DT',#3,';');
  Delay(200);
  Write(D,'SP4;');
  Write(D, 'PA',Round(Min_X)+Round((Max_X-Min_X)/30) );
  Delay(200);
  Write(D,',',-2*Round(Ymax/20),';');
  Delay(200);
  Write(D, 'LBScanning: ',DeviceString);
  Delay(200);
  Write(D,RETURN,#10,#3);
  DElay(200);
  Write(D, 'LBDisplay: ',DisplayString,RETURN,#10,#3);
 End;

Begin
 Display_Plotting(True);
 Too_Large:=0;
 Assign(D,'COM1');
 REWRITE(D);

 {Initialize Plotter}

 Write(D,'IP;');
 Write(D,'DF;');
 Write(D,'SP1;');
 Write(D,'T1,1;');
 Write(D,'IP 1000,1001,9000,7200;');  {Set Plot Area}
 Min_X:=Xmin;
 Max_X:=Xmax;
 If Max_X<10 then Begin
  Max_X:=Max_X*100;
  Min_X:=Min_X*100;
  End;

 PlotMax:=YMax;

 If Ymax>32767 then begin   { Check if Data Maximum is too large for
                              Plotter}
  PlotMax :=YMax/10;
  Too_Large:=1;
  end;


 Write(D,'SC',Min_X:5:2,',',Max_X:5:2,',',0,',',Round(PlotMax),';');
 {Scale to Data Values}
 Case Mode of
```

```
  0: Begin
     Tics;
     PlotDat;
     Lables;
     Messages;
     End;
  1: Begin;
     PlotDat;
     End;
  End;{Case}

  Write(D,'PU;SP0;');
  Close(D);
  Display_Plotting(False);
 End;


PROCEDURE Main_Menue(var Ch:char);

 Begin
            Case {ReadKey} Ch of

                     F1: Begin
                         case help_page of
                            false: begin
                                      SetVisualPage(1);
                                      While not keypressed do
                                         begin
                                         end;
                                      help_page:=true;
                                   end;
                             true: begin
                                      SetVisualPage(0);
                                      help_page:=false;
                                   end;
                         end; {case help_page}
                      End;    {F1}

                     F3: Reset_Device;

                     F4:   Begin
                              Clear_Arrays;
                              ReDraw(P.num_chan);
                           End;

                     F5: Begin
                           If Data <> SignalandBackground then
                           begin
                              Data:=Signalandbackground;
                              DisplayString:='Sig and Back';
                              Find_Array_Max;
                              ReDraw(p.num_chan);
                              Display_Display;
                           end;
                      End;

                     F6: Begin
                           If Data <> Background then
                           begin
                              Data:=BackGround;
                              DisplayString:='Background';
```

```
                        Find_Array_Max;
                        ReDraw(p.num_chan);
                        Display_Display;
                     end;
               End;

            F7: Begin
                  If Data <> Signal then
                     begin
                        Data:=Signal;
                        DisplayString:='Signal';
                        Find_Array_Max;
                        ReDraw(p.num_chan);
                        Display_Display;
                     end;
               End;

            F8: Begin
                  If Data <> Power then
                     begin
                        Data:=Power;
                        DisplayString:='Power';
                        Find_Array_Max;
                        ReDraw(p.num_chan);
                        Display_Display;
                     end;
               End;



            F9: Key_Mode;

            F10: Begin

              if device = laser then
              begin

              start_w_length           := P.Start_W;
              stop_w_length            := P.End_W;
              Laser_Narrow:=p.Etalon_IN;
              Case P.Etalon_in of
               False:
init_laser_scan(P.Start_W,P.End_W,P.num_chan,p.etalon_in);
              End; {Case}
              {if p.etalon_in then set_etalon_normal;}
              end;
              Scan;
              End;


         ShiftF2: HP_Plotter(0);  {Nice Plot}

         ShiftF4: begin
                     {closegraph;
                     dyecontrol;
                     init_graphics;
                     Init_Help_Page;
                     ReDraw(p.num_chan);
                     Display_Bottom_Info(Actual_Channel);}
                  end;
```

```
            SHIFTF3: Begin
                        Set_Timing;
                        Redraw(p.num_chan);
                        display_bottom_info(actual_channel);
                     end;

            ShiftF9: Begin
                        Make_Device_Menu;
                        Init_Help_Page;
                        Clear_Arrays;
                        ReDraw(p.num_chan);
                        Display_Bottom_Info(Actual_Channel);
                      End;

            SHIFTF5: Begin
                        Find_Array_max;
                        ReDraw(p.num_chan);
                     End;

            SHIFTF6: Begin
                        YMAX:=YMAX/10;
                        ReDraw(p.num_chan);
                     End;

            SHIFTF7: Begin
                        YMAX:=YMAX/100;
                        ReDraw(p.num_chan);
                     End;

            SHIFTF8: Begin
                        YMAX:=YMAX/1000;
                        ReDraw(p.num_chan);
                     End;

            SHIFTF1: Begin
                        Make_Save_Menu;
                        Init_Help_Page;
                        Find_Array_Max;
                        Redraw(p.num_chan);
                        Display_Bottom_Info(actual_channel);
                     End;
              AltF5: Begin
                       Integrate_Display;
                     End;
              AltF9: Begin
                        Parameters_Form;
                        Init_Help_Page;
                        Redraw(p.num_chan);
                        Display_Bottom_Info(actual_channel);
                     End;

                F2 : HP_Plotter(1); {Speed Plot}

           CtrlF10 : Begin
                           CloseGraph;
                           Halt;
                     End;

          End; {Case Ch}

        End; {main_menue}
```

```
PROCEDURE Scan_Menue(var Ch:char);

 Begin
            Case {ReadKey} Ch of

                     F1: Begin
                            case help_page of
                               false: begin
                                         SetVisualPage(1);
                                         While not keypressed do
                                            begin
                                            end;
                                         help_page:=true;
                                      end;
                                true: begin
                                         SetVisualPage(0);
                                         help_page:=false;
                                      end;
                            end; {case help_page}
                         End;    {F1}


                     F3: If Halt_Scan = true then
                            Reset_Device;

                     F4: If Halt_Scan = true then
                            Begin
                               Clear_Arrays;
                               ReDraw(p.num_chan);
                            End;

                     F5: Begin
                            If Data <> SignalandBackground then
                               begin
                                  Data:=Signalandbackground;
                                  DisplayString:='Sig and Back';
                                  Find_Array_max;
                                  Rescale_Diagram;
                                  Display_Display;
                               end;
                         End;

                     F6: Begin
                            If Data <> Background then
                               begin
                                  Data:=BackGround;
                                  DisplayString:='Background';
                                  Find_Array_max;
                                  Rescale_Diagram;
                                  Display_Display;
                               end;
                         End;

                     F7: Begin
                            If Data <> Signal then
                               begin
                                  Data:=Signal;
                                  DisplayString:='Signal';
                                  Find_Array_max;
                                  Rescale_Diagram;
                                  Display_Display;
```

```
                        end;
                    End;

                F8: Begin
                       If Data <> Power then
                       begin
                          Data:=Power;
                          DisplayString:='Power';
                          Find_Array_max;
                          Rescale_Diagram;
                          Display_Display;
                       end;
                    End;

            SHIFTF5: Begin
                       Find_Array_Max;
                       Rescale_Diagram;
                    End;

            SHIFTF6: Begin
                       YMAX:=YMAX/10;
                       Rescale_diagram;
                    End;

            SHIFTF7: Begin
                       YMAX:=YMAX/100;
                       Rescale_Diagram;
                    End;

            SHIFTF8: Begin
                       YMAX:=YMAX/1000;
                       Rescale_Diagram;
                    End;

           SHIFTF10: Begin
                       case halt_scan of
                          false: begin
                                    halt_scan:=true;
                                    Display_Status;
                                 end;
                           true: begin
                                    halt_scan:=false;
                                    Display_Status;
                                 end;
                       end;  {case halt}
                     end; {ShiftF10}
        AltF5: Begin
                     Integrate_Display;
                   End;
        F10 :  if halt_scan then
                     Begin            { Abort Scan }
                      scanning  := false;
                      halt_scan := true;
                      Display_Up_down;
                      Display_Channel(actual_channel);
                      Display_Scan;
                    end;

    End; {Case Ch}

End; {scan_menue}
```

```
{ MAIN PROGRAM }

BEGIN

    Init_Graphics;
    Initialize;
    Initialize_CAMAC;
    Init_Help_Page;

    E:=200;
    I:=1;
    Actual_channel := 1;

    Display_Bottom_Info(Actual_Channel);
    ReDraw(p.num_chan);

    Repeat
       Ch:=Readkey;
       If Ch = #0 then
       Begin
          Ch:=Readkey;
          Main_Menue(Ch);
       End;
    Until CH=Ctr1F10;

    CloseGraph;
    Release_GPIB;

END.
```

Appendix 2

Data Analysis Program

```
{$N+}    {Change to $N+ if you have a numeric coprocessor}
{$I-}
PROGRAM Analysis6;

{*  (c) 1990, J.M. Price, All rights reserved.

     Program to manipulate a series of input vectors and generate a
series of output vectors from equations typed in by the user.  Makes use
of the Vector3 unit which dynamically allocates and manipulates the
vectors.  Input and output files are of the same format as that of the
data aquisition program.
     The latest version now supports the HP 7475 Plotter through calls
to the GraphAdd unit.  1 Oct 90. *}


USES

  Dos,          {Unit Supplied By Borland}
  Crt,          {          "           }
  Graph,        {          "           }
  Forms,        { " and Modified by JMP  }
  JPTools,      {     }
  JPDos,        {By JMP. Contains the Directory Displaying Functions}
  MenuMax,      {By JMP. To Generate the 'Scroll Bar' Menus  }
  Grafmax,      {By JMP. Contains the Functions for Plotting to Screen}
  Vector3,      {By JMP. The Singly Linked List Vector Object.
                 Does its own Mathematical Manipulations, and handles its
                 own memory Allocation.}
  Common,       {Provided With Borland's Numerical Recipies Toolbox. I
                 Use it for the Convenient I/O Error Checking Routines}
  GraphAdd;     {*.BGI Device Driver Unit for the HP 7475 plotter and
                 assorted other output devices.  Allows the same commands
                 used to manipulate the screen to manipulate the devices.
                 By Fleming Software.}

CONST
  {Default Values:}

  Input_Dir:String[12]='A:\';
  Output_Dir:string[12]='A:\';
  Input_Data_File: String[25] ='20p197.a';
  Output_Data_File: String[25]='                         ';
  Num_Inputs = 5;
  Num_outputs = 5;
  Command_String_Length=40;
  Input_Title_Length=10;
  Num_Chan :Integer =1000;


  {HP Plotter Output Stuff}

  info : DrvINFO = (DrvMem:64000; DrvWrkdrive:' ';
  DrvOutfile : ''; escchk : TRUE; nohead : FALSE );

  { Change these to match your hardware }
  MyPath : string = 'c:\tp5';
  MyPort : integer = PortCOM1;
  MyDevice : string = '$HP7475';
  MyMode : integer = DraftPL;
  XON : boolean = TRUE;
  MyComm : word = Baud2400 or ParNone or Data8 or Stop1;
```

```
TYPE

  InTitles        = Array[1..num_Inputs]  of
                    String[Input_Title_Length];
  Command_Strings = Array[1..num_Outputs] of
                    String[Command_String_Length];

  Analysis_Form   = record
     Input_Directory: String[30];
     Input_File_Name: String[12];
     Output_Directory: String[30];
     Output_File_Name: String[12];
     Input_Titles: InTitles;
     Output_Titles:Command_Strings;
  end;

  Plot_Form    = record
      Main_Title:String[50];
      Y_Title:String[50];
      X_Title:String[50];
     Plot_List:Array[1..Num_Outputs] of integer;
     XAuto_Scale:Integer;
     Xmin,Xmax:Real;
     YAuto_Scale:Integer;
     Ymin,Ymax: Real;
      Lines_Points:Integer;
      Plot_Versus:LongInt;
  end;


  Comrec = Record
   Com : String[80];
   VCO : Integer;
  End;

  Comlist=Array[1..10] of Comrec;
  Com_list_Length = Integer;

  VectorPTR =^Vector;
  RealPTR   =^Real;

VAR

  Menu,menu2,Menu3:Menuarray;
  HeapTop : ^Word;
  F:   Form;
  P,D: Analysis_Form;
  E,H: Plot_Form;
  I,J: Integer;
  B: Text;

  { The Input And output Vectors }

  In_Vectors: Array[1..Num_Inputs] of Vector;
  Out_Vectors:Array[1..Num_Outputs] of Vector;

  { The Commands entered into each output field are stored in
    A list in the Comlist_Array.  The number of commands in each
    list are held in the Com_List_Length_Array... }

  ComList_Array:Array[1..Num_Outputs] of ComList;
  Com_List_Length_Array:Array[1..Num_Outputs] of Com_List_Length;
```

```
  Input_VectorPtrs: Array[1..Num_Inputs] of VectorPtr;
  Output_VectorPtrs:Array[1..Num_Outputs] of VectorPtr;

  Analyzed_Toggle: Boolean;
  Retrieved_Toggle:Boolean;
  Saved_Toggle:Boolean;
  Plot_Select_Toggle:Boolean;
  Exec_Toggle:Boolean;

  Name:String[25];

  {Graphics Driver Variables}
  drv, mode, driverID : integer;
  ierr : shortint;
  status : word;


PROCEDURE AbortM ( msg:string );
 { Abort the Program With A Message. }
  BEGIN
   WriteLn(msg);
   Halt(1);
  END;

{*************************************************************************}


PROCEDURE MA;
 {Probably ought to tuck this in the JPDos unit
  Tells the amount of memory remaining in RAM }
 BEGIN
   TextColor(Yellow);
   BOX(49,22,75,24,2);
   GOTOXY(52,23);
   WRITE(MEMAVAIL div 1000,' K Bytes Available');
 END;


PROCEDURE Init_Vectors;
{ Initialize all the Arrays }
 Var I:integer;
 Begin

  If Retrieved_Toggle then
    Begin
      For I:=1 to Num_Inputs do In_Vectors[I].done;
      For I:=1 to Num_Outputs do  Out_Vectors[I].done;
    End;

  For J:=1 to Num_Inputs do
   Begin
    New(Input_VectorPtrs[j]);
    Input_VectorPtrs[j]:=@In_vectors[J];
    In_Vectors[J].Init(Num_Chan);
   End;

  For J:=1 to Num_Outputs do
   Begin
    New(Output_VectorPtrs[j]);
    Output_VectorPtrs[j]:=@Out_vectors[J];
    Out_Vectors[J].Init(Num_Chan);
```

```
    End;

  End;

PROCEDURE Init_D;
{ Initialize the Analysis Form }
 Begin
  { Look for options on the program Command Line }

  If ParamStr(1)<>'' Then
    Begin
     D.Input_Directory:='';
     D.Input_File_Name:=ParamStr(1)
    End
  Else
    Begin
     D.Input_Directory:=Input_Dir;
     D.Input_File_Name:=Input_Data_File;
    End;

  If ParamStr(1)<>'' Then
    Begin
     D.Output_Directory:='';
     D.Output_File_Name:=ParamStr(2)
    End
  Else
    Begin
     D.Output_Directory :=Output_Dir;
     D.Output_File_Name:=Output_Data_File;
    End;

  For I:=1 to Num_Inputs do D.Input_Titles[i]:='';
  For I:=1 to Num_Outputs do
   Begin
    D.Output_Titles[i]:='|';
   End;
 End;

Procedure Init_E;
{ Initialize the Plot Form }
 Begin
  E.Main_Title:='';
  E.Y_Title:='';
  E.X_Title:='';
  For I:= 1 to Num_Outputs do E.Plot_List[i]:=0;
  E.XAuto_Scale:=1;
  E.Xmin:=0;
  E.Xmax:=Num_Chan;
  E.YAuto_Scale:=1;
  E.Ymin:=-10;
  E.YMax:=1000;
  E.Lines_Points:=1;
  E.Plot_Versus:=0;
 End;


PROCEDURE Save_Retrieve_Data(Save_Ret:Integer);
{ Reads the titles of and the data for the Vectors in the Raw Data
File }
 Var
    K: Integer;
    Num_Chan_Text:String[18];
```

```
   Num:Array[1..Num_Inputs] of Real;
Begin

   For I:=1 to 3 do
     Case Save_Ret of
      1:Readln(b);
      2:Writeln(b);
     End;

   Case Save_Ret of
   1: Begin
       Readln(b,Num_chan_Text,Num_chan);
       Init_Vectors;
       For I:=1 to 11 do Readln(b);
       For I:=1 to Num_Inputs do Read(B,D.Input_Titles[I]);
       Readln(B);
       For J:=1 to Num_Inputs do In_Vectors[J].VMark(1);
       For I:= 1 to num_Chan Do
        Begin
         For J:=1 to num_Inputs do Read(B,Num[j]);

          For K:=1 to num_Inputs do
            Begin
             In_Vectors[K].VReplace(Num[K]);
             In_Vectors[K].VAdvance;
            end;
         Readln(b);
        End;
      End;
   2: Begin
       Num_Chan_Text:='Number of Channels';
       Writeln(b,Num_chan_Text,Num_chan);
       For I:=1 to 11 do Writeln(b);
       For I:=1 to Num_Outputs do Write(B,D.Output_Titles[I]);
       Writeln(B);
       For J:=1 to Num_Outputs do Out_Vectors[J].VMark(1);
       For I:= 1 to num_Chan Do
        Begin
         For J:=1 to num_Outputs do
           Begin
            Write(B,Out_Vectors[j].Value,' ');
            Out_Vectors[j].VAdvance;
           end;
         Writeln(b);
        End;
      End;
   End;
   Close(B);
End;

PROCEDURE Set_Up_Screen;
{ Prepares the Screen for the Form }
 Begin
  TextMode(CO80);
  TextBackground(blue);
  ClrScr;

  TextColor(Cyan);
  Box(1,1,79,25,2);
  GotoXY(2, 1);
  TextColor(Yellow);
  Write(' VECTOR Data Analysis Program:  Version 1.0.  (C) 1990, John M.
```

```
Price.  ');
  GotoXY(3, 25);
  TextColor(Yellow);
  Write(' <F2> -Execute Output Commands.   <Esc> -Quit Without
Executing.');
 End;

PROCEDURE Make_Analysis_Form;
{ Make the Form from which Commands may be Entered }
 Var S:String[2];
 Begin
  F.Init(2, 3, 78, 24);
  F.Add(New(FStrPtr, Init(1, 1, ' Input  Directory: ',30)));
  F.Add(New(FStrPtr, Init(33,1, ' Input  Data File: ',12)));
  F.Add(New(FStrPtr, Init(1, 3, ' Output Directory: ',30)));
  F.Add(New(FStrPtr, Init(33,3, ' Output Data File: ',12)));
  For I:= 1 to num_Inputs do
   Begin
    Str(I:2,S);
    F.Add(New(FStrPtr,
         Init(1, I*3+4, ' Input '+S+': ',Input_Title_Length)));
   End;
  For I:= 1 to num_Outputs do
   Begin
    Str(I:2,S);
    F.Add(New(FStrPtr,
         Init(25,I*3+4, ' Output '+S+': ',Command_String_Length)));
   End;
  P := D;
  F.Put(P);
  F.Show(True);
  Case  F.Edit of
   CSave: Begin
            F.Get(P);
            D:=P;
            Analyzed_Toggle:=True;
          End;
   CEsc: Analyzed_Toggle:=False;
  End; {Case}
  F.Done;
  ClrScr;
 End;

PROCEDURE Make_Plotting_Form;
{ Make the Form from which Plots may be modified }
 Var S:String[2];
 Begin
  F.Init(2, 3, 78, 24);

  F.Add(New(FstrPTR,Init(3,2,' Main Title: ',50)));
  F.Add(New(FstrPTR,Init(3,3,' Y Title:    ',50)));
  F.Add(New(FstrPTR,Init(3,4,' X Title:    ',50)));

  For I:=1 to num_Outputs do
   Begin
    Str(I:2,S);
    F.Add(New(JPbuttonPtr,
         Init(3, I*2+4, ' Plot Output '+S+': ')));
   End;

    F.Add(New(JPButtonPtr,Init(30,6,' Scale X Automatically: ')));
    F.Add(New(FrealPtr,Init(30,8,' Manual Scale X min: ',10,2)));
```

```
    F.Add(New(FrealPtr,Init(30,9,' Manual Scale X max: ',10,2)));
    F.Add(New(JPButtonPtr,Init(30,11,' Scale Y Automatically: ')));
    F.Add(New(FrealPtr,Init(30,13,' Manual Scale Y min: ',10,2)));
    F.Add(New(FrealPtr,Init(30,14,' Manual Scale Y max: ',10,2)));
    F.Add(New(JPButtonPTR,Init(30,16,' Lines Instead of Points:')));
    F.Add(New(FIntPTR,Init(30,18,' X-Axis Source:',0,5)));

   H := E;
   F.Put(H);
   F.Show(True);

  If F.Edit = CSave then
   Begin
    F.Get(H);
    E:=H;
    For I:=1 to num_outputs do
      If E.Plot_List[i]=1 then Plot_Select_Toggle:=True;
   End;
  F.Done;
  ClrScr;
 End;


PROCEDURE Init_ComList;
{ Initializes the Command list Array }
 Begin
  For I:=1 to Num_Outputs do Com_List_Length_Array[I]:=0;
  For J:=1 to Num_Outputs do
   For I:=1 to 10 do
   Begin
    ComList_Array[J][I].Com:='';
    ComList_Array[J][I].VCO:=0;
   End;
 End;

PROCEDURE Command_List_Generator;
{ Translates the String input in Reverse Polish Notation into
  A list of ComRec's that can be evaluated by Execute_Command_List
 }

 Var
     S : String[20];
     SR: String[10];
     M,K: Integer;
     Which_Vector:Integer;
     Value:String[80];
     Code:Integer;

 Begin
   Init_ComList;
   For J:=1 TO Num_Outputs do
    Begin
     M:=1;
     For I:=1 to Command_String_Length do
     Begin
     Case Upcase(D.Output_Titles[J][I]) of
      '|':Begin
          I:=Command_String_Length;
          COM_List_Length_Array[j]:=M-1;
         End;
      'I':Begin
          Case Upcase(D.Output_Titles[J][I+1]) of
```

```
            '1'..'5':Begin
            Comlist_Array[j][m].com:=Upcase(D.Output_Titles[J][I+1]);
            Comlist_Array[j][m].VCO:= 1;
            M:=M+1;
            End;
           End; {Case}
          End;

      'M':Begin
            Val(ComList_Array[j][m-1].com,which_Vector,code);
            Case Upcase(D.Output_Titles[J][I+1]) of
             'X': Begin
                  STR(In_Vectors[which_Vector].max,value);
                  I:=I+1;
                  End;
             'N': Begin
                  Str(In_Vectors[which_Vector].min,value);
                  I:=I+1;
                  End;
            End;
            Comlist_Array[j][m-1].com:=Value;
            Comlist_Array[j][m-1].vco:=2;
           End;
      '+', '-', '/', '*', '^' :
          Begin
           Comlist_Array[j][m].Com:=D.Output_Titles[J][I];
           Comlist_Array[j][m].VCO:= 3;
           M:=M+1;
          End;
      '0'..'9', ' ', '.':
          Begin
           If Upcase(D.Output_Titles[J][I-1])<> 'I' then
           Begin
            K:=0;
            Repeat
             Comlist_Array[j][m].Com:=Comlist_Array[j][m].Com+
                                      D.output_Titles[J][K+I];
             Comlist_Array[j][m].VCO:=2;
             K:=K+1;
            Until (D.output_Titles[J][I+K]=',') or
                  (D.output_Titles[J][I+K]=' ') or
                  (D.output_Titles[J][I+K]='+') or
                  (D.output_Titles[J][I+K]='-') or
                  (D.output_Titles[J][I+K]='*') or
                  (D.output_Titles[J][I+K]='/') or
                  (D.output_Titles[J][I+K]='^') ;
            M:=M+1;
            I:=I+K-1;
           End;
          End;
    End;
   End;
  End;
 End;

PROCEDURE Execute_Command_List;
{ Takes the Array of Comrec generated above, and executes the
  Vector operations after interpreting the commands. }
 Var

   Vector_Registers : Array[1..5] of Vector;
   Const_Registers: Array[1..5] of Real;
```

```
    Max_Vector_Reg:Integer;
    Max_Const_Reg:Integer;

    InputINT: Integer;
    Code: Integer;


    ConstantVal:Real;
    N,Z: Integer;


    MEMOMARK1:POINTER;  {Markers to tell The Mark/Release Functions how
                         Allocate/Deallocate RAM}
    MemoMark2:Pointer;

  Begin
    MARK(MEMOMARK1);
    Window(25,10,55,14);
    TextBackground(Blue);
    TextColor(White);
    ClrScr;
    Box(1,1,30,5,2);
    gotoXY(15-length('Calculating.') div 2,3);
    Write('Calculating.');

    For n:=1 to 5 do Const_Registers[n]:=0.0;

      For I:= 1 to Num_Outputs do
       Begin
        Mark(MemoMark2);
        n:=1;
        Max_Vector_Reg:=0;
        Max_Const_Reg :=0;
        For J:=1 to Com_List_Length_Array[I] do
         Begin

          Case Comlist_Array[i][j].VCO of
          1:Begin
             Val(Comlist_Array[i][j].com,InputInt,Code);
             Vector_Registers[n].Init(Num_Chan);
             N:=N+1;

Vector_Registers[Max_Vector_Reg+1].Vident(In_Vectors[InputInt]);
             Max_Vector_Reg:=Max_vector_Reg+1;
            End;

          2:Begin
             Val(Comlist_Array[i][j].com,ConstantVal,Code);
             Const_Registers[Max_Const_Reg+1]:=ConstantVal;
             Max_Const_Reg:=Max_Const_Reg+1;
            End;

          3:Begin
             Case Comlist_Array[i][j].COM[1] of
              '+': Begin
                     If Max_Const_Reg>0 then
                      Begin
                      Vector_Registers[Max_Vector_Reg].
                             VAddC(Const_Registers[Max_Const_Reg]);
                      Max_Const_Reg:=Max_Const_Reg-1;
                     End
```

```
        Else
         Begin
         Vector_Registers[Max_Vector_Reg-1].
                VAdd(Vector_Registers[Max_Vector_Reg]);
         Max_Vector_Reg:=Max_Vector_Reg-1;
        End;
      End;

'/': Begin
        If Max_Const_Reg>0 then
         Begin
         Vector_Registers[Max_Vector_Reg].
                VDivC(Const_Registers[Max_Const_Reg]);
         Max_Const_Reg:=Max_Const_Reg-1;
        End

        Else
         Begin
         Vector_Registers[Max_Vector_Reg-1].
                VDiv(Vector_Registers[Max_Vector_Reg]);
         Max_Vector_Reg:=Max_Vector_Reg-1;
        End;
      End;


'-': Begin
        If Max_Const_Reg>0 then
         Begin
         Vector_Registers[Max_Vector_Reg].
                VSubtC(Const_Registers[Max_Const_Reg]);
         Max_Const_Reg:=Max_Const_Reg-1;
        End

        Else
         Begin
         Vector_Registers[Max_Vector_Reg-1].
           VSubt(Vector_Registers[Max_Vector_Reg]);
         Max_Vector_Reg:=Max_Vector_Reg-1;
        End;
      End;


'*': Begin
        If Max_Const_Reg>0 then
         Begin
         Vector_Registers[Max_Vector_Reg].
                VMultC(Const_Registers[Max_Const_Reg]);
         Max_Const_Reg:=Max_Const_Reg-1;
        End

        Else
         Begin
         Vector_Registers[Max_Vector_Reg-1].
           VMult(Vector_Registers[Max_Vector_Reg]);
         Max_Vector_Reg:=Max_Vector_Reg-1;
        End;
      End;

'^': Begin
        If Max_Const_Reg>0 then
         Begin
         Vector_Registers[Max_Vector_Reg].
```

```
                        VRaiseC(Const_Registers[Max_Const_Reg]);
                       Max_Const_Reg:=Max_Const_Reg-1;
                      End

                      Else
                       Begin
                       Vector_Registers[Max_Vector_Reg-1].
                         VRaise(Vector_Registers[Max_Vector_Reg]);
                       Max_Vector_Reg:=Max_Vector_Reg-1;
                      End;
                    End;


                End; {Case}

              End;{Case}

           End;
        End;

       Out_Vectors[I].Vident(Vector_Registers[1]);
       Release(MemoMark2);
      End;
      Exec_Toggle:=True;

    ClrScr;
    Box(1,1,30,5,2);
    gotoXY(15-length('Done')div 2,3); Write('Done.');
    Delay(1000);
    Window(1,1,80,25);
    RELEASE(MEMOMARK1);
  End;


PROCEDURE Plot_Data;

 Var Ymin,Ymax:Real;
      Xmin,Xmax:Real;
     Title:String[80];
      YLast,XLast:Real;

 Begin
  If Plot_Select_Toggle then
  Begin

    {NB: All Graphics Coordinates in My Programs are in Relative
     Coordinates. -- Relative to the GetMaxX and GetMaxY's of the
     Output Device. -- This means a display will look the same on
     EGA screens, and VGA, etc.}


    SetViewPort(GetMaxX Div 5,
                GetMaxY div 20,
                getMaxx-GetMaxX div 5,
                Getmaxy-GetMaxY Div 20,clipon);
    ClearViewPort;
    SetColor(White);
    Draw_Axis;
    Set_Title(E.Main_Title);
    Set_X_Lable(E.X_Title);
    Set_Y_Lable(E.Y_Title);
```

```
X_Dec_Places:=2;
Case E.XAuto_Scale of
1: Begin
    If E.Plot_Versus <>0 then
     Begin

      Xmin:=In_Vectors[E.Plot_Versus].Min;
      Xmax:=In_Vectors[E.Plot_Versus].Max;

      Set_X_Min(Xmin);
      Set_X_Max(Xmax);
      Set_X_Dec_Places(XMin,XMax);
     End
    Else
    Begin
     Set_X_Min(0);
     Set_X_Max(Num_Chan);
    End;
  End;
0: Begin
   Set_X_Min(E.Xmin);
   Set_X_Max(E.Xmax);
  End;
End; {Case}

Case E.YAuto_Scale of
1: Begin
   Ymax:=-100000000;
   Ymin:= 100000000;
   For J:=1 to Num_Outputs do
     If E.Plot_List[j]=1 then
     Begin
        If Out_Vectors[j].Min<ymin then
            Ymin:=Out_Vectors[j].Min;
         If Out_Vectors[j].Max>ymax then
            Ymax:=Out_Vectors[j].Max;
     End;
   Set_Y_Min(Ymin-0.01);
   Set_Y_max(Ymax+0.01);
    Set_Y_Dec_Places(YMin,YMax);

  End;
0:Begin
   Set_Y_Min(E.Ymin);
   Set_Y_Max(E.Ymax);
   Set_Y_Dec_Places(E.Ymin,E.Ymax);
  End;
End; {Case}

SetColor(Red);
Lable_Titles;
SetColor(Yellow);
Lable_Axis;

For J:=1 to Num_Outputs do Out_Vectors[J].Vmark(1);
 {Set All the output Vectors to their First Entry}

For J:=1 to Num_Outputs do
 {For Each Output, Plot it.}

 Begin
  If E.Plot_Versus<>0 then In_vectors[E.Plot_Versus].Vmark(1);
```

```
      {If you are plotting the data against one of the input channels
       then set that input vector to its first entry.}

     YLast:=Out_Vectors[J].Val;
     If E.Plot_VErsus <>0 then XLast:=In_Vectors[E.Plot_Versus].Val Else
     XLast:=0;

     For I:=1 to Num_Chan do
     Begin
      If E.Plot_List[J]=1 then
       Begin
        Case E.Lines_Points of
         0:Begin
             Case E.Plot_Versus of
             0: Begin
                  Plot_Point2(I,Out_Vectors[J].Val,J+1);
                  Out_Vectors[J].Vadvance;
                End;
             1..5:Begin

Plot_Point2(In_Vectors[E.Plot_Versus].Val,Out_Vectors[J].val,J+1);
                  Out_Vectors[J].Vadvance;
                  In_Vectors[E.Plot_Versus].Vadvance;
                 End;
            End;
           End;


         1:Begin
             Case E.Plot_Versus of
             0:Begin
                Plot_Line2(I-1,YLast,I,Out_Vectors[J].val,J+1);
                YLast:=Out_Vectors[j].val;
                Out_Vectors[J].Vadvance;
                In_Vectors[E.Plot_Versus].Vadvance;
               End;
             1..5:Begin

Plot_Line2(XLast,YLast,In_Vectors[E.Plot_Versus].val,Out_Vectors[J].val,
J+1);
                YLast:=Out_Vectors[j].val;
                XLast:=In_Vectors[E.Plot_Versus].val;
                Out_Vectors[J].Vadvance;
                In_Vectors[E.Plot_Versus].Vadvance;

               End;
            End;
           End;
       End; {Case}
      End;
    End;
  End;


  End
  Else
  Begin
   Write('  Need to Select Plotting Range(s). ');
   Delay(1500);
  End;
 End;
```

```
PROCEDURE HP_Output;
 {I just grabbed the Freman sample program for the graphic driver and
  stuck it in here.}
 BEGIN

    Init_Graphics;   {I found you need these commands for some reason.}
    Close_Graphics;

    { Install the driver }
    driverID := InstallUserDriver(MyDevice,nil);
    ierr := GraphResult;
    if ierr<>0 then AbortM (GraphErrorMsg(ierr));

    { Set up the serial port }
    if (MyPort=PortCOM1) or (MyPort=PortCom2) then
    begin
        if XON then
        begin
            SPinstall(MyPort);
            ExitProc := @SPrestore;
        end;
        SPinit(MyPort,MyComm);
        if XON and (Copy(MyDevice,1,3)='$HP') then
            SPsend(MyPort,HPinit);
    end;

    { Enter Graphics Mode }
    mode := MyMode or MyPort;
    drv := driverID + 5;
    bInitGraph ( drv, mode, MyPath, @info);
    ierr := GraphResult;
    if ierr<>0 then AbortM (GraphErrorMsg(ierr));
    status := GraphStatus;
    if (status and $8000) <> 0 then begin
        bCloseGraph;
        AbortM (GraphStatusMsg(status));
    end;

    {*****************   Draw Graph     **********************}
    Plot_Data;
    {************************************************************}

    { Print the graph }
    ClearDevice;
    status := GraphStatus;
    if (status and $8000) <> 0 then begin
        bCloseGraph;
        AbortM (GraphStatusMsg(status));
    end;

    { Exit Graphics }
    bCloseGraph;
 END; {Output}


PROCEDURE Store_Main_Menu;
 Begin
  Storemenu (menu[1],' A. Analyze Data ',3,5);
  Storemenu (menu[2],' B. Retrieve Data ',5,5);
  Storemenu (menu[3],' C. Save Data ',7,5);
  Storemenu (menu[4],' D. Plot Data to Screen ',9,5);
  Storemenu (menu[5],' E. Plot Data to Plotter ',11,5);
```

```
  Storemenu (menu[6],' F. Plotting Parameters ',13,5);
  Storemenu (menu[7],' G. Exit VECTOR  ',15,5);
 End;

PROCEDURE Store_Retrieve_Menu;
 Begin
  Storemenu (menu2[1],' A. Current DIR: ',1,1);
  Storemenu (menu2[2],' B. Current File Name: ',3,1);
  Storemenu (menu2[3],' C. Retrieve ',5,1);
  Storemenu (menu2[4 ,' D. Directory ',7,1);
  Storemenu (menu2[5],' E. Return ',9,1);

 End;

PROCEDURE Store_Save_Menu;
 Begin
  Storemenu (menu3[1],' A. Current DIR: ',1,1);
  Storemenu (menu3[2],' B. Current File Name: ',3,1);
  Storemenu (menu3[3],' C. Save ',5,1);
  Storemenu (menu3[4],' D. Directory ',7,1);
  Storemenu (menu3[5],' E. Return ',9,1);

 End;


PROCEDURE Small_Window;
 Begin
   Window(30,5,78,16);
   TextBackground(Blue);
   Textcolor(White);
   ClrScr;
   GotoXY(24,1);
   ClrEol;
 End;


BEGIN
  MA;
  Store_Main_Menu;            {Store All the Menu Arrays Needed}
  Store_Retrieve_Menu;
  Store_Save_Menu;

  Register_Drivers_and_Fonts; {This allows the executable program to
                               be independent of the *.BGI Screen
                               drivers. -- It increases the size of the
                               *.EXE file, however. -- This function
                               is found in the GRAFMAX Unit. }

  Init_ComList;               {Initialize the lists and forms}
  Init_D;
  Init_E;

  Analyzed_Toggle:=False;
  Retrieved_Toggle:=False;
  Saved_Toggle:=False;
  Plot_Select_Toggle:=False;
  Exec_Toggle:=False;

  MenuChoice :=0;

  MA;
```

```
Repeat;
 ClrScr;
 Set_Up_Screen;
 GotoXy(30,5);
 Writeln('Filename: ',D.Input_Directory+D.Input_File_Name);
 GotoXy(30,7);
 Writeln('Filename: ',D.Output_Directory+D.Output_File_Name);
 MA;
 MakeMenu(Menu,7);
 Case MenuChoice of
 1: Begin
     If Retrieved_Toggle Then
      Begin
       Set_Up_Screen;
       Make_Analysis_Form;
       If Analyzed_Toggle then
        Begin
         Command_List_Generator;
         Execute_Command_List;
        End;
      End
      Else Begin
            Write('  Need to Retrieve Data First. ');
            Delay(1500);
           End;
   End;
 2: Begin
     Repeat
      Small_Window;
      Writeln(D.Input_Directory);
      GotoXY(24,3);
      Writeln(D.Input_File_Name);
      MakeMenu(Menu2,5);
      Case MenuChoice of
        1: Begin
            Name:=D.Input_Directory;
            Window(0,0,80,25);
            F.Init(30,5,78,5);
          F.Add(New(FStrPtr,Init(1,1,' A. Current Directory: ',25)));
            F.Put(Name);
            If F.Edit = CSave then
             Begin
              F.Get(Name);
              D.Input_Directory:=Name;
             End;
            F.Done;
           End;
        2: Begin
            Name:=D.Input_File_Name;
            Window(0,0,80,25);
            F.Init(30,7,78,7);
            F.Add(New(FStrPtr,Init(1,1,' B. Current File Name:
',12)));
            F.Put(Name);
            If F.Edit = CSave then
             Begin
              F.Get(Name);
              D.Input_File_Name:=Name;
             End;
            F.Done;
           End;
        3: Begin
```

```
                Assign(b, D.Input_Directory+D.Input_File_Name);
                Reset(b);
                IOCheck;
                If not IOerr then
                 Begin
                  Save_Retrieve_Data(1);
                  Retrieved_Toggle:=True;
                 End;
                IOerr:=False;
               End;
            4: Begin
                Dirlist(D.Input_Directory);
                MA;
               End;
          End;
          Until Menuchoice=5;
        Window(1,1,25,80);
       End;
    3: Begin
        Repeat
         Small_Window;
         Writeln(D.Output_Directory);
         GotoXY(24,3);
         Writeln(D.Output_File_Name);
         MakeMenu(Menu3,5);
         Case MenuChoice of
           1: Begin
               Name:=D.Output_Directory;
               Window(0,0,80,25);
               F.Init(30,5,78,5);
               F.Add(New(FStrPtr,Init(1,1,' A. Current Directory:
',25)));
               F.Put(Name);
               If F.Edit = CSave then
                Begin
                 F.Get(Name);
                 D.Output_Directory:=Name;
                End;
               F.Done;
              End;
           2: Begin
               Name:=D.Output_File_Name;
               Window(0,0,80,25);
               F.Init(30,7,78,7);
               F.Add(New(FStrPtr,Init(1,1,' B. Current File Name:
',12)));
               F.Put(Name);
               If F.Edit = CSave then
                Begin
                 F.Get(Name);
                 D.Output_File_Name:=Name;
                End;
               F.Done;
              End;
           3: Begin
               If analyzed_Toggle then
                Begin
                 Assign(b, D.Output_Directory+D.Output_File_Name);
                 Rewrite(b);
                 IOCheck;
                 If not IOerr then
                  Begin
```

```
                    Save_Retrieve_Data(2);
                    Saved_Toggle:=True;
                   End;
                  IOerr:=False;
                 End
                 Else
                  Begin
                   Write('  Need to Analyze Data first. ');
                   Delay(1500);
                  End;
               End;
          4: Begin
              Dirlist(D.Output_Directory);

              {D.Output_File_Name:=
               Select_File(16,24,D.Output_Directory);}

              MA;
             End;
        End;
        Until Menuchoice=5;
       Window(1,1,25,80);
      End;

   4: Begin
       If Analyzed_Toggle then
       Begin
        Init_Graphics;
        Plot_Data;
        Readln;
        Close_graphics;
       End
       Else Begin
              Write('  Need to Analyze Data First. ');
              Delay(1500);
            End;
      End;

   5: Begin
       HP_Output;
      End;

   6: Begin
      Set_up_Screen;
      Make_Plotting_Form;
      End;

  End; {Case}

 Until MenuChoice = 7;


 If Retrieved_Toggle then
   Begin
     For I:=1 to Num_Inputs do In_Vectors[I].done;
     For I:=1 to Num_Outputs do  Out_Vectors[I].done;
   End;

 MA;
End.
```

LAWRENCE BERKELEY LABORATORY
UNIVERSITY OF CALIFORNIA
INFORMATION RESOURCES DEPARTMENT
BERKELEY, CALIFORNIA 94720